EXPERT CONSENSUS DOCUMENT

ACCF/ACR/AHA/NASCI/SCMR
2010 Expert Consensus Document on
Cardiovascular Magnetic Resonance

A Report of the American College of Cardiology Foundation Task Force on
Expert Consensus Documents

Writing Committee Members

W. Gregory Hundley, MD, FACC, FAHA, *Chair**

David A. Bluemke, MD, PhD, FAHA†
J. Paul Finn, MD†
Scott D. Flamm, MD‡
Mark A. Fogel, MD, FACC, FAHA, FAAP§
Matthias G. Friedrich, MD, FESC‡
Vincent B. Ho, MD, MBA, FAHA‖**
Michael Jerosch-Herold, PhD
Christopher M. Kramer, MD, FACC, FAHA*
Warren J. Manning, MD, FACC*
Manesh Patel, MD

Gerald M. Pohost, MD, FACC, FAHA¶
Arthur E. Stillman, MD, PhD, FACR, FAHA#
Richard D. White, MD, FACC, FAHA#
Pamela K. Woodard, MD, FACR, FAHA‖

*American College of Cardiology Foundation Representative; †North American Society for Cardiovascular Imaging Representative; ‡Society for Cardiovascular Magnetic Resonance Representative; §American Academy of Pediatrics; ‖American College of Radiology Representative; ¶ACCF Task Force Liaison; #American Heart Association Representative. **The findings and conclusions in this expert consensus document reflect ACCF policy and do not necessarily represent the views of the Uniformed Services University of the Health Sciences, the U.S. Department of Defense, or the U.S. Government, by whom Dr. Ho is employed.

TABLE OF CONTENTS

Preamble

This document was developed by the American College of Cardiology Foundation (ACCF) Task Force on Clinical Expert Consensus Documents (ECDs) and cosponsored by the American College of Radiology (ACR), American Heart Association (AHA), North American Society for Cardiovascular Imaging (NASCI), and the Society for Cardiovascular Magnetic Resonance (SCMR), to provide a perspective on the current state of cardiovascular magnetic resonance (CMR). ECDs are intended to inform practitioners and other interested parties of the opinion of the ACCF and document cosponsors concerning evolving areas of clinical practice and/or technologies that are widely available or new to the practice community. Topics are chosen for coverage because the evidence base, the experience with technology, and/or the clinical practice are not considered sufficiently well developed to be evaluated by the formal ACCF/AHA practice guidelines process. Often the topic is the subject of ongoing investigation. Thus, the reader should view the ECD as the best attempt of the ACCF and document cosponsors to inform and guide clinical practice in areas where rigorous evidence may not be available or the evidence to date is not widely accepted. When feasible, ECDs include indications or contraindications. Typically, formal recommendations are not provided in ECDs as these documents do not formally grade the quality of evidence, and the provision of "Recommendations" is felt to be more appropriately within the purview of the ACCF/AHA Practice Guidelines. However, recommendations from ACCF/AHA Clinical Practice Guidelines and ACCF Appropriate Use Criteria are presented where pertinent to the discussion. The writing committee is in agreement with these recommendations. Finally, some topics covered by ECDs will be addressed subsequently by the ACCF/AHA Practice Guidelines Committee.

The task force makes every effort to avoid any actual or potential conflicts of interest that might arise as a result of an outside relationship or personal interest of a member of the writing panel. Specifically, all members of the writing panel are asked to provide disclosure statements of all such relationships that might be perceived as real or potential conflicts of interest to inform the writing effort. These statements are reviewed by the parent task force, reported orally to all members of the writing panel at the first meeting, and updated as changes occur. The relationships and industry information for writing committee members and peer reviewers are published in Appendix 1 and Appendix 2 of the document, respectively.

Robert A. Harrington, MD, FACC, FAHA
Chair, ACCF Task Force on
Clinical Expert Consensus Documents

1. Introduction

1.1. Writing Committee Organization

The writing committee consisted of acknowledged experts in the field of CMR, as well as a liaison from the ACCF Task Force on Clinical ECDs, the oversight group for this document. In addition to 2 ACCF members, the writing committee included 1 representative from the American Academy of Pediatrics (AAP) and 2 representatives from the ACR, AHA, NASCI, and the SCMR. Representation by an outside organization does not necessarily imply endorsement.

1.2. Document Development Process

1.2.1. Relationships With Industry

At its first meeting, each member of the writing committee reported all relationships with industry and other entities relevant to this document topic. This information was updated, if applicable, at the beginning of all subsequent meetings and full committee conference calls. As noted in the Preamble, relevant relationships with industry and other entities of writing committee members are published in Appendix 1.

1.2.2. Consensus Development

During the first meeting, the writing committee discussed the topics to be covered in the document and assigned lead authors for each section. Authors conducted literature searches and drafted their sections of the document outline. Over a series of meetings and conference calls, the writing committee reviewed each section, discussed document content, and ultimately arrived at a consensus on a document that was sent for external peer review. Following peer review, the writing committee chair engaged authors to address reviewer comments and finalize the document for document approval by participating organizations. Of note, teleconferences were scheduled between the writing committee chair and members who were not present at the meetings to ensure consensus on the document.

1.2.3. External Peer Review

This document was reviewed by 8 official representatives from the ACCF, ACR, AHA, NASCI, and SCMR, as well as 4 content reviewers, resulting in 279 peer review comments. See list of peer reviewers, affiliations for the review process, and corresponding relationships with industry and other entities in Appendix 2. Peer review comments were entered into a table and reviewed in detail by the writing committee chair. The chair engaged writing committee members to respond to the comments, and the document was revised to incorporate reviewer comments where deemed appropriate by the writing committee.

In addition, a member of the ACCF Task Force on Clinical ECDs served as lead reviewer for this document. This person conducted an independent review of the doc-ument at the time of peer review. Once the writing committee documented its response to reviewer comments and updated the manuscript, the lead reviewer assessed whether all peer review issues were handled adequately or whether there were gaps that required additional review. The lead reviewer reported to the task force chair that all comments were handled appropriately and recommended that the document go forward to the task force for final review and sign-off.

1.2.4. Final Writing Committee and Task Force Sign-Off on the Document

The writing committee formally signed off on the final document, as well as the relationships with industry that would be published with the document. The ACCF Task Force on Clinical ECDs also reviewed and formally approved the document to be sent for organizational approval.

1.2.5. Document Approval

The final version of the document along with the peer review comments and responses to comments were circulated to the ACCF Board of Trustees for review and approval. Several issues arose during board review that were addressed by the writing committee. The document was approved in November 2009. The document was then sent to the governing boards of the ACR, AHA, NASCI, and SCMR for endorsement consideration, along with the peer review comments/responses for their respective official peer reviewers. All 4 organizations formally endorsed this document. This document will be considered current until the ACCF Task Force on Clinical ECDs revises or withdraws it from publication.

1.3. Purpose of This Expert Consensus Document

This document is the first ACCF/ACR/AHA/NASCI/SCMR Expert Consensus Document on CMR. It serves the following purposes: 1) it introduces the basic instrumentation, physics, scan techniques, safety parameters, and contraindications associated with CMR acquisitions; 2) it reviews the use of CMR for assessing patients with cardiovascular disease processes; and 3) unique capabilities of image data generated with CMR are provided relative to other imaging techniques. Finally, recommendations from ACCF/AHA clinical practice guidelines and ACCF appropriate use criteria are presented where pertinent. In addition, new recommendations for the use of CMR in clinical practice were developed by this writing committee and are presented for those situations where guidelines are unavailable.

1.4. Document Overview

CMR is an imaging modality that provides a mechanism to assess cardiac or vascular anatomy, function, perfusion, and tissue characteristics in a highly reproducible manner during a single examination. Images can be acquired in patients of various body habitus, in a time-efficient fashion, without an

invasive procedure or exposure to ionizing radiation or iodinated intravenous contrast medium.

1.5. CMR Physics

CMR is based on the detection of signals from hydrogen nuclei which are in very high concentration within the body (approximately 100 M) (1). Upon a patient entering a scanner, hydrogen nuclei align with and "precess" about the axis of the magnetic field. This precession can be perturbed by application of additional small magnetic field pulses. By applying these pulses in a controlled manner in the form of "pulse sequences," signals can be received and processed to produce an image of the spatial distribution of the spins or protons within the body. A unique feature of CMR is the availability of multiple types of pulse sequences for imaging that can define cardiac structure, characterize tissue, or measure cardiovascular function.

1.6. Magnetic Field Strength

The strength of the magnetic field within the scanner is measured in Tesla (T) (2). Typical commercially available CMR field strengths for use in patients with cardiovascular disease are 1.0-, 1.5-, and 3.0-T. In general, images acquired at higher field strengths exhibit proportionally greater signals, and thus can produce images with higher spatial resolution and more precise delineation of cardiac or vascular structures. On occasion, however, artifacts become more prominent at higher field strengths, which may sometimes negate the advantage provided by the higher spatial resolution.

1.7. Configuration and Instrumentation Within the CMR Suite

CMR suites are comprised of 5 components: 1) the room housing the scanner; 2) the console room used to direct the scanning process; 3) an image interpretation room; 4) a space allocated for the preparation and recovery of patients; and 5) a technical room for magnet-related equipment. In addition to the magnet, accessory equipment for the scanning procedure is also present in the CMR scanner room. This equipment includes special devices that function in a high magnetic field to monitor heart rate and blood pressure, as well as administer intravenous medications or CMR contrast agents. The operator console for the scanner is located outside of the scanning room. This master console is utilized by the technologist or physician to direct image acquisition, implement pulse sequences, and to display images for immediate review after acquisition. Once images are acquired, they are often transferred to other computer workstations for the purpose of image analysis, storage, and physician review.

1.8. Advantages of CMR

CMR possesses several advantages for the study of patients with cardiovascular disease (3). First, images are acquired without application of ionizing radiation or the administration of radioactive isotopes or iodinated contrast. The noninvasive acquisition of images without the use of ionizing radiation facilitates the diagnosis and subsequent monitoring of medical conditions without incurring the risk of developing conditions related to ionizing radiation exposure. Second, CMR images can be acquired throughout the body in any tomographic plane without limitations imposed by body habitus. This feature can be helpful in patients with acoustic window limitations during transthoracic echocardiography or attenuation artifacts during radionuclide scintigraphy.

Third, CMR is a flexible imaging modality that allows assessment of multiple different parameters of cardiovascular anatomy and function. As mentioned, CMR can define cardiovascular anatomy and structure, characterize tissue composition (including myocardial viability), measure function in terms of heart wall motion or blood flow, assess metabolism with spectroscopic techniques, visualize and quantify myocardial perfusion, and define the course and orientation of epicardial coronary arteries. Importantly, recent advances allow for the acquisition of this type of information throughout the body; thus, the ability exists to precisely define cardiovascular phenotype in patients with disease processes such as atherosclerosis, cardiomyopathies, diabetes, and hypertension that commonly affect individuals with cardiovascular disease (3).

A fourth advantage of CMR imaging is the ability to quantify with relatively high spatial and temporal resolution meaningful measures of cardiovascular structure or performance that discriminate normal from abnormal pathologic conditions or denote adverse cardiovascular prognoses (3). At 1.5-T, voxel sizes of $1 \times 1 \times 3$ cm can be acquired with most pulse sequence strategies. When cine sequences are required, frame rates of 20 to 40 ms are routinely available allowing for the characterization of time-dependent processes such as left ventricular (LV) diastolic function. Measurements of myocardial mass; blood flow through vessels or across valves; LV or right ventricular (RV) myocardial thickening, strain, or tissue perfusion; infarct size; or plaque burden can be quantified in absolute terms. Studies have confirmed high reproducibility and low variance of these measures in repeated samples indicating marked precision of CMR for use in clinical or research examinations (4).

2. Assessment of Cardiovascular Structure and Function With CMR

2.1. Dimension and Morphology

2.1.1. Dark Blood Imaging

Dark blood imaging sequences, for example those acquired with spin echo or inversion recovery techniques, are used to acquire morphologic images of the heart (5–8). In these techniques, protons in nonmoving or slowly moving structures such as the myocardium provide high signal in the

images, while rapidly flowing blood within the heart and great vessels moves out of the imaging slice (and are therefore not exposed to both of the radiofrequency pulses), resulting in a signal void (hence the term "dark blood").

Dark blood imaging strategies are used throughout the spectrum of cardiovascular diseases, including the assessment of cardiac and great vessel morphology in congenital heart disease and thoracic aortic disease (9–11), the assessment of myocardial masses, and the evaluation of the pericardium (12–14).

2.1.2. Bright Blood Imaging

Bright blood imaging is advantageous for acquiring high temporal resolution cine movies of LV and RV systolic and diastolic function. Imaging strategies include gradient echo (GRE), segmented k-space GRE, GRE hybridized with an echo-planar readout, and steady-state free precession (SSFP) techniques. These sequences produce images in which the blood pool is bright relative to the adjacent intermediate signal intensity of the myocardium. These techniques can also be used to identify intravoxel dephasing related to turbulent blood flow from valvular stenosis or regurgitation (15).

Cine CMR for evaluation of cardiac volumes and systolic function is considered a standard of reference by which other modalities are validated (7). This includes normal physiology such as atrial or right-sided myocardial assessment, as well as pathological conditions with low flow states such as congestive heart failure.

2.2. Myocardial Function

CMR is an accurate and highly reproducible technique for measuring ejection fraction and ventricular volumes in 3 dimensions (16). Unlike 2-dimensional (2D) projection techniques, cine CMR imaging does not rely on geometric assumptions or calculations based on incomplete sampling of the cardiac volumes (17–19). Newer SSFP techniques have largely replaced conventional GRE for cine CMR assessment of myocardial volumes, mass, and systolic function (20,21). An offset exists between the older conventional GRE techniques and SSFP cine-generated CMR measures. The offset between volumes and mass between the 2 CMR methods is linear over the range of interest, so that normal databases for myocardial function may be adapted for the newer SSFP cine CMR method (22).

For CMR measurement of myocardial volume and mass, consecutive breath-hold short axis 6- to 10-mm tomographic cine short-axis cross-sections of the heart are obtained; the summation of discs method is then applied to determine the total myocardial mass and volume (3). A series of long-axis views rotated around the anatomical axis of the left ventricle can also be used to assess LV function with comparable accuracy (23–25). In a typical application, the temporal resolution of cine CMR for myocardial function determination is 50 ms or less. Breath-hold time for each cross-sectional slice is approximately 5 to 10 seconds;

the lower imaging times are achieved with newer CMR scanners that use parallel imaging techniques. For myocardial mass, the total volume of the myocardial wall at end-diastole is multiplied by the specific gravity of the myocardium (1.05 g/mm^3). Myocardial mass and ventricular volumes are commonly adjusted for body size by dividing raw measures by body surface area to derive indexed values. Single acquisition, 3-dimensional (3D) CMR acquisition methods for the heart are available. The temporal resolution in thin, relatively new acquisition is typically lower (100 ms) than the slice-by-slice acquisition methods; spatial resolution is lower as well. The primary advantage is a single breath-hold of 20 to 30 seconds to cover the entire myocardium in this cine 3D mode.

A significant advantage of CMR for evaluation of myocardial mass and volume is its reproducibility and accuracy compared with 2D planar or projection techniques that depend on geometric assumptions in order to define mass and volume determinations. As a result, small changes in myocardial mass and/or volume can be detected over time or as a result of therapy. This is particularly useful for determining the impact of therapy or for research purposes in clinical trials where sample size can be reduced by an order of magnitude compared with planar or projection techniques using LV geometric assumptions (26,27). CMR LV size and systolic function are precisely determined with standard errors of about 5% (16,19,28–30).

Using CMR, normal LV volumes and mass have been determined to be smaller for women than men even after adjustment for body size (16). In normal individuals, LV mass is relatively constant with increasing age in adults, although LV volumes decrease by about 3% per decade from age 45 years. Asian-American men tend to have slightly smaller body size–adjusted LV mass and volumes (5%) compared with Whites, African-Americans, and Hispanics.

Regional myocardial function may be assessed using CMR tagging (31,32). In this method, specialized radiofrequency pulses are applied prior to the beginning of the cine CMR pulses sequence. These additional pulses result in alteration of the magnetic properties of the heart, typically in a grid stripe pattern. The grids or stripes are dark relative to the remaining myocardium, and the grids are displaced as a result of myocardial motion/contraction. For research purposes, specialized software is available for dynamic analysis of the spacing between the magnetic stripes, allowing regional myocardial strain to be calculated. CMR tagging has allowed precise quantification of regional heterogeneity in myocardial contraction in the setting of coronary artery disease (CAD) and nonischemic cardiomyopathy (33–36). In clinical practice, CMR tagging is most commonly interpreted qualitatively rather than quantitatively. New methods (DENSE [displacement encoding with stimulated echoes in CMR] [37] and HARP [harmonic phase] [38]) may offer more automated methods for myocardial strain analysis.

2.3. Metabolism

CMR can be used to assess myocardial metabolism without the need for administration of radioactive tracers; the basis for the assessment of myocardial metabolism is magnetic resonance spectroscopy. For spectroscopy, nuclei other than hydrogen may be studied, but there are substantial scanner hardware modifications and signal-to-noise compromises involved in using other nuclei. At the time of writing, clinical cardiac spectroscopy is not available as a routine tool. Spectroscopic approaches have been applied to evaluate the behavior of the high-energy phosphates; phosphorus-31 provides the basis for such evaluation (39). The spectrum is represented by a series of peaks, each of which represents 1 or more molecular species, including adenosine triphosphate (ATP), phosphocreatine (PCr), and inorganic phosphate. The position of a spectral peak is determined by the phenomenon of chemical shift, which is related to the chemical nature and environment of the molecule. For example, the position of or chemical shift of the inorganic phosphate peak is related to the intracellular pH. With ischemia, the environment becomes acidic, and the inorganic phosphate peak is shifted to the right. Due to the relatively low concentration of ^{31}P, a large volume of myocardium (20 to 30 cm^3) must be interrogated to generate a ^{31}P spectrum at 1.5-T. Spectral resolution can be improved by using a higher field strength, for example, 3.0-T, and thus, 3.0-T is often preferred.

2.4. Phase-Contrast Blood Flow

In addition to the magnitude data used to generate cine CMR images of cardiac function, the phase data collected from the image acquisition can be used to measure velocity (40). The use of the phase data, termed the "phase-contrast" (PC) technique, relies on the fact that blood flowing through a magnetic field gradient produces a phase shift that is proportional to the velocity of flow (41). By summing the PC-generated velocities within the area of the lumen throughout the cardiac cycle, blood flow within the vessel can be calculated. PC-CMR measures of blood flow agree strongly with those obtained in phantom models as well as by both noninvasive and other accepted invasive techniques (42,43). Conventional PC magnetic resonance (MR) usually encodes the velocity in a single direction. More recently developed tridirectional PC MR allows velocity encoding in multiple directions, facilitating direct visualization of flow disturbances such as vortices or turbulent flow (44).

Clinically, PC-CMR measures of blood flow velocity have been acquired in the aorta (43), the pulmonary arteries (45), coronary artery bypass grafts (46), and across heart valves (47). These data are useful for identifying abnormalities of blood flow in patients with diseases of the aorta (aortic dissection, aneurysms, or coarctation) (46), congenital heart disease (either through native vessels or surgically placed conduits) (48,49), or stenotic/regurgitant valve lesions (3).

2.5. Myocardial Perfusion

Myocardial perfusion imaging by CMR is most commonly achieved with rapid dynamic imaging during the first pass of a tracer or contrast agent (50). Coronary autoregulation provides an efficient mechanism for maintaining adequate myocardial blood flow during resting conditions in the presence of flow-limiting epicardial lesions. However, during stress, myocardial perfusion is inadequate in the setting of flow-limiting epicardial coronary artery stenoses. The myocardial perfusion examination therefore consists of a measurement at baseline (rest) and a comparative measurement during stress. The term *stress* is used here in a generic form, and in most cases, a vasodilator is administered to induce maximal hyperemia and determine the coronary flow capacitance. The pharmacological agents that are most widely used for myocardial perfusion imaging with CMR include adenosine and dipyridamole. Exercise-induced stress is currently performed in specialized academic centers.

Contrast agents used for CMR generally reduce both the longitudinal (T1) and transverse (T2) relaxation times (51). Pulse sequence techniques sensitive to T1, T2, or both can be employed to detect the transit of contrast agent through a perfusion bed. Currently, myocardial perfusion studies are mostly based on T1-weighted 2D, multislice imaging, with 3 to 5 slices being considered the minimum for coverage of the heart. As an alternative to vasodilator perfusion imaging, dobutamine can be administered for assessment of regional contractile response during rest and stress conditions. Recent data on the prognostic value of CMR perfusion imaging indicate that patients with a normal myocardial vasodilator perfusion reserve and normal dobutamine stress (DS) wall motion have a 3-year event-free survival rate of 99.2% (52).

In patients with suspected coronary disease, myocardial perfusion reserve measured by CMR yields high diagnostic accuracy for the detection of flow-limiting lesions (53–55). CMR perfusion imaging has also been used to assess functional improvements after percutaneous coronary interventions (56–58). Microvascular dysfunction and microvascular obstruction after myocardial infarction are detected by CMR (59,60), and the presence of microvascular obstruction detected by early hypoenhancement carries valuable prognostic information, independent of infarct size (61–63). The extent and incidence of microvascular obstruction observed with CMR has been associated with the duration of ischemia before coronary intervention (64).

An international, multicenter study demonstrated that CMR perfusion imaging exhibits high specificity for detecting coronary disease (65). Other single-center studies have shown similar findings (66). High spatial resolution provides high utility for detecting flow deficits within the subendocardium layer (66–68), the portion of the ventricular wall most vulnerable to any flow reductions. CMR perfusion imaging, by virtue of its excellent spatial resolution, may also be indicated in pediatric

patients, where any exposure to ionizing radiation is of particular concern (69).

2.6. Angiography

Magnetic resonance angiography (MRA) exhibits benefits related to its lack of exposure to ionizing radiation, iodinated contrast agents, or arterial access (70–72). Moreover, MRA image acquisitions are typically 3D and afford improved visualization of complex geometries through image postprocessing of maximum intensity projection and multiplanar reformations of 3D data sets. MRA techniques exhibit high utility for assessing the carotid arteries, aorta, renal arteries, and peripheral vasculature.

CMR offers a variety of methods for visualizing vascular pathology. Conventional T1- and T2-weighted dark blood techniques (e.g., spin echo, fast spin echo, and double inversion recovery fast spin echo) enable proper depiction of vessel walls (73). Bright blood imaging techniques (Table 1; time-of-flight, phase contrast, SSFP, and contrast-enhanced magnetic resonance angiography [CE-MRA]) provide the ability to evaluate blood flow and to generate images of vessel lumens that allow selective display of vascular anatomy in 3D projections. With improvements in scanner speed, it is now possible to perform rapid frame rate MRA, also known as time-resolved MR angiography, allowing direct visualization of flow dynamics, which may be important for assessment of vascular shunts or dissections.

2.7. Tissue Characterization

A unique feature of CMR is the ability to use characteristics of proton relaxation, typically referred to as the relaxation times T1, T2, and T2*, to characterize myocardial or vascular tissue. Whereas T1 images are often used for contrast-enhanced studies (see the following text), T2 and T2* imaging mostly have been used in noncontrast approaches. For example, within the myocardium, T2-weighted CMR imaging is sensitive to regional or global increases of myocardial water content. Increased myocardial water content has been shown in acute heart diseases such as transplant rejection, acute myocarditis, and acute myocardial infarction (74) (Figure 1A).

Another noncontrast tissue characterization technique relates to the T2* relaxation of the tissue. T2* times are significantly altered by the myocardial iron content; their quantification provides an excellent marker for iron overload (see Section 3.5.8, Hemochromatosis).

Contrast agents such as gadolinium (Gd) chelates shorten the T1 relaxation time within the surrounding tissue and increase the signal intensity of regions with high Gd concentration during T1-weighted imaging. In essence, Gd chelates facilitate water visualization in the intravascular (blood) or in the extravascular organ tissue space. This can be used to selectively identify areas with reduced or increased "uptake" of Gd (Figure 1B). Regional differences of Gd inflow characteristics after intravenous injection ("first-pass imaging") can be used to assess myocardial perfusion.

T1-weighted sequences with 3 to 5 slices per heartbeat have been used in the diagnostic workup for CAD with a very high negative-predictive value (52,75). Early after the first pass of Gd, a significant fraction of the injected Gd enters the interstitial space. Several minutes after intravenous administration of Gd, the larger volume of distribution available in necrotic or fibrotic myocardium results in a higher concentration of contrast agent than what is present in viable myocardium. This is typically referred to as "delayed (hyper)enhancement" or "late gadolinium enhancement" (LGE) (76). The transmural extent of myocardial scars as defined by LGE predicts functional recovery after revascularization (77) and is related to prognosis (78).

Patterns other than the endocardial accumulation of LGE can occur. For example, LV epicardial and midwall enhancement are known to be associated with infectious causes of myocardial inflammation (Figure 1C). Also, inflammatory conditions involving the heart, such as with sarcoidosis, are associated with midwall accumulation of LGE. A special mechanism may be the cause for Gd accumulation in cardiac amyloidosis. Data indicate that a molecular binding of Gd to amyloid may lead to the extensive uptake of the agent in myocardial tissue, typically associated with a very rapid washout from blood (79).

3. Important Applications

3.1. Heart Failure

CMR may be used for assessment of LV and RV size and morphology, systolic and diastolic function, and for characterizing myocardial tissue for the purpose of understanding the etiology of LV systolic or diastolic dysfunction. The writing committee recognizes the potential capabilities of spectroscopic techniques for acquiring metabolic information of the heart when evaluating individuals with heart failure.

When assessing patients with heart failure, CMR is useful in several aspects (80). Questions that may be answered by CMR include understanding of the presence and severity of morphological and functional abnormalities of the LV or RV myocardium, determining the underlying etiology (e.g., ischemic versus nonischemic disease) of LV or RV dysfunction, and identifying prognostic factors related to patient outcomes. Often, follow-up studies are required during or after therapeutic interventions. CMR offers more accurate assessment of function and morphology than most available imaging modalities, providing reliable volumetric data with high diagnostic image quality in nearly all patients. Table 2 displays quantitative and qualitative parameters, each of which can be used as diagnostic markers or descriptors in patients with suspected heart failure.

In general, cine SSFP sequences are used to visualize and quantify global left and right atrial and ventricular systolic function with reference data sets for normal subjects (16,81,86). Regional LV and RV systolic function can be

Table 1. Cardiovascular Evaluation of Structure and Function Using Cardiovascular Magnetic Resonance

Target of Evaluation	Technique	Description	Advantage	Common Clinical Indication(s)
Dimension and morphology	SE and double IR	"Dark blood"	• Vessel and myocardial wall evaluation	• LV dimensions, relationships of heart to other structures in chest • Myocardial masses, pericardial disease
	GRE/SSFP (not cine)	"Bright blood"	• Less sensitive to motion artifact than dark blood SE	• Aortic dimensions and internal lesions, including intimal flap of dissection
Function	Cine SSFP (1.5-T) or cine GRE (higher field strengths; e.g., 3.0-T) Tissue tagging	"Bright blood" cine with temporal resolution of ∼30–60 ms	• High temporal resolution • Relatively flow-independent • 2D and 3D high accuracy and reproducibility	• LV and RV volumes and ejection fraction, such as in heart failure • LV and RV regional wall motion • Valvular heart disease • With tagging, useful for quantifying LV and RV systolic and diastolic function
Metabolism	MR spectroscopy with ^{31}P	Detection of spectral peaks for ^{31}P metabolites	• High specificity	• Ischemia evaluation
Blood flow velocity	Phase-contrast imaging	Blood velocity leads to phase shift displayed on gray scale	• High accuracy • Velocity and flow quantitation • Locating and identifying intracardiac shunts or valvular lesions	• Valvular poststenotic and regurgitant flow • Large (aorta) and medium (renal, femoral, carotid) arterial flow • Pulmonary artery and vein blood flow • Qp/Qs (intracardiac shunts) • Determination of true and false lumen blood flow
Perfusion	T1-sensitive sequences, single-shot, multislice acquisitions w/GRE or GRE-EPI hybrid sequences	Contrast-based first-pass imaging for detection of hypoperfused myocardial segments	• High spatial resolution (∼2 mm in-plane) • Rapid results	• Ischemia evaluation, including detection of CAD under stress • Microvascular disease
Angiography	Noncontrast MRA (e.g., TOF, proximal compression, SSFP)	Relies on blood flow (TOF and proximal compression) or T2/T1 ratio (SSFP)	• No contrast required	• Coronary artery angiography for detection of stenosis or anomalous origin/course
	3D CE-MRA	T1 shortening with contrast-enhanced MRA image	• Fast and reliably provides "luminogram" for most vascular territories	• Bypass graft stenosis • Aortography • Carotid angiography • Renal angiography • Peripheral angiography
Tissue characterization	**Noncontrast**			
	T1-weighted spin echo	Fat has very high signal intensity	• Sensitive for increased fat content	• ARVC/D • Cardiac mass
	T2-weighted spin echo	Low signal-to-noise ratio, but very sensitive to edema	• Sensitive for increased water content	• Acute infarction • Acute myocarditis
	T2*-weighted sequences	Iron leads to T2* shortening, quantitative evaluation is required	• Sensitive for iron	• Hemochromatosis
	Contrast-based			
	T1-weighted spin echo	Early enhancement reflects hyperemia and capillary leak	• Inflammation	• Myocarditis • Acute MI
	T1-weighted/inversion recovery Late enhancement	Late enhancement reflects areas with delayed wash out of gadolinium	• Sensitive for necrosis, fibrosis, and myocardial amyloid	• MI • Myocarditis • Infiltrative disease (e.g., amyloid, sarcoid) • Hypertrophic or eosinophilic cardiomyopathy

2D indicates 2-dimensional; 3D, 3-dimensional; ARVC/D, arrhythmogenic right ventricular cardiomyopathy/dysplasia; CAD, coronary artery disease; CE-MRA, contrast-enhanced magnetic resonance angiography; GRE, gradient echo; GRE-EPI, gradient echotype planar imaging; IR, inversion recovery; LV, left ventricular; MI, myocardial infarction; MR, magnetic resonance; Qp/Qs, pulmonary to systemic flow ratio; RV, right ventricular; SE, spin echo; SSFP, steady state free precession; T, Tesla; and TOF, time-of-flight.
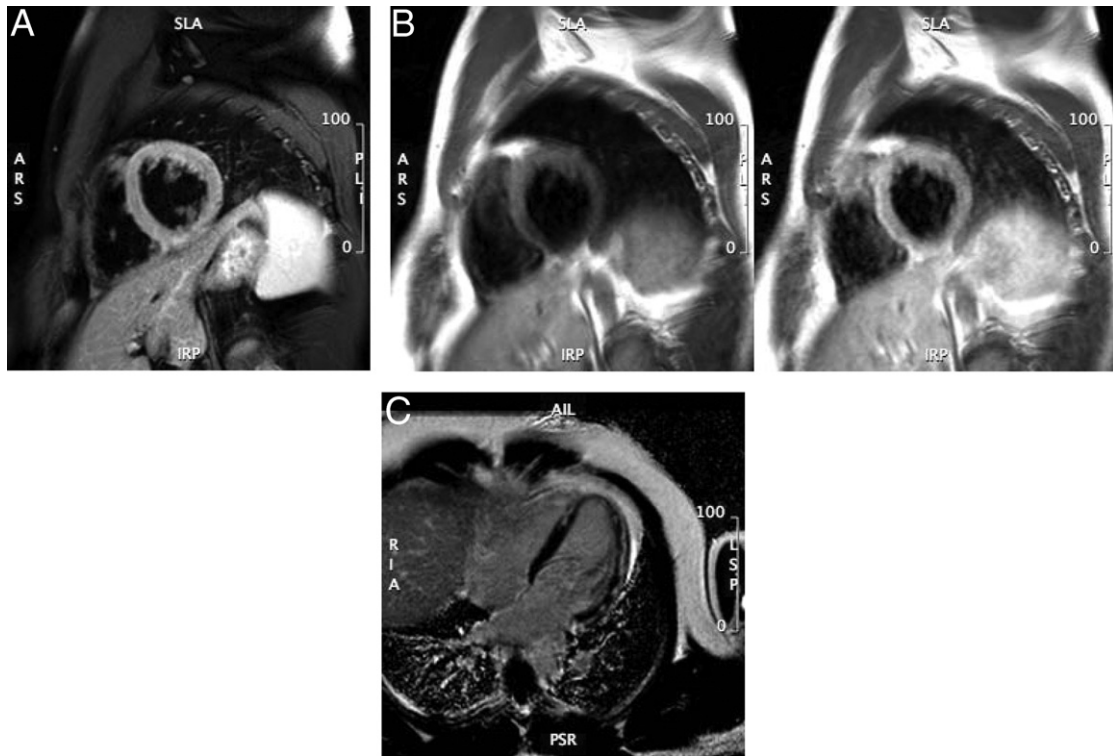
Figure 1. Cardiovascular Magnetic Resonance of Acute Myocarditis

Panel A: T2-weighted image of LV myocardial edema showing global bright signal intensity (ratio 2.2) of the left ventricle relative to the myocardium. Panel B: Early enhancement (T1-weighted spin echo) before (left) and after (right) Gd administration; enhancement ratio 5.4. Panel C: Arrows indicating late enhancement (T1-weighted gradient echo sequence with myocardial nulling) 10 minutes after Gd. Gd indicates gadolinium; and LV, left ventricular.

assessed in great detail using myocardial tagging, with circumferential strain the most widely described parameter (82,87).

Diastolic LV function has also been assessed with CMR. For this purpose, analogous echocardiographic parameters such as transmitral flow pattern or the presence of end-diastolic pulmonary vein forward flow can be utilized (83). In addition, CMR provides approaches for quantifying LV myocardial tissue velocity and strain/strain rates. Indicating

Table 2. Cardiovascular Magnetic Resonance–Derived Parameters in Patients With Suspected Heart Failure

	Parameters	Acronym	Units	Reference
Systolic function	LV and RV end-diastolic volumes and indices	LVEDV(I), RVEDV(I),	mL, mL/cm$_{height}$, mL/m^2$_{BSA}$	(16,79,81)
	LV and RV end-systolic volumes and indices	LVESV(I), RVESV(I)	mL, mL/cm$_{height}$, mL/m^2$_{BSA}$	
	LV and RV stroke volume and index	LVSV(I), RVSV(I)	mL, mL/cm$_{height}$, mL/m^2$_{BSA}$	
	LV and RV ejection fraction	LVEF, RVEF	%	
	Cardiac output and cardiac index	CO, CI	mL/min, mL/min/m^2$_{BSA}$	
	Regional and global systolic wall thickening		%	
	Regional or global measures of myocardial strain	Ecc	(%), (%)/s	
Morphology	LV mass and indices	LVM	g, g/cm$_{height}$, g/m^2$_{BSA}$	(16,79,81)
	Mean and maximum myocardial wall thickness	MWT	mm	
	Assessment of pericardium		mm	
Wall stress	End-systolic wall stress	ESWS	N/m^2 × 1000	(30)
Diastolic function	Circumferential strain and strain rate	Ecc	(%), (%)/s	(82)
	Peak untwisting rate		°/s	
	End-diastolic forward flow in pulmonary veins			
	E/A ratio	E/A, Ea		(83)
Reversible acute injury	Edema (regional or global high signal intensity in T2-weighted images)			(84)
Irreversible injury, prognosis	Myocardial fibrosis (late enhancement)		% of LV mass or myocardial segment	(85)

BSA indicates body surface area; E/A, early/atrial (late) ratio for ventricular filling; LV, left ventricular; N, Newton; and RV, right ventricular.

its usefulness, strain analysis has been used for detecting regional abnormalities in patients with LV hypertrophy despite normal systolic function and lack of clinical evidence for heart disease (33).

CMR may also provide important information regarding tissue abnormalities (see Section 2.7, Tissue Characterization). Focal fibrosis defined by LGE has provided novel insights into etiology and risk assessment of patients with LV dysfunction. Of great importance, the regional distribution of scarring allows an accurate discrimination of ischemic from nonischemic cardiomyopathies (88). In contrast to subendocardial involvement, patients with nonischemic etiologies of heart failure either do not have detectable focal scars or have a nonsubendocardial distribution that is very distinct from ischemic subendocardial and transmural patterns. Even within the group of nonischemic cardiomyopathies, the regional distribution may help to identify the underlying etiology. In hypertrophic cardiomyopathy (HCM), the LGE is typically found in hypertrophied regions and in the interventricular septum close to the RV insertion areas. In dilated cardiomyopathy, an intramural layer of septal fibrosis has been described as a typical feature and is of strong prognostic value (85,89). Typical regional patterns of LGE in various etiologies have been reviewed elsewhere (90).

In patients with acute heart failure, T2-weighted CMR may be useful to detect myocardial inflammation due to acute myocarditis (91). In cardiac iron overload, quantification of T2* relaxation times (92) have proven useful for estimating intramyocardial iron content.

Abnormal high-energy phosphate metabolism has been studied by ^{31}P-CMR spectroscopy in patients with dilated cardiomyopathy (93) and HCM (94). ^{31}P-CMR spectroscopy, however, is limited by a strong signal from water-bound protons and difficulties in spectral interpretation due to the weak ^{31}P signal. Due to these limitations, ^{31}P-CMR spectroscopy does not yet have a clinical role in the management of heart failure.

3.1.1. Potential Advantages of CMR Relative to Other Imaging Modalities

CMR measurements of biventricular function and volumes are highly reproducibile, accurate, and can be acquired with a high temporal resolution, thereby allowing precise identification of the point in time in which end-systole and end-diastole occurs. High precision and avoidance of ionizing radiation allows CMR to be used in longitudinal serial evaluations of patients with heart failure and to assess response to medical intervention or to evaluate disease progression (26,95). Furthermore, CMR has unique approaches to visualize tissue pathology, such as fibrosis, and therefore provides important diagnostic information. Importantly, CMR is highly advantageous in patients that may have body habitus limitations with other imaging techniques (i.e., acoustic window limitations or attenuation artifacts).

3.1.2. Summary of Existing Guidelines and Appropriate Use Criteria

The ACC/AHA 2005 Guideline Update for the Diagnosis and Management of Chronic Heart Failure in the Adult indicates that CMR may be useful in evaluating chamber size and ventricular mass, as well as assessing cardiac function and wall motion (96). CMR may also be used to identify myocardial viability and scar tissue in patients with heart failure. CMR of the heart or liver may be useful for confirming the presence of iron overload (96).

The ACCF/ACR/SCCT/SCMR/ASNC/NASCI/SCAI/SIR 2006 Appropriateness Criteria for Cardiac Computed Tomography and Cardiac Magnetic Resonance Imaging lists CMR evaluation of LV function as an appropriate indication in heart failure patients or those with technically limited echocardiograms (97).

3.2. Coronary Artery Disease

CMR may be useful for identifying coronary artery anomalies and aneurysms, and for determining coronary artery patency. In specialized centers, CMR may be utilized to identify patients with multivessel CAD without exposure to ionizing radiation or iodinated contrast medium.

Over the past decade, CMR has evolved into an important diagnostic modality for patients with suspected anomalous CAD and coronary artery aneurysms. In specialized academic centers of excellence, CMR has reached sufficient maturity for discrimination of patients with multivessel CAD. This may be especially helpful among patients presenting with a dilated cardiomyopathy in the absence of a clinical history of myocardial infarction.

Coronary CMR is more technically challenging than CMR of other vascular beds due to several unique issues including: the small caliber of the coronary arteries (3- to 6-mm diameter), the near constant motion of the coronary arteries (during both the respiratory and the cardiac cycles), the high level of tortuosity of the coronary arteries, and the surrounding signal from adjacent epicardial fat and myocardium (98–105). To overcome these obstacles, CMR approaches employ 1) cardiac triggering (e.g., vector electrocardiogram [ECG]) to suppress bulk cardiac motion; 2) respiratory motion suppression (e.g., breath-hold, CMR navigators); 3) prepulses to enhance contrast-to-noise ratio of the coronary arterial blood (e.g., fat saturation, T2 preparation); and 4) 3D acquisition that offers superior postprocessing capabilities. Bright blood (segmented k-space GRE and SSFP) are most commonly used without an exogenous contrast agent (e.g., Gd diethylene triamine pentaacetic acid). A special consideration in this population is intracoronary stents (see Section 4, CMR Safety), which are generally CMR compatible but demonstrate a local signal void/image distortion that is dependent on both the stent material and the CMR sequence, thereby preclud-

Table 3. CMR Identification of Anomalous Coronary Vessels

Investigators (Reference)	n	Correctly Classified Anomalous Vessels
McConnell et al. (101)	15	14 (93%)
Post et al. (102)	19	19 (100%)*
Vliegen et al. (105)	12	11 (92%)†
Taylor et al. (104)	25	24 (96%)
Bunce et al. (98)	26	26 (100%)‡

*Includes 3 patients originally misclassified by X-ray angiography. †Includes 5 patients unable to be classified by X-ray angiography. ‡Includes 11 patients unable to be classified by X-ray angiography.

ing direct evaluation of intrastent and peristent coronary integrity.

3.2.1. Anomalous Coronary Artery Identification

Although unusual (less than 1% of the general population [106]) and usually benign, congenital coronary anomalies in which the anomalous segment courses between the aorta and pulmonary artery are a well-recognized cause of myocardial ischemia and sudden cardiac death, especially among young adults (99). Catheter-based X-ray angiography has traditionally been the diagnostic imaging test to identify these anomalies, but the presence of an anomalous vessel is sometimes only suspected after the procedure, particularly in a situation where there was unsuccessful engagement or visualization of a coronary artery.

3.2.2. Potential Advantages of CMR Relative to Other Imaging Modalities

CMR has several advantages for diagnosing coronary artery anomalies. CMR does not require ionizing radiation (likely to be an important consideration among adolescents and younger adults with suspected anomalous CAD) or iodinated contrast agents. Both 2D breath-hold and targeted 3D or whole-heart free-breathing navigator coronary CMR methods have been used with similar excellent results (Table 3), (Figures 2 and 3) (98,100–105), including several instances in which the 3D aspects of coronary CMR were of marked utility relative to 2D projection techniques (Table 3). The use of coronary CMR for suspected anomalous coronary disease is also very helpful when an intramural course is suspected or present (107).

3.2.3. Coronary Artery Aneurysms

In the absence of a percutaneous intervention, the vast majority of acquired coronary aneurysms are due to mucocutaneous lymph node syndrome (Kawasaki's disease). These aneurysms are the source of both short- and long-term morbidity and mortality (108). Coronary CMR (Figure 4) studies have confirmed the high accuracy of coronary CMR for both the identification and the characterization (diameter/length) of these aneurysms (109–111). Similar data have been reported for ectatic coronary arteries and fistulas (112).
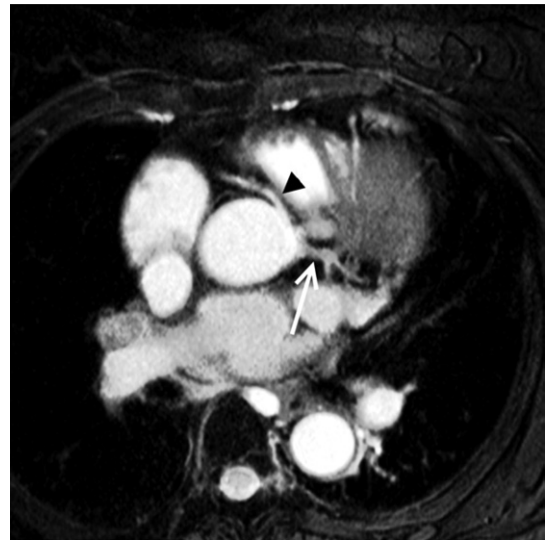
Figure 2. Cardiovascular Magnetic Resonance of a Coronary Artery Anomaly

An oblique axial reconstruction is presented from a "whole-heart coronary MRA" sequence. The white arrow notes the normally arising left main coronary artery from the left sinus of Valsalva. The black arrowhead highlights the right coronary artery arising anomalously from the anterior aspect of the left sinus of Valsalva superior to the left main origin and then coursing between the aortic root and the outflow tract of the right ventricle. MRA indicates magnetic resonance angiography.

3.2.4. Coronary CMR for Identification of Native Vessel Coronary Stenoses

Data regarding the clinical utility of coronary CMR for native vessel integrity are based on high-risk populations referred for X-ray angiography. No data are available
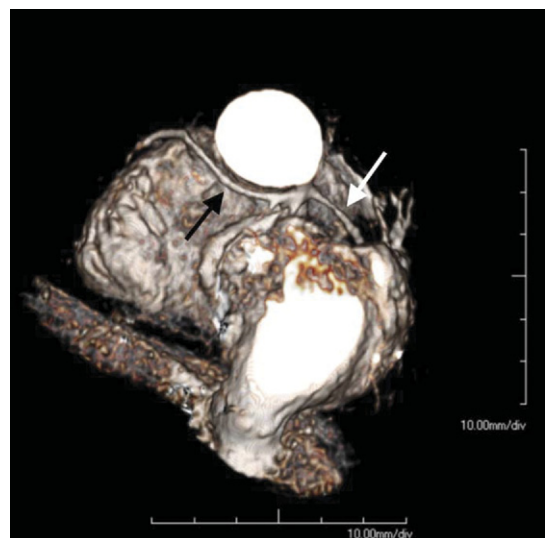
Figure 3. Cardiovascular Magnetic Resonance of a Single Coronary Artery

A 3-dimensional volume-rendered reconstruction from a "whole-heart coronary MRA" sequence in a patient with single ventricle and a single coronary artery. The white arrow denotes the proximal right coronary artery, whereas the black arrow highlights the elongated left main coronary artery arising from a common origin with the right coronary artery. MRA indicates magnetic resonance angiography.
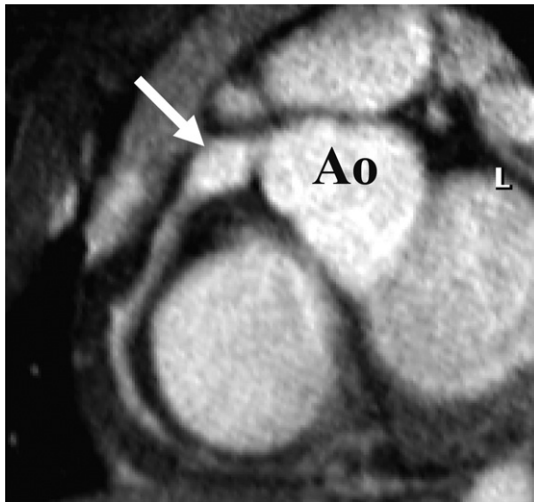
Figure 4. Cardiovascular Magnetic Resonance of a Proximal Aneurysm

Transverse targeted 3-dimensional T2 prepulse coronary MRA of a subject with a proximal right coronary artery aneurysm. Ao indicates aorta; L, left coronary artery; and MRA, magnetic resonance angiography.

regarding the use of coronary CMR for patients presenting with chest pain or for screening purposes of even high-risk patients. In addition, the majority of CMR data has been generated in a few highly specialized centers.

Using modern free-breathing, navigator-gated 3D-segmented GRE methods, good results have been shown, especially for the proximal coronary segments and in subjects with high image quality scans (Table 4) (113–123). Focal disease is depicted as local signal attenuation. An international multicenter, free-breathing, 3D volume-targeted coronary

CMR study of patients without prior X-ray angiography using common hardware and software demonstrated a very high sensitivity (100%) and modestly high specificity (85%) with very high negative-predictive value (100%) of coronary CMR for the identification of left main and multivessel CAD (greater than or equal to 50% diameter stenosis by quantitative coronary angiography) (Table 4) (118). The results were not as useful for identifying single-vessel disease. Accordingly, coronary CMR is especially valuable for patients who present with a dilated cardiomyopathy in the absence of clinical infarction. Data suggest it is useful and can supplement LGE methods for determining the underlying etiology (ischemic versus nonischemic) of the cardiomyopathy (124).

Increasing data are now available on whole-heart SSFP coronary CMR methods. Although the technique utilizes an inferior in-plane spatial resolution, data appear to be at least as accurate as free-breathing methods (Table 4) (117,121,122). This type of data may be useful in heavily calcified lesions (107). Coronary MRA may also be useful for assessing heavily calcified arteries on computed tomography where blooming artifact may obscure the vessel lumen (125).

3.2.5. Coronary CMR for Coronary Artery Bypass Graft Assessment

In comparison with the native coronary arteries, reverse saphenous vein and internal mammary artery grafts are relatively easy to image due to their minimal motion during the cardiac and respiratory cycles and the larger lumen of reverse saphenous vein grafts. With schematic knowledge of the origin and touchdown site of each graft, a variety of CMR sequences have been used to identify graft patency (126–131).

Table 4. Free-Breathing 3D Gradient Echo Coronary CMR Using Prospective Navigators for Identification of Focal ≥50% Diameter Coronary Stenoses

Investigators (Reference)	n	Technique	For ≥50% Diameter Stenosis	
			Sensitivity (%)	Specificity (%)
Prospective navigators with real-time correction-targeted 3D				
Bunce et al. (98)*	34		88	72
Sommer et al. (123)†	112		74	63
			88 (good quality)	91 (good quality)
Bogaert et al. (113)	19		85–92	50–83
Dewey et al. (115)	15‡	SSFP	86	98
Maintz et al. (119)		TFE	92	67
		SSFP	81	82
Ozgun et al. (120)	20	SSFP	82	82
Jahnke et al. (116)	21	SSFP	79	91
Prospective navigators with real-time correction whole-heart SSFP				
Sakuma et al. (121)	101		82	91
Jahnke et al. (117)	55		78	91
Sakuma et al. (122)	106		82	90
Kim et al. (118)	109		93 (patient)	59 (patient)
			100 (LM/3VD)	85 (LM/3VD)

3D indicates 3-dimensional; CMR, cardiovascular magnetic resonance; LM/3VD, left main coronary artery or 3-vessel disease; SSFP, steady-state free precession; and TFE, turbo fast-echo.
*Excludes 5 patients for "lack of cooperation" and 15 segments for being uninterpretable. †Based on 74% of coronary artery segments analyzable by CMR. ‡Based on 60% of patients with good free breathing CMR images.

Limitations of coronary CMR bypass graft assessment include difficulties related to local signal loss/artifact due to implanted metallic objects (hemostatic clips, ostial stainless steel graft markers, sternal wires, coexistent prosthetic valves and supporting struts or rings, and graft stents). Imaging strategies used to image coronary arteries have also been applied to saphenous vein grafts (132) and reported to be quite accurate for assessment of saphenous vein graft stenoses, with very good agreement between quantitative X-ray angiography for assessment of both graft occlusion (sensitivity 83% [36% to 100%]; specificity 100% [92% to 100%]) and graft stenosis (greater than or equal to 50%; sensitivity 82% [57% to 96%]; specificity 88% [72% to 97%]) (133). Saphenous vein and internal mammary artery bypass graft CMR can also be combined with rest and adenosine stress graft flow assessment using phase velocity CMR techniques (133) and suggest superior results.

3.2.6. Potential Advantages of CMR Relative to Other Imaging Modalities

In addition to coronary artery anomalies, CMR is highly advantageous for identifying aneurysms or fistula without the use of contrast materials or exposing patients to ionizing radiation. These particular advantages are well suited for assessing both children and relatively young women that experience an increased risk of adverse events associated with exposure to ionizing radiation. At expert centers, early data suggest CMR may have a role in identifying coronary arterial stenoses in arterial bypass grafts, as well as excluding the presence of left main or 3-vessel coronary arterial disease.

3.2.7. Summary of Existing Guidelines and Appropriate Use Criteria

The ACC/AHA 2002 Guideline Update for the Management of Patients With Chronic Stable Angina indicates that coronary CMR is a suitable method to identify anomalous origins of coronary arteries. It may be particularly useful in younger individuals with signs or symptoms of myocardial ischemia for the purpose of identifying coronary artery anomalies and in individuals with the presence of a continuous murmur for identifying an anomalous origin of the left anterior descending or circumflex artery from the pulmonary artery or coronary arterial venous fistulas (134).

Similarly, the ACCF/ACR/SCCT/SCMR/ASNC/NASCI/SCAI/SIR 2006 Appropriateness Criteria for Cardiac Computed Tomography and Cardiac Magnetic Resonance Imaging indicates that it is appropriate to use CMR to evaluate patients suspected of exhibiting coronary anomalies (97).

3.3. Ischemic Heart Disease

The combination of CMR stress perfusion, function, and LGE allows the use of CMR as a primary form of testing for: 1) identifying patients with ischemic heart disease when there are resting ECG abnormalities or an inability to exercise; 2) defining patients with large vessel CAD and its distribution who are candidates for interventional procedures; or 3) determining patients who are appropriate candidates for interventional procedures. Assessment of LV wall motion after low-dose dobutamine in patients with resting akinetic LV wall segments is useful for identifying patients that will develop improvement in LV systolic function after coronary arterial revascularization. The writing committee recognizes the potential advantages of spectroscopic techniques for identifying early evidence of myocardial ischemia that may or may not be evident using existing non-CMR methods.

CMR is well suited to detect many of the physiologic consequences of ischemia through the assessment of myocardial abnormalities of perfusion, diastolic and systolic performance, and metabolism.

3.3.1. Myocardial Perfusion Imaging

CMR perfusion imaging is performed using a T1-weighted sequence to visualize first passage of a Gd-based contrast agent in transit through the heart. Following peripheral injection, the contrast is detected against the background of nulled (dark) myocardium with rapid enhancement during vasodilation stress. Signal intensity correlates with contrast concentration and analysis can be performed in a quantitative, semiquantitative, or qualitative fashion. Qualitatively, an experienced observer examines the myocardium for regions of low signal or hypoperfusion relative to normally perfused segments (Figure 5). Because the contrast agents rapidly redistribute into the extracellular space, quantitative analysis is limited to the initial upslope in the tissue intensity curve, which has been shown to correlate well with measures of microsphere blood flow (135).

Validation of CMR perfusion in humans has been performed in a number of clinical studies employing a variety of contrast agents, analysis techniques, and reference standards (136) (Table 5). One study examined signal-intensity time curves in both patients and controls following dipyridamole infusion and bolus injection of a Gd chelate (55). Using a linear fit to determine the upslope, a threshold value was defined to distinguish between normal and ischemic myocardium. Diagnostic accuracy was 87% with a high level of interobserver agreement. CMR perfusion, ^{13}N-ammonia positron emission tomography, and quantitative coronary angiography were compared in a study using calculation of regional signal intensity upslopes (67). Analysis of the subendocardial upslope data showed a sensitivity and specificity of 91% and 94%, respectively, when compared to ^{13}N-ammonia positron emission tomography and greater than 85% when compared to quantitative angiography. A study combining qualitative analysis of CMR perfusion images with LGE identification of myocardial infarction yielded a sensitivity of 89%, specificity of 87%, and overall accuracy of 88% compared to X-ray angiography (142). A meta-analysis of all CMR perfusion studies demonstrated a sensitivity of 91% and specificity of 81% for the diagnosis of
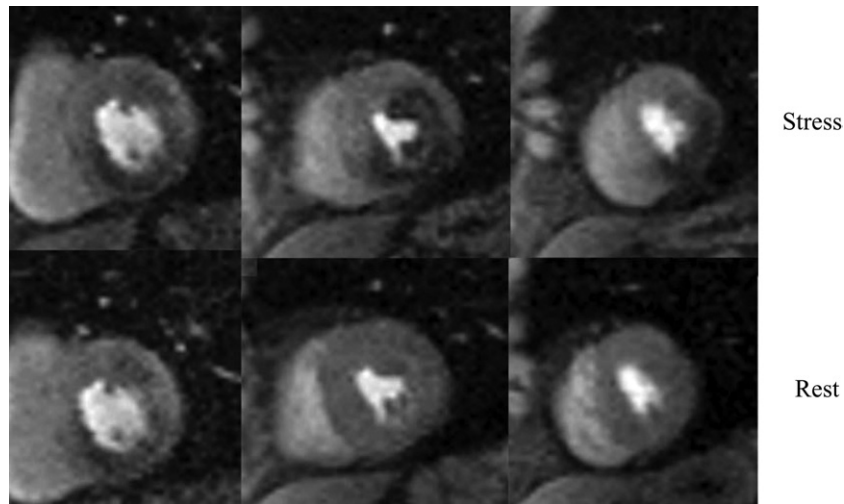
Figure 5. Myocardial Perfusion Imaging

First-pass contrast-enhanced perfusion images from a 73-year-old diabetic man using a hybrid gradient echo–echo planar pulse sequence with parallel imaging during infusion of 0.075 mM/kg of gadolinium chelate at 4 cc/s. The top panel of short-axis images was obtained during adenosine stress, a 4-minute infusion at 0.14 mg/kg, and the bottom panel obtained in the same short-axis slices 10 minutes later at rest. The base of the left ventricle on the left demonstrates an inferior wall perfusion abnormality seen at both stress and rest, consistent with myocardial infarction. The mid left ventricle demonstrates a large perfusion defect only at stress in the anterolateral and inferior walls. The apical left ventricle shows an inferolateral perfusion defect at stress but is normal at rest. cc indicates cubic centimeter; and mM, millimolar.

CAD on a per-patient level (146). A multicenter study comparing CMR perfusion to SPECT suggests a higher specificity of CMR perfusion but similar overall accuracy (65). Clinically, it is important to note that to accomplish results associated with these multicenter results, appropriate physician and staff training is required, and a facility capable of performing the stress testing is required.

3.3.2. Stress Imaging of Ventricular Function

Dobutamine is commonly administered to evaluate stress-function CMR with a qualitative evaluation of wall motion as the dose of dobutamine is increased, an application similar to DS echocardiography. CMR safety and efficacy have been assessed extensively. CMR exhibits major complications (i.e., the development of sustained ventricular tachycardia) in less than 0.1% of subjects, findings that are similar to those observed with DS echocardiography (147).

Studies have shown breath-hold GRE DS CMR to have a high accuracy for detecting ischemia, related in part to excellent LV endocardial visualization throughout dobutamine/atropine stress protocols (148). DS CMR appears to be particularly valuable for patients who are poor candidates for DS echocardiography (149). A list of DS cine CMR studies is shown in Table 6. A meta-analysis of stress-functional CMR studies demonstrated a sensitivity of 83% and specificity of 86% for the demonstration of CAD on a per-patient level (146).

Table 5. Sensitivity and Specificity of Recent CMR Perfusion Studies on a Per-Patient Basis for Detecting Coronary Arterial Luminal Narrowings ≥50%

Investigators (Reference)	n	Stress Agent	Sensitivity (%)	Specificity (%)
Cury et al. (137)	46	Dipyridamole	97	75
Doyle et al. (138)	184	Dipyridamole	57	78
Giang et al. (139)	44	Adenosine	93	75
Ishida et al. (140)	104	Dipyridamole/isometric handgrip exercise	90	85
Kawase et al. (141)	50	Nicorandil	94	94
Klem et al. (142)	92	Adenosine	89	87
Nagel et al. (55)	84	Adenosine	88	90
Pilz et al. (143)	171	Adenosine	96	83
Plein et al. (144)	68	Adenosine	96	83
Plein et al. (144)	82	Adenosine	88	74
Sakuma et al. (66)	40	Dipyridamole	81	68
Schwitter et al. (67)	47	Dipyridamole	86	70
Takase et al. (145)	102	Dipyridamole	93	85

CMR indicates cardiovascular magnetic resonance.
Modified from Nandalur et al. (146).

Table 6. Sensitivity and Specificity of Recent CMR Wall Imaging Studies on a Per-Patient Basis in Detecting Coronary Arterial Luminal Narrowings ≥50%

Investigators (Reference)	n	Stress Agent	Sensitivity (%)	Specificity (%)
Baer et al. (150)	23	Dipyridamole	78	NA
Baer et al. (151)*	32	Dobutamine	84	NA
Hundley et al. (149)	41	Dobutamine and atropine	83	83
Jahnke et al. (152)	40	Dobutamine	89	75
Nagel et al. (148)	172	Dobutamine	86	86
Paetsch et al. (153)	79	Adenosine	91	62
Paetsch et al. (153)	79	Dobutamine and atropine	89	81
Paetsch et al. (154)	150	Dobutamine	78	88
Pennell et al. (155)	40	Dipyridamole	62	100
Pennell et al. (156)	25	Dobutamine	91	100
Rerkpattanapipat et al. (157)	27	Exercise	79	85
Schalla et al. (158)	22	Dobutamine	81	83
van Rugge et al. (159)	45	Dobutamine	81	100
van Rugge et al. (160)	39	Dobutamine	91	0.83

CMR indicates cardiovascular magnetic resonance; and NA, not available.

*Utilized 2 perfusion territories (left anterior descending coronary artery and combined left circumflex artery/right coronary artery. Modified from Nandalur et al. (146).

CMR tagging may further improve the accuracy of DS CMR for detecting ischemia (161). In addition, in patients with resting LV wall motion abnormalities, low-dose dobutamine CMR is useful for identifying contractile reserve indicative of potential for recovering systolic thickening after coronary arterial revascularization (162). In summary, DS CMR is useful for identifying inducible myocardial ischemia and identifying contractile reserve of LV wall motion after coronary artery revascularization.

3.3.3. Stress Perfusion and Functional Imaging for Prognosis Assessment

Prognostic data are now available using both vasodilator and DS CMR methods (52). Three-year event-free survival has been reported at 99.2% for patients with normal stress perfusion CMR or DS CMR and 83.5% for those with abnormal stress perfusion or DS CMR. Ischemia suggested by stress perfusion CMR or DS CMR is predictive of cardiac events over the 3-year period with hazard ratios of 12.5 and 5.4, respectively, compared with those without evidence of myocardial ischemia. In summary, abnormalities observed during stress CMR serve as independent predictors of adverse cardiac events.

3.3.4. Magnetic Resonance Spectroscopy

Spectroscopy provides the CMR basis for the assessment of myocardial metabolism without the need for contrast agents or radionuclides (93,163,164). Hydrogen spectroscopy may be useful for assessing myocardial cellular triglyceride levels. Phosphorus spectroscopy has been used to measure myocardial energetics. In an early clinical application of Neubauer and his colleagues, 39 patients with dilated cardiomyopathy underwent ^{31}P myocardial spectroscopy and were followed up at approximately 30

months (93). Kaplan-Meier analysis showed significantly reduced total and cardiovascular mortality for patients with greater than 1.6 versus patients with low or less than 1.6 PCr/ATP; a Cox model for multivariate analysis showed that the PCr-to-ATP ratio offered significant independent prognostic information on cardiovascular mortality. In patients with left anterior descending CAD, Weiss et al. (164) used spatially localized ^{31}P magnetic-resonance spectra from the anterior myocardium before, during, and after isometric hand-grip stress. In patients with significant LAD or left main CAD (n=16), the ratio decreased from 1.45 ± 0.31 at rest to 0.91 ± 0.24 during stress (p<0.001) and recovered to 1.27 ± 0.38 2 minutes after exercise.

In a more recent study, handgrip stress was used in association with ^{31}P spectroscopy in women with cardiac symptoms, but without significant angiographic CAD. Of 35 women studied, 20% demonstrated an abnormal reduction in PCr/ATP with stress (163). In a follow-up study, the women with an abnormal PCr/ATP had a significantly greater incidence of recurrent symptoms and rehospitalizations compared with patients with a normal PCr/ATP response to exercise (165).

3.3.5. Potential Advantages of CMR Relative to Other Imaging Modalities

CMR provides high spatial and temporal resolution images of myocardial perfusion, myocardial function, and identification of infarcts using LGE techniques. This unique combination offers the ability to reliably identify subendocardial ischemic processes. There is future promise of potentially incorporating spectroscopic techniques that may provide informative information regarding myocardial metabolism.
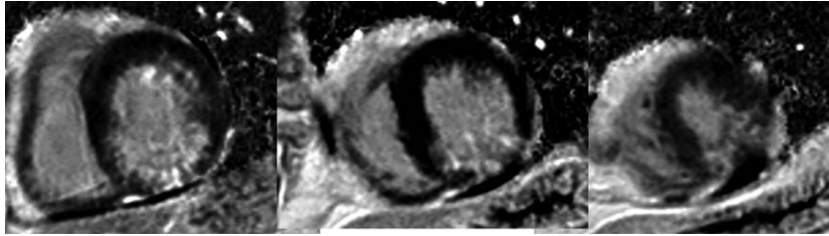
Figure 6. Infarct Imaging

Images from the same patient as in Figure 5. The panel of images demonstrates phase-sensitive inversion recovery gradient echo images in the same 3 short-axis locations obtained 10 minutes after 0.15 mM/kg of gadolinium was infused intravenously. The basal left ventricle shows a 50% transmural inferior infarction while the mid and apical left ventricle show a 25% to 50% transmural inferior infarction. Putting this data together with Figure 5, the findings are consistent with an inferior infarction with peri-infarct ischemia in the mid and apical inferior walls as well as mid anterolateral ischemia, consistent with multivessel coronary artery disease. mM indicates millimolar.

3.3.6. Summary of Existing Guidelines and Appropriate Use Criteria

The ACC/AHA 2002 Guideline Update for the Management of Patients With Chronic Stable Angina indicates that CMR may be used to assess LV performance including ejection fraction (134). In the ACC/AHA Guidelines for the Management of Patients With ST-Elevation Myocardial Infarction, CMR is recommended for differentiating ST-segment elevation myocardial infarction from aortic dissection in patients for whom this distinction is initially unclear (Class I, *Level of Evidence: B*) (166). Within the ACC/AHA/ESC 2006 Guidelines for Management of Patients With Ventricular Arrhythmias and the Prevention of Sudden Cardiac Death, CMR is probably indicated in patients with ventricular arrhythmias when echocardiography does not provide accurate assessment of LV and RV function and/or evaluation of structural changes (Class IIa, *Level of Evidence: B*) (167).

The ACCF/ACR/SCCT/SCMR/ASNC/NASCI/ SCAI/SIR 2006 Appropriateness Criteria for Cardiac Computed Tomography and Cardiac Magnetic Resonance Imaging indicates that the use of CMR stress testing (vasodilator or dobutamine) is appropriate in individuals with intermediate pretest probability of CAD or those with an uninterpretable ECG or those who are unable to exercise. CMR is also appropriate to determine viability prior to revascularization and establish the likelihood of recovery of systolic function with mechanical revascularization. CMR is appropriate to assess myocardial viability when determinations from other forms of noninvasive testing are equivocal or exhibit indeterminate results. The use of CMR stress testing is appropriate for identifying cardiac risk in patients with prior coronary angiography or stenoses of unclear significance (97).

At present, ACCF/ACR/SCCT/SCMR/ASNC/NASCI/ SCAI/SIR 2006 Appropriateness Criteria for Cardiac Computed Tomography and Cardiac Magnetic Resonance Imaging is uncertain of the utility of CMR stress testing procedures in individuals with: 1) an interpretable ECG and better ability to exercise; 2) a high pretest probability of coronary disease; 3) acute chest pain with an intermediate pretest probability of coronary disease; 4) no ECG changes, with serial cardiac enzymes remaining negative; 5) a prior equivocal stress test from another modality; 6) intermediate CAD risk profile using Framingham criteria; 7) intermediate preperioperative cardiovascular risk; or 8) post percutaneous intervention myocardial necrosis (97).

3.4. Myocardial Infarction/Scar

LGE-CMR can be used for identifying the extent and location of myocardial necrosis in individuals suspected of having or possessing chronic or acute ischemic heart disease.

3.4.1. Infarct Imaging

The spatial extent of LGE closely mirrors the distribution of myocyte necrosis in the early period following infarction and that of collagenous scar seen at 8 weeks (168), whereas in regions of the heart subjected to reversible injury, the retention of contrast does not occur (76). LGE accurately delineates infarction as defined by histology at various time points following injury (169) (Figure 6). When compared with SPECT, LGE is more reliable in detecting subendocardial infarct scar (68,170). LGE also improves the detection of RV infarction (171).

Transmural extent of infarct scar, as determined on LGE, is inversely related to the functional recovery of LV wall motion following acute infarction. Previous studies have noted an inverse relationship between transmural extent of LGE and segmental recovery of function (172). The best predictor of improved wall thickening and global function was the extent of dysfunctional myocardium that had either no LGE or less than 25% transmurality of LGE.

Investigators have exploited the enhanced sensitivity of LGE to study small infarctions after percutaneous intervention (173,174), demonstrating enzyme leak and discrete areas of LGE in the target vessel territory. LGE persists at follow-up scans 3 to 12 months after initial procedures. Similar studies have been performed in patients undergoing coronary artery bypass surgery (175).

Evidence suggests that the presence of any LGE may be a valuable tool for predicting major adverse cardiac events and cardiac mortality. In a study of patients evaluated for ischemic heart disease for various reasons, the presence of

any LGE was found to be the strongest predictor of major or adverse cardiac events, independent of LV ejection fraction and other conventional clinical markers (78). A study of randomly chosen patients greater than 70 years old showed that more than 24% had evidence of LGE, over three fourths of which were unrecognized myocardial infarction (176). Thus, the finding of LGE is likely to become an important marker of silent infarction and prognosis.

Border zones of infarcts may have prognostic utility in patients sustaining prior infarction. These regions experience LGE at a level above the intensity of normal background intensity, but below the 2 standard deviations in intensity above background normal tissue that is used to identify infarcts. This "intermediate" intensity is due in part to a mixture of healthy and diseased myocytes and, in small studies, had been found associated with future incidences of ventricular arrhythmias (34,177). Investigators have also established the clinical importance of microvascular obstruction (MO) regions, sometimes referred to as no-reflow zones (178). Acutely, tissue edema, hemorrhage, and inflammation can increase infarct volume by as much as 25% (179). Beyond these necrotic regions, dysfunctional, nonnecrotic tissue coexists, which has the potential for functional recovery (180). Thus, a region of systolic dysfunction following myocardial infarction will generally consist of a combination of reversibly injured (stunned) and irreversibly injured (infarcted) myocardium, with the severity of dysfunction a poor marker for the transmural extent of necrosis (181). With the development of LGE, these tissue states can be distinguished within the same segment of myocardium (Figure 7). Studies have demonstrated that regions with MO are nonviable with no recovery of function at 7 to 8 weeks post-myocardial infarction in these territories (182,183). MO, defined as hypoenhancement at 1 to 2 minutes after Gd injection, is also a prognostic marker of postinfarction complications even after controlling for absolute infarct size (62). Furthermore, MO is a better predictor of major adverse cardiac events than LGE-defined infarct size (62).

3.4.2. LV Remodeling After Acute Myocardial Infarction

The technique of LGE has enabled investigators to simultaneously chronicle changes in infarct scar and LV function and geometry following acute myocardial infarction. LGE infarct size and transmurality appear to slightly decline over the first 1 to 2 months from acute myocardial infarction, with involution of LGE contours (184), observed to a greater degree among patients with MO. Apoptosis and cellular loss likely play a role in this infarct involution (178).

3.4.3. Potential Advantages of CMR Relative to Other Imaging Modalities

Due to high spatial resolution and few limitations imposed by body habitus, CMR provides a noninvasive mechanism to reliably identify subendocardial or transmural infarctions.
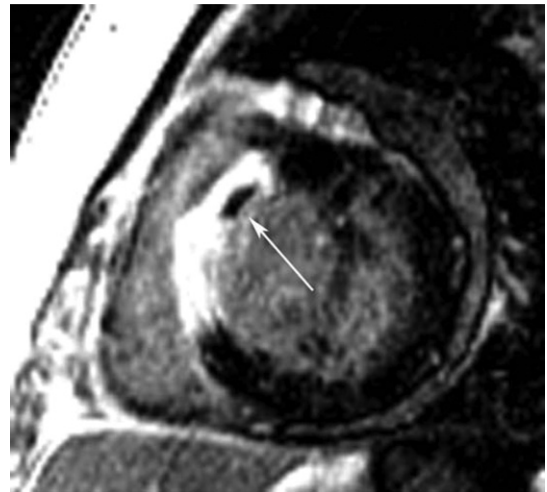
Figure 7. Microvascular Obstruction of a Patient After Anteroseptal Myocardial Infarction

This figure is a short-axis late gadolinium-enhanced inversion recovery gradient echo axis image obtained 10 minutes after gadolinium infusion in a patient on Day 3 after reperfused anteroseptal myocardial infarction. Note the transmural late gadolinium enhancement in the anteroseptum. The arrow points to a region of microvascular obstruction in the core of the infarction that represents a region of capillary damage to the extent that contrast is unable to fill this region even 10 minutes after contrast. MO is generally only seen in the first 7 to 10 days post-myocardial infarction and signifies an infarction and patient with poorer prognosis than those without MO. MO indicates microvascular obstruction.

Regions of microvascular obstruction can be identified within infarcts. This imaging may be combined with other structural or functional heart assessments to provide a comprehensive cardiac assessment of patients sustaining myocardial injury.

3.4.4. Summary of Existing Guidelines and Appropriate Use Criteria

The ACC/AHA 2005 Guideline Update for the Diagnosis and Management of Chronic Heart Failure in the Adult indicates the use of LGE to identify myocardial viability in scar tissue (96).

The ACCF/ACR/SCCT/SCMR/ASNC/NASCI/SCAI/SIR 2006 Appropriateness Criteria for Cardiac Computed Tomography and Cardiac Magnetic Resonance Imaging indicates the appropriate use of LGE for determining the location and extent of myocardial necrosis including no-reflow regions, assessments of patients post acute myocardial infarction, assessing viability prior to revascularization, establishing the likelihood of recovery of function with coronary artery revascularization, and to determine viability prior to revascularization, and assessing viability when low-dose dobutamine echocardiography has provided indeterminate results (97).

3.5. Nonischemic Cardiomyopathy/Myocarditis

CMR may be used for assessment of patients with LV dysfunction or hypertrophy, or suspected forms of cardiac injury not related to ischemic heart disease. When the diagnosis is unclear, CMR may be considered to

identify the etiology of cardiac dysfunction in patients presenting with heart failure including: 1) evaluation of dilated cardiomyopathy in the setting of normal coronary arteries; 2) patients with positive cardiac enzymes without obstructive atherosclerosis on angiography; 3) patients suspected of amyloidosis or other infiltrative diseases; 4) HCM; 5) arrhythmogenic RV dysplasia; or 6) syncope or ventricular arrhythmia.

Nonischemic cardiomyopathies include genetic forms (HCM, arrhythmogenic right ventricular cardiomyopathy [ARVC], LV noncompaction, and others), mixed forms (dilated cardiomyopathies [DCM], and restrictive cardiomyopathies), and acquired forms (myocarditis, stress-induced cardiomyopathy, peripartum cardiomyopathy, and others). Knowledge of the etiology of a cardiomyopathy is important for diagnosis, therapy, and prognosis. CMR provides a noninvasive measure to provide this knowledge through determination of cardiac chamber size and structure, LV and RV regional and global function, perfusion, metabolism, and tissue composition.

3.5.1. Hypertrophic Cardiomyopathy

Inappropriate myocardial hypertrophy, loss of diastolic function, development of intramyocardial fibrosis, and possible dynamic systolic obstruction of the LV outflow tract are hallmarks of HCM. CMR accurately quantifies myocardial mass and regional wall thickness in all myocardial segments. In obstructive HCM, systolic anterior movement of the anterior mitral valve apparatus and a turbulent jet can be identified on long-axis cine bright blood imaging studies. The area of the obstructed LV outflow tract can be quantified for diagnosis and directing therapy longitudinally over time (185). Specific patterns of focal or regional LGE have been reported in HCM (186) and found to be associated with regional hypertrophy, decreased systolic thickening, and perfusion deficits (187). These patterns can be scattered throughout the hypertrophied myocardium and are dissimilar to the endocardial based patterns of LGE seen after myocardial infarction. Preliminary data suggest a prognostic relevance of LGE in patients with HCM (89,186). CMR is also very sensitive for detecting HCM in the first-degree relatives of those with clinical HCM (188). During treatment, CMR can readily identify the effects of alcohol septal ablation (25). LGE in hypertrophied muscle has been shown to be associated with increased fibrosis within the LV myocardium.

3.5.2. Arrhythmogenic Right Ventricular Cardiomyopathy

Characteristics of ARVC include global or regional dilatation and dysfunction of the RV (and in some cases, the LV) myocardium. Furthermore, fatty and/or fibrous replacement may be found. Morphological and functional targets for CMR include regional or global wall motion abnormalities, aneurysms, and segmental or global dilation, as well as global hypokinesis, with quantitative analysis of RV volume and function (189,190). The role of CMR in ARVC has been
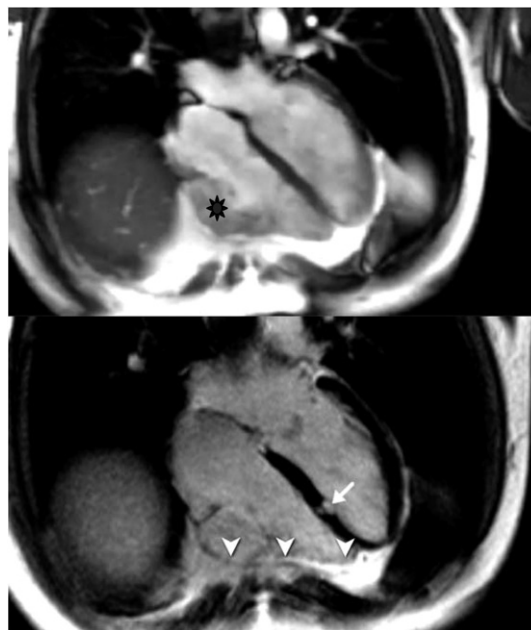
Figure 8. Late Gadolinium Enhancement in ARVC in a Patient With Family History of ARVC

Upper panel: irregular silhouette of the free RV wall with microaneurysm. Lower panel: evidence for LGE of the RV wall (arrowheads), but also focal fibrosis of the interventricular septum (arrow). ARVC indicates arrhythmogenic right ventricular cardiomyopathy; LGE, late gadolinium enhancement; and RV, right ventricular.

recently reviewed (191). In contrast to earlier reports, the identification of myocardial fat is not the only structural wall abnormality associated with ARVC (192) and may be less specific for the disease (192). LGE of RV fibrosis has been reported as a useful marker (Figure 8) (193). Combined protocols involving determination of wall motion and RV tissue characteristics may provide an excellent diagnostic accuracy, as shown in patients with genetically defined disease (194). Recent studies in gene carriers have also emphasized the important role of LV involvement in ARVC (195).

3.5.3. Noncompaction Cardiomyopathy

Noncompaction cardiomyopathy is described as a cardiomyopathy that occurs due to an autosomally dominant inherited trait in which the middle and apical segments exhibit a thin compact wall with regional dilatation, dysfunction, and significant hypertrabeculation (Figure 9). An end-diastolic ratio of noncompacted to compacted LV myocardium of greater than or equal to 2.3 defines the condition (196). Also, LV wall motion abnormalities, global dysfunction, or coronary intraventricular thrombi are often present in the disorder. Refined diagnostic criteria may be forthcoming as this disorder becomes recognized with greater frequency.

3.5.4. Dilated Cardiomyopathy

Diagnostic targets for CMR in DCM include progressive LV dilation, LV systolic dysfunction, and regional midwall myocardial fibrosis (88). Recently, focal septal fibrosis in DCM, the so-called "midwall sign," has been linked to
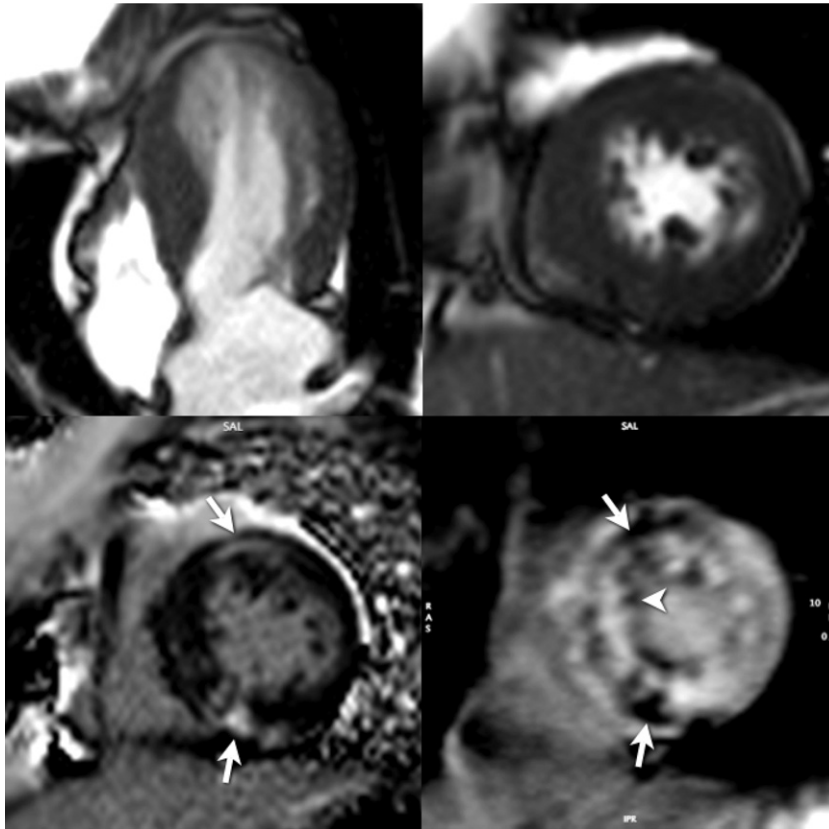
Figure 9. Late Gadolinium Enhancement in Left Ventricular Noncompaction

Upper panels: systolic long-axis (left) and short-axis (right) still frames. Lower panels: left: short-axis late Gd enhancement image showing several areas of fibrosis. Right: late Gd enhancement study using a short inversion time (fibrosis appears with low SI). Confirmation of lesions in the myocardium (arrows) and in the trabecular tissue (arrowhead) are shown. Gd indicates gadolinium; LGE, late gadolinium enhancement; and SI, signal intensities.

ventricular arrhythmia (197). The presence of fibrosis identified with LGE has been found to be associated with adverse cardiac events (85).

3.5.5. Acute Viral Myocarditis

Quantification of global myocardial signal intensity changes on T2-weighted CMR reflecting inflammation and especially edema offers a high diagnostic accuracy to detect acute myocarditis (198). Reflecting irreversible injury, a typical pattern of regional, typically subepicardial fibrosis, can be visualized (90) (Figure 10). With combined analysis of T1- and T2-weighted scans, heightened diagnostic accuracy for identifying active myocarditis is achieved (198,199). CMR is considered one of the most important diagnostic tools in the workup of patients with myocarditis (91,200). An expert consensus document on the application, evaluation, and reporting of CMR in myocarditis has been developed (201).

3.5.6. Sarcoidosis

Up to 50% of patients with pulmonary sarcoidosis have cardiac involvement, although only 5% have cardiac symptoms. Myocardial involvement, however, is the leading cause of death in these patients. CMR can visualize myo-

cardial inflammation using contrast-enhanced techniques. Early contrast enhancement identifies territories exhibiting myocardial inflammation, whereas LGE shows areas of irreversible injury (Figure 11) (202).

3.5.7. Amyloidosis

Myocardial amyloid infiltration is frequent among patients with systemic amyloidosis and leads to apparent myocardial hypertrophy with impaired ventricular function. Because of abnormally short T1 and T2 relaxation times and a significant accumulation of Gd within affected tissue (79), the diagnosis of cardiac amyloidosis can be established with a high accuracy. It is important to note that in amyloidosis, Gd is cleared much faster from the blood than in other patients. Blood will therefore appear with a low signal in contrast-enhanced T1-weighted images (Figure 12).

3.5.8. Hemochromatosis

Cardiac iron overload in diseases such as thalassemia may lead to dilatation, hypertrophy, and dysfunction. The introduction of myocardial T2* quantification offers a reliable parameter for monitoring patients undergoing chelation therapy (203). T2* correlates well with LV systolic function,
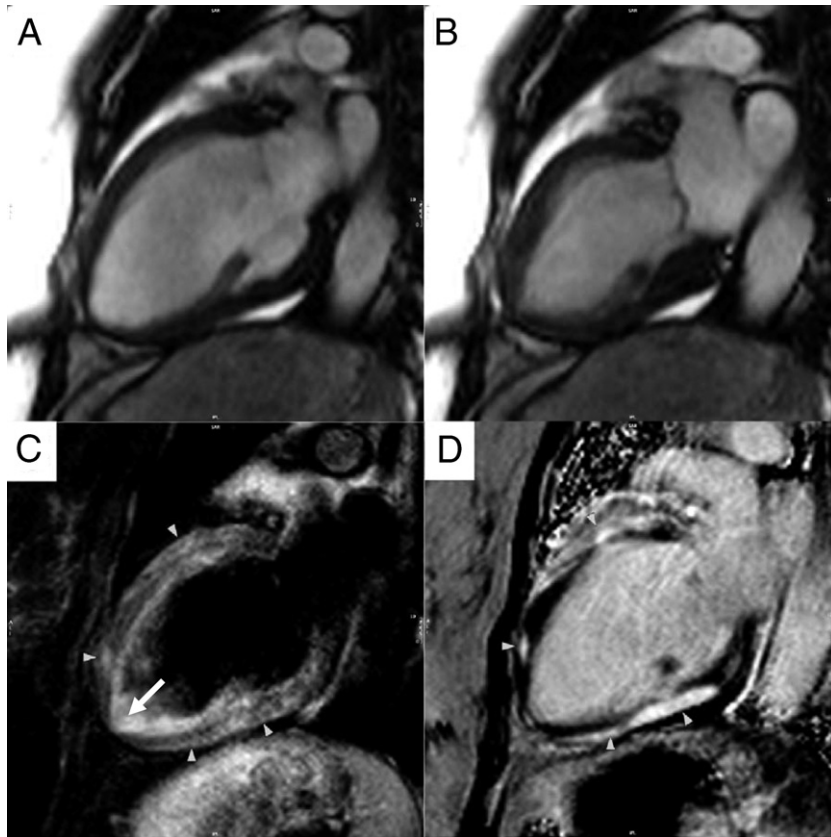
Figure 10. Cardiovascular Magnetic Resonance Tissue Characterization in a Patient With Acute Myocarditis

Images obtained by different sequences in the same 2-chamber view are shown. Panels A (diastolic) and B (systolic) indicate a basal-anterior and apical-inferior wall motion abnormality. Panel C shows increased signal intensity in a T2-weighted image, indicating edema as a feature of acute injury (arrowheads). Note the increased signal of the apical blood due to slow blood flow (thin arrow). Panel D visualizes a delayed gadolinium washout indicating irreversible injury (arrowheads).

but not with liver iron content or serum ferritin. Since prognosis is mainly determined by cardiac involvement, T2* quantification within the LV myocardium has been shown to be a more efficacious marker of cardiac iron involvement and guidance of chelation therapy than serial liver biopsies (203,204).

3.5.9. Potential Advantages of CMR Relative to Other Imaging Modalities

CMR can be used to provide excellent serial assessment of LV and RV function and volumes. In addition, it can reliably visualize the cardiac apex (95). This is important in
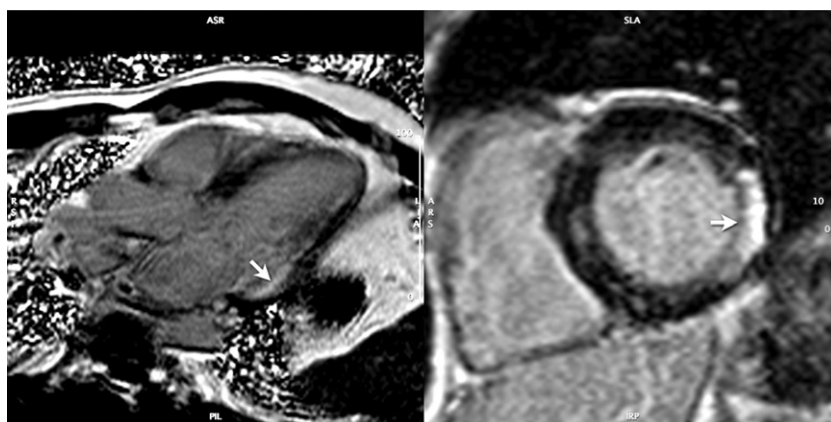
Figure 11. Late Gadolinium Enhancement in Arrhythmogenic Right Ventricular Cardiomyopathy in a Patient With Cardiac Sarcoidosis

Left panel: long-axis view of a late gadolinium enhancement study showing a transmural lesion in the basal lateral wall (arrow). Right panel: cross-referenced short-axis view with the same lesion (arrow).
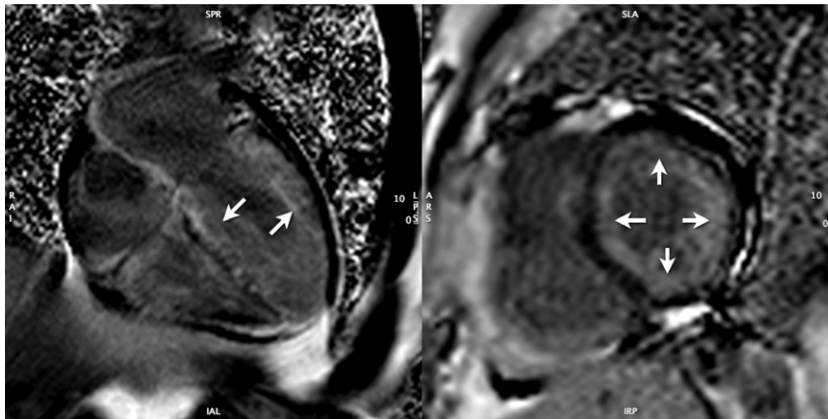
Figure 12. Late Gadolinium Enhancement in Arrhythmogenic Right Ventricular Cardiomyopathy in a Patient With Cardiac Amyloidosis

Left panel: long-axis view of a late Gd enhancement study (10 min post Gd administration) showing extensive, diffuse myocardial Gd uptake (arrows) with early clearance from blood pool (low signal intensity of the ventricular lumen). Right panel: confirmative short-axis view showing the mainly subendocardial distribution of the Gd (arrow). Gd indicates gadolinium.

planning therapeutic interventions. Importantly, the unique ability of CMR to characterize disease-specific tissue abnormalities and assess cardiac function affords physicians an ability to diagnose the etiology and monitor therapy in patients with cardiomyopathy.

3.5.10. Summary of Existing Guidelines and Appropriate Use Criteria

The ACC/AHA 2005 Guideline Update for the Diagnosis and Management of Chronic Heart Failure in the Adult indicates the utility of CMR to confirm the presence of iron overload (96).

The writing committee recognizes the ACCF/ACR/SCCT/SCMR/ASNC/NASCI/SCAI/SIR 2006 Appropriateness Criteria for Cardiac Computed Tomography and Cardiac Magnetic Resonance Imaging for utilizing CMR to evaluate dilated cardiomyopathy in the setting of normal coronary arteries, or evaluating cardiomyopathies in individuals with positive cardiac enzymes without obstructive atherosclerosis on angiography. In addition, CMR is appropriate to evaluate specific cardiomyopathies including infiltrative (amyloid, sarcoid), HCM, LV dilated cardiomyopathy (including cardiotoxic therapy), patients suspected of ARVC, or individuals suspected of cardiomyopathy presenting with syncope or ventricular arrhythmia (97).

3.6. Assessment of Valvular Heart Disease

CMR may be used for assessing individuals with valvular heart disease in which evaluation of valvular stenosis, regurgitation, para- or perivalvular masses, perivalvular complications of infectious processes, or prosthetic valve disease are needed. CMR is particularly useful in identifying serial changes in LV volumes or mass in patients with valvular dysfunction.

In patients with valvular heart disease, CMR is uniquely suited to identify and assess the magnitude of valvular stenosis or regurgitation, as well as determine the influence of the valve lesion on LV performance. The subjective presence or absence of valvular disease can be made on cine GRE sequences by visualization of a signal void/turbulent jet above or below the valve in systole or diastole. Although SSFP imaging is the preferred cine CMR method for most functional imaging, standard GRE imaging may be preferable for jet visualization because of its longer echo time (205,206). Sequences such as these with relatively high temporal resolution (20 to 40 ms) can be used to measure the area of valve leaflet opening in systole for either aortic valve stenosis (207), or in diastole for mitral valve stenosis. Although CMR planimetry of the aortic valve has been shown to be relatively accurate, CMR is likely to underestimate mitral stenosis (i.e., overestimate the valve area) (208,209) because of the translational motion of the heart. Newer sequences, currently in development, that incorporate mitral annular tracking devices, may help resolve this issue.

A quantitative assessment of single-valve regurgitant disease can be obtained by calculating the difference between RV and LV stroke volumes (210). A more elegant quantitative assessment of valvular stenosis and regurgitation may also be performed using velocity-encoded PC sequences (210,211). These sequences display both a magnitude and a phase image. The phase image can be used to obtain the peak and mean velocity of a stenotic jet as well as flow through a prescribed area. Velocities can then be applied in the modified Bernoulli equation to calculate the pressure gradient (47,212,213) across a stenotic valve (47,212). Forward and reverse volume across a valve can also be assessed to determine the regurgitant volume and regurgitant fraction to quantify the extent of valvular insufficiency (3,214–216). In-plane PC-CMR can be used to assess direction of highly eccentric jets such as occur in mitral regurgitation. Importantly, CMR defines the consequence of the valvular lesion on LV performance (LV regional

function, dimensions, volumes, mass, and ejection fraction): all parameters used to direct medical therapy or determine the optimal time for surgical intervention (3,217).

CMR may also be useful in assessing valvular masses. These masses can include either true primary valvular tumors such as papillary fibroelastomas, or valvular vegetations or thrombi such as in bacterial endocarditis (218–220). Sequences used to assess the valve for masses would include cine SSFP in the plane of the valve to assess for mass mobility (218). As valvular vegetations may be quite small, 3D SSFP imaging with a T2 preparatory pulse and fat suppression may be useful in the plane of the valve (221). In cases where the tumor or vegetation is causing valvular insufficiency, quantitative evaluation should be performed.

3.6.1. Potential Advantages of CMR Relative to Other Imaging Modalities

Principles (modified Bernoulli equation, continuity equation, planimetry) used in other modalities to determine valvular stenosis are similar in CMR, with the latter using PC sequences to obtain transvalvular velocity measures (211). In individuals with valvular regurgitation, CMR is unique in that it is used to directly quantify valvular regurgitation in mL/min rather than provide an estimate using another surrogate measure. Although several small studies identify potential utility of CMR in assessing patients with valvular heart disease, studies with larger patient numbers and comparisons with echocardiography would be useful to extend applicability. In addition, CMR can be used for serial assessments that accurately quantify LV and RV volume and function, important information in patients with chronic valvular heart disease that is often used to determine the optimal time for surgical or percutaneous interventions.

3.6.2. Summary of Existing Guidelines and Appropriate Use Criteria

The ACC/AHA 2006 Guidelines for the Management of Patients With Valvular Heart Disease recommends CMR for initial and serial assessment of LV volume and function at rest in patients with aortic regurgitation and suboptimal echocardiograms (Class I, *Level of Evidence: B*) (222). In addition, CMR is recommended in patients with bicuspid aortic valves when morphology of the aortic root or ascending aorta cannot be assessed accurately by echocardiography (Class I, *Level of Evidence: C*) and is probably recommended in patients with bicuspid aortic valves when aortic root dilation is detected by echocardiography to further quantify severity of dilation and involvement of the ascending aorta (Class IIa, *Level of Evidence: B*) (222).

The ACCF/ACR/SCCT/SCMR/ASNC/NASCI/SCAI/SIR 2006 Appropriateness Criteria for Cardiac Computed Tomography and Cardiac Magnetic Resonance Imaging indicates the use of CMR to characterize native and prosthetic cardiac valves including planimetry of stenotic valves and quantification of regurgitant disease. CMR

may be especially useful in individuals with technically limited images from echocardiography or in those patients who are not candidates for transesophageal echocardiography. CMR is also useful for assessing serial changes in LV or RV mass or volumes and quantification of valvular heart disease (97).

3.7. Cardiac Masses

CMR may be used for clinical evaluation of cardiac masses, extracardiac structures, and involvement and characterization of masses in the differentiation of tumors from thrombi.

CMR can be a valuable adjunct for the evaluation of patients with suspected pericardial or cardiac masses. Cardiac masses can be categorized as intracavitary thrombus, primary tumors (arising from cardiac tissue), and secondary cardiac tumors (metastasis from noncardiac tissue) (223,224). A standard CMR approach for evaluation of structure and function would routinely involve dark blood images in the axial, sagittal, and coronal planes of the entire chest followed by bright blood (e.g., SSFP) cine imaging of the heart from base to apex in both short- and long-axis views. Common structures that may mimic or raise concern for true cardiac tumors, often due to incomplete coverage or visualization, include prominent eustachian valves, Chiari network, crista terminalis, lipomatous interatrial septum, pericardial cysts, and large hiatal hernias. Often many of these pseudocardiac tumors are incompletely categorized on other noninvasive cardiac imaging studies. In patients with cardiac masses, CMR can be used to characterize tissue within the mass (225).

3.7.1. Characterization of Cardiac Masses

For intracavitary cardiac masses, the ability to distinguish a cardiac tumor from thrombus is important. Cardiac thrombi occur in the left atrial appendage in association with atrial fibrillation, and LV thrombi often occur with dilated ischemic cardiomyopathy. Intracavitary mural thrombi may be difficult to identify using other imaging techniques. CMR has been shown to be very sensitive for the detection of LV thrombi (226–228). This is in part due to the utility of CMR tissue characterization with LGE. LGE, which is typically used for detection of myocardial fibrosis or scar, can be used with long inversion recovery times for improved differentiation of enhancing cardiac masses from nonenhancing bland thrombus (229). CMR may have utility for identifying cardiac cavitary thrombi in patients sustaining cardioembolic stroke.

3.7.2. Benign Versus Malignant Cardiac Masses

Once a cardiac mass is identified, the presence of heterogeneous infiltration of the myocardium, vascular invasion, or other signs of metastasis (e.g., metastatic pleural effusion and/or mediastinal adenopathy) can be used to differentiate benign versus malignant tumors (230,231). Primary cardiac tumors including myxomas, papillary fibroelastomas, fibromas, and lipomas are often benign. Many of these tumors

have characteristic anatomic locations and specific tissue characteristics. The most common primary malignant tumors of the heart can be classified as cardiac sarcomas (the most common subtype is angiosarcomas), and primary cardiac lymphomas. These malignant tumors can extend locally and involve the pericardium and, with tissue characterization, have indistinct margins and heterogeneous Gd enhancement. First-pass imaging through a cardiac mass may help distinguish vascularized lesions, such as renal carcinoma metastases, from other nonvascular lesions.

3.7.3. Potential Advantages of CMR Relative to Other Imaging Modalities

CMR has been shown to be beneficial for characterizing of cardiac tumors as benign or malignant (232). In comparison to other imaging modalities, CMR has the benefits of multiplanar image acquisition, high spatial resolution imaging, large field of view, and tissue characterization.

3.7.4. Summary of Existing Guidelines and Appropriate Use Criteria

The writing committee recognizes that no existing guidelines are established for the evaluation of cardiac mass with CMR.

The ACCF/ACR/SCCT/SCMR/ASNC/NASCI/ SCAI/SIR 2006 Appropriateness Criteria for Cardiac Computed Tomography and Cardiac Magnetic Resonance Imaging indicates the use of CMR for evaluation of intracardiac and extracardiac masses including suspected tumors or LV thrombi (97).

3.8. Pericardial Disease (Constrictive Pericarditis)

CMR may be used as a noninvasive imaging modality to diagnose patients with suspected pericardial disease. CMR can provide a comprehensive structural and functional assessment of the pericardium as well as evaluate the physiological consequences of pericardial constriction.

In 2 respects, CMR is useful for assessing patients suspected of constrictive pericardial disease. First, with CMR, the entire pericardium can be visualized without regard to body habitus or prior surgical procedures (233–237). In constriction, a pericardial thickness greater than or equal to 4 mm is abnormal and visually seen. Second, CMR can be used to evaluate the physiologic impact of abnormal pericardial thickening. Distension of the hepatic veins and flattening of the interventricular septum are signs of accompanying elevated right-sided pressures. Paradoxical motion of the interventricular septum may be seen as the right-sided pressures equalize or exceed those on the left during diastole. Real-time cine CMR can be used to evaluate for ventricular interdependence to help distinguish constrictive pericarditis from restrictive cardiomyopathy (238,239).

Effusive constriction results from a pericardial effusion that has become organized or gelatinous (240). The peri-
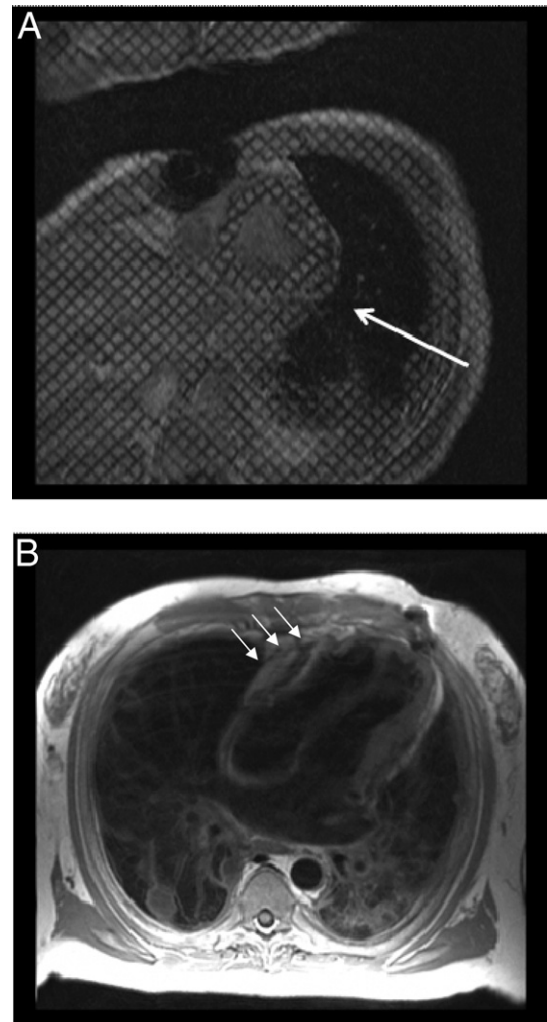
Figure 13. Cardiovascular Magnetic Resonance Findings Associated With Pericardial Disease

Panel A: a short-axis, cine-tagged imaging is provided. Along the posterior wall of the left ventricle (white arrow), tag deformation is absent, indicating pericardial adhesions. Panel B: dark blood T1-weighted spin echo images are provided, indicating thickened pericardium along the anterior surface of the right ventricle and corresponding tubular deformity of the ventricles. Advanced lung disease is also noted.

cardial space tends not to be homogeneous on various pulse sequences. Tagged cine can be used to demonstrate failure of the tags to distort with systole. Pericardial adhesions may be seen with a normal-thickness pericardium and result in functional constriction. They are best appreciated with tagged cine (Figure 13) (241). Rather than the normal slippage of the pericardium across the myocardium during systole, there is tethering of the myocardium, which impairs diastolic filling.

Right heart catheterization has been used to identify the hemodynamic consequence of right-sided heart failure, but the initial criteria that examined end-diastolic pressure relationships have been of limited predictive value (242). Abnormal ventricular interdependence can improve the diagnostic accuracy of right heart catheterization (243).

3.8.1. Potential Advantages of CMR Relative to Other Imaging Modalities

The marked utility of CMR for assessment of pericardial disorders resides in the fact that comprehensive visualization of the LV endocardium may occur, and the physiologic consequences of abnormal pericardial thickening can be obtained without exposure to ionizing radiation (244).

3.8.2. Summary of Existing Guidelines and Appropriate Use Criteria

The writing committee recognizes that no existing guidelines are established for assessment for pericardial disease with CMR.

The ACCF/ACR/SCCT/SCMR/ASNC/NASCI/ SCAI/SIR 2006 Appropriateness Criteria for Cardiac Computed Tomography and Cardiac Magnetic Resonance Imaging indicates CMR is appropriate for evaluation of pericardial conditions, including pericardial mass and pericardial constriction (97).

3.9. Congenital Heart Disease

CMR may be used for assessing cardiac structure and function, blood flow, and cardiac and extracardiac conduits in individuals with simple and complex congenital heart disease. Specifically, CMR can be used to identify and characterize congenital heart disease, to assess the magnitude or quantify the severity of intracardiac shunts or extra cardiac conduit blood flow, and to evaluate the aorta and pulmonary arteries to assess the pathological and physiologic consequences of congenital heart disease on left and right atrial and ventricular function and anatomy.

CMR can be used to characterize 3 important aspects of patients with congenital heart disease both pre- and postoperatively: the anatomy of the lesion (including the atria, ventricle, and great vessels and their respective connections), the physiology (including cardiac and conduit blood flow), and the assessment of ventricular function (in order to determine how the heart is handling the abnormal anatomy and/or physiology). CMR is especially attractive in congenital heart disease where complex anatomic details need to be ascertained, as well as in the pediatric age range where ionizing radiation is a grave concern.

3.9.1. Anatomy

CMR has been used to delineate anatomic details of congenital heart disease for over 2 decades. CMR determination of anatomy has been validated against other gold standard techniques and often CMR-derived information alters therapy (245,246). 3D SSFP and Gd imaging has been shown to be particularly useful in giving an overview of complex anatomy in congenital heart disease.

3.9.2. Physiology

Cine and PC velocity mapping CMR provide physicians with a noninvasive method to assess the physiologic importance of consequential heart lesions. For example, the pulmonary to systemic flow ratio (Qp/Qs) of shunt lesions (e.g., atrial and ventricular septal defects) can be quantified using CMR (48,247,248). PC-CMR can also provide quantification of collateral blood flow in aortic coarctation (249,250), determine caval contributions to each lung in Fontan patients (251), measure cerebral blood flow in superior-cavopulmonary connections (252), or quantify regurgitant fractions in patients after repair of tetralogy of Fallot (253,254). Newer techniques such as ultrafast, time-resolved 3D contrast-enhanced MRA expand the utility of CMR to assess physiology in congenital heart disease. This is particularly useful in assessing disorders of the pulmonary circulation (Figure 14).

3.9.3. Biventricular Function

There are multiple studies reinforcing the accuracy of CMR for biventricular function in congenital heart disease (255,256). The high accuracy and reproducibility of CMR for ventricular cavity size and systolic function is particularly useful in the congenital heart disease population because these patients undergo numerous procedures that change the physiology and may affect ventricular performance due to cardiopulmonary bypass or deep hypothermic circulatory arrest (257,258).

3.9.4. Congenital Aortic Disease

Coarctation, Complete Interruption, and Pseudo-Coarctation

Coarctation of the aorta, representing abnormal placation of the tunica media of the posterior aortic wall proximal to the ligamentum arteriosum, accounts for approximately 5% of all congenital heart disease (259). Most coarctations found in adults are juxtaductal in location and "simple," being found in the absence of other cardiovascular abnormalities. On the other hand, "complex" coarctations are often present in infancy due to their associated intracardiac anomalies.

Anatomic CMR (combined spin echo and cine GRE or SSFP) (114,118,120–122) and/or CE-MRA (121–123) alone has been shown to be comparable to conventional angiography for delineation of the location and degree of stenosis due to coarctation. A large series of patients with angiographically confirmed congenital obstructive aortic anomalies, including coarctation and interruption, reported a diagnostic sensitivity of 89%, specificity of 84%, and accuracy of 86% for CMR (spin echo and cine GRE or SSFP) and 98%, 99%, and 98%, respectively, for CE-MRA (260). However, a general superiority of CMR (spin echo, cine, dynamic PC) with CE-MRA over other imaging modalities, including echocardiography, for combined anatomic (location and severity of narrowing) and physiologic (trans-coarctation pressure gradient determination, collat-
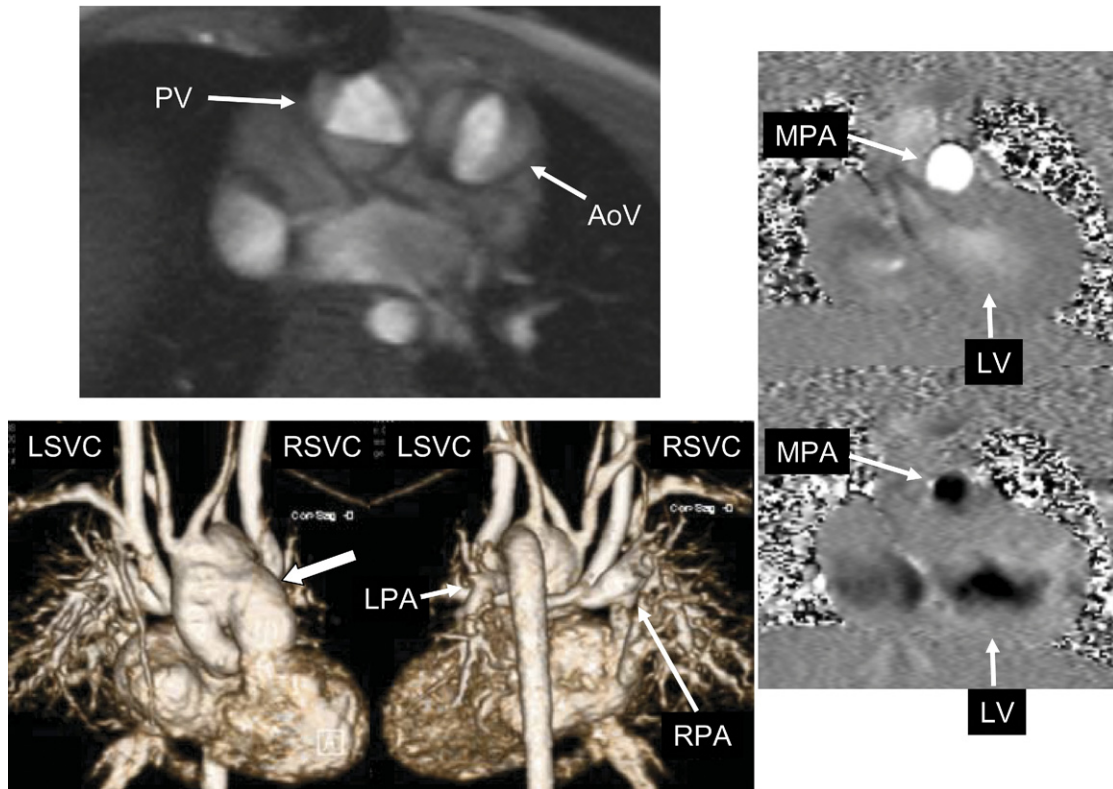
Figure 14. Examples of Cardiovascular Magnetic Resonance in Congenital Heart Disease

The upper left panel is a cine CMR of a patient with double outlet right ventricle demonstrating semilunar valve morphology. The PV is trileaflet, whereas the AoV is bicuspid. The lower left panel is a 3-dimensional reconstruction of a single-ventricle patient after aortic to pulmonary anastamosis (arrow on leftward image, which is an anteroposterior view) and a bilateral bidirectional cavopulmonary connection where the LSVC and RSVC are connected to the LPAs and RPAs (best visualized on the rightward image, which is a posterior view). The rightward panels are from a patient with tetralogy of Fallot after repair with pulmonary regurgitation using through-plane phase-contrast imaging of the MPA. This technique encodes flow into and out of the imaging plane with directionality encoded as white or black; the top image demonstrates antegrade flow (white), and the bottom image demonstrates retrograde or regurgitant flow (black). The frames were acquired at peak systole and diastole. AoV indicates aortic valve; CMR, cardiovascular magnetic resonance; LPA, left pulmonary artery; LSVC, left superior vena cava; MPA, main pulmonary artery; PV, pulmonary valve; RPA, right pulmonary artery; and RSVC, right superior vena cava.

eral flow measurement) assessment of coarctation has been demonstrated (114,118,121,126,129,260,261). Accordingly, CMR (262) or CE-MRA (263) can effectively distinguish pseudocoarctation (no hemodynamically significant narrowing, poststenotic flow, or collateral vessels) from true coarctation of the aorta. In addition, CMR can be used to identify aneurysms of the central nervous system circulation in patients with coarctation.

CMR and CE-MRA can also be effectively used to assess postoperative complications for coarctation, including restenosis and pseudoaneurysm formation (114,121,135,264). Direct visualization of collateral vessels by CE-MRA and percent increase in flow from proximal to distal descending thoracic aorta are more reliable indicators of hemodynamic significance of restenosis following surgical repair of coarctation than arm–leg blood pressure gradient (136). The presence of metallic stents following angioplasty can interfere with postintervention assessment of the coarctation site by CMR/CE-MRA. However, physiologic evaluation of changes in collateral circulation before and after intervention is still feasible (142).

Arch Anomalies and Vascular Rings

The failure of embryonic vascular arches to fuse and regress in the usual manner during the formation of the aortic arch, pulmonary arteries, and ductus arteriosus can cause a wide spectrum of vascular congenital abnormalities of the aortic arch and its branches (265). These abnormal vascular structures, especially when they constitute a true vascular ring (i.e., double aortic arch, right aortic arch with aberrant left subclavian artery, or mirror-image right aortic arch with left-sided ligamentum arteriosum) may cause varying degrees of compression of the trachea and/or esophagus, with resulting symptoms ranging from none to severe stridor, dyspnea, cyanosis, and dysphagia. These arch anomalies/vascular rings require specific surgical corrective measures based on well-delineated anatomic and physiologic assessment of the abnormalities by imaging, such as CMR and/or CE-MRA (148). CE-MRA, complemented by flow-sensitive techniques to evaluate stenosis, is very useful for detecting congenital vascular abnormalities (123,129, 149,164) and diagnosing potentially life-threatening com-

plications, especially airway compression from vascular rings (163).

3.9.5. Potential Advantages of CMR Relative to Other Imaging Modalities

CMR is advantageous for the assessment of patients with congenital heart disease because it can visualize structures within and external to the heart with minimal impediments related to body habitus. In lesions affecting the right heart, CMR provides excellent visualization and comprehensive volume determinations regardless of RV shape. This is particularly important in patients with congenital heart disease in which abnormalities of pulmonary artery anatomy or blood flow can raise RV afterload. Importantly, CMR can be used to quantify in 3D anatomy, physiology, and function and, in pediatric patients can be used to acquire information relating to congenital heart disease without ionizing radiation (266,267), or the need for iodinated contrast (268,269). Because of concerns regarding exposure of pediatric patients to ionizing radiation (270), the writing committee feels CMR (rather than cardiovascular computed tomography) may be preferred to address questions related to pediatric congenital heart disease when 1) there is an appropriate indication for tomographic imaging and 2) there is local expertise present to perform and interpret the CMR studies.

3.9.6. Summary of Existing Guidelines and Appropriate Use Criteria

The ACC/AHA 2008 Guidelines for the Management of Adults With Congenital Heart Disease recommends CMR (Class I, *Level of Evidence: B*) for assessment of patients with aortic coarctation and (Class I, *Level of Evidence: C*) for subsequent evaluations of repaired aortic coarctations. CMR is also recommended (Class I, *Level of Evidence: C*) for baseline imaging of patients with pulmonary stenosis. In centers with adequate expertise, CMR is useful (Class I, *Level of Evidence: B*) for the initial screening of patients with suspected congenital coronary anomalies. Patients with arteriovenous fistula that have a continuous murmur should be evaluated with CMR (Class I, *Level of Evidence: C*). In patients with congenital heart disease, CMR is useful for evaluating patients with suspected pulmonary hypertension (Class I, *Level of Evidence: C*) and patients with tetralogy of Fallot (Class I, *Level of Evidence: C*). CMR is also recommended to evaluate the great arteries and veins in patients with prior atrial baffle procedures (Class I, *Level of Evidence: B*) and congenitally corrected transposition of the great arteries (Class I, *Level of Evidence: C*) and managing patients with complex congenital heart disease (Class I, *Level of Evidence: C*). Finally, CMR is reasonable in patients with arterial switch operations to evaluate the anatomy and hemodynamics in more detail (Class IIa, *Level of Evidence: C*) (271).

In addition, the ACC/AHA 2008 Guidelines for the Management of Adults With Congenital Heart Disease indicates that CMR provides additional noninvasive imaging information in any situation in which findings generated by echocardiography are uncertain. This includes evaluation of patients with intracardiac communication such as atrial and ventricular septal defects (271).

The ACCF/ACR/SCCT/SCMR/ASNC/NASCI/SCAI/SIR 2006 Appropriateness Criteria for Cardiac Computed Tomography and Cardiac Magnetic Resonance Imaging indicates that CMR is appropriate to assess complex congenital heart disease including anomalies of the coronary circulation, great vessels, cardiac chambers, and valves (97). CMR is particularly useful in this regard in children in which exposure to ionizing radiation is to be avoided.

3.10. Pulmonary Angiography

CE-MRA may be used in patients with a strong suspicion of pulmonary embolism in whom the results of other tests are equivocal or for whom iodinated contrast material or ionizing radiation are relatively contraindicated (272). The writing committee agrees that data in the literature are insufficient to recommend where pulmonary CE-MRA should fit into a diagnostic pathway for pulmonary embolism.

CMR imaging can be used to assess the pulmonary arteries for acute and chronic thromboembolic disease, pulmonary arterial stenoses (as in congenital heart disease), or acquired pulmonary arterial pathology such as iatrogenic pseudoaneurysms. Pulmonary arterial size in patients with pulmonary arterial hypertension can also be assessed. Primarily, pulmonary CE-MRA is used with the bolus timed to opacify the pulmonary arteries at the center of k-space data acquisition. Time-resolved contrast-enhanced MRA is particularly useful for imaging the pulmonary vasculature as it allows complete separation of the pulmonary and systemic phases.

3.10.1. Pulmonary Emboli

There are few studies regarding the utility of data for pulmonary CE-MRA for the diagnosis of acute pulmonary embolism (273). Although a few prospective single-center studies assessing CE-MRA have been performed (274–277), no large randomized, controlled, multicenter trial has been reported. Data from these smaller single-center studies, however, are promising, with the sensitivity for pulmonary CE-MRA to detect pulmonary emboli ranging from 77% to 100% and the specificity ranging from 95% to 100%.

Real-time CE-MR pulmonary perfusion methods can be added to raise the sensitivity for pulmonary embolism detection (275,278). Techniques used for this purpose have a lower spatial resolution, which may preclude direct visualization of emboli; however, these methods display segmental and subsegmental perfusion defects analogous to nuclear medicine techniques, which can then be used to indirectly predict the presence of embolus.

The Gd-based MR contrast agent administered for pulmonary CE-MRA can potentially be used to passively opacify the veins of the pelvis and lower extremities to provide information about deep venous thrombosis during the same examination. The addition of lower extremity venous imaging, especially from the femoral veins to the popliteals, has the potential to increase the overall sensitivity for pulmonary thromboembolic disease (279). Experience with MRA, even without the use of a CMR contrast agent, for the detection of proximal deep venous thrombosis and extension into the pelvic veins has shown a sensitivity of 94% to 100% and a specificity of 90% to 100% (280–282).

3.10.2. Summary of Existing Guidelines and Appropriate Use Criteria

At present, the writing committee recognizes that there are no guidelines or appropriate use criteria highlighting the utility of CMR for assessment of pulmonary artery diseases exclusive of congenital heart disease.

3.11. Atrial Fibrillation

CMR may be used for assessing left atrial structure and function in patients with atrial fibrillation. The writing committee recognizes that evolving techniques utilizing LGE may have high utility for identifying evidence of fibrotic tissue within the atrial wall or an adjoining structure. Standardization of protocols and further studies are needed to determine if CMR provides a reliable effective method for detecting thrombi in the left atrial appendage in patients with atrial fibrillation. CMR may be useful for identifying pulmonary vein anatomy prior to or after electrophysiology procedures without need for patient exposure to ionizing radiation.

When assessing patients with atrial fibrillation, CMR can be used to determine the size and shape of the left atrium and to determine pulmonary vein orientation in patients receiving surgical or percutaneous ablation to control heart rate and rhythm. As with determinations of LV and RV chamber size and volumes, CMR has been used to characterize left atrial chamber dimensions and volumes (81,283–289).

3.11.1. Preablation Planning

Preprocedural CMR can provide the 3D orientation of the pulmonary vein and atrium for the purpose of reducing the time necessary to locate ablation sites during the procedure. Important considerations include the presence of atrial thrombus and variations of pulmonary venous anatomy (290). Most of the required planning and follow-up information may be obtained with a CE-MRA (291–293). CMR may prove to be useful for guiding ablation procedures (294,295). Time-resolved MRA is the method of choice for assessing the pulmonary veins. For "at-risk" patients, where Gd administration is undesirable, noncontrast MRA using 3D SSFP is a useful alternative.

Pulmonary vein stenosis is a potential complication of ablation by pulmonary vein isolation with an incidence ranging from 1.5% to 42% depending on how stenosis is defined and on the imaging method (296–299). Uncommonly, pulmonary vein occlusion may lead to pulmonary infarction. CMR can be used to identify pulmonary infarction (300,301).

There are also emerging data to suggest that CMR may have a role in determining postablation scar formation in patients with atrial fibrillation. In this strategy, LGE techniques are employed to outline the extent of scarred atrial myocardium after ablation. Acquiring a stack of images encompassing the atrium allows for the determination of scar volume (302).

3.11.2. Potential Advantages of CMR Relative to Other Imaging Modalities

At present, the role of CMR in management pathways for diagnosing left atrial or atrial appendage thrombus (303) is not defined. Further studies are required to determine the clinical role of CMR in identifying left atrial thrombi (304). In centers with expertise, CMR provides an accurate method to obtain pulmonary vein orientation without exposure to ionizing radiation or iodinated contrast.

3.11.3. Summary of Existing Guidelines and Appropriate Use Criteria

At present the writing committee recognizes that there are no guidelines established for the use of CMR in assessing patients with atrial fibrillation.

The ACCF/ACR/SCCT/SCMR/ASNC/NASCI/SCAI/SIR 2006 Appropriateness Criteria for Cardiac Computed Tomography and Cardiac Magnetic Resonance Imaging indicates that CMR is an appropriate test to evaluate pulmonary veins prior to radiofrequency ablation for atrial fibrillation and to identify left atrial and pulmonary venous anatomy including dimensions of veins for mapping purposes (97).

3.12. Peripheral Arterial Disease

CMR for peripheral arterial disease (PAD) may be used to diagnose anatomic location and degree of stenosis and is useful in selecting patients with lower extremity PAD who are candidates for intervention. Additionally, MRA of the lower extremities is appropriate for patients with claudication (305).

PAD has been estimated to affect more than 5 million adults in the United States (306). CMR provides a noninvasive method to evaluate peripheral vessels and to identify the location and severity of PAD. Proper vascular evaluation of PAD requires illustration from at least the aortic bifurcation through the distal trifurcation vessels (and pedal arch in cases of limb-threatening ischemia). This imaging re-

Table 7. Peripheral CMR: 2D Time of Flight and Contrast-Enhanced Magnetic Resonance Angiography

Technique	Strengths	Limitations
2D TOF	• No intravenous contrast media requirement	• Long examination times (greater than 2 hours) • Highly susceptible to flow-related artifacts that may result in the overestimation of stenoses or erroneously mimic arterial occlusion
CE-MRA (i.e., bolus chase CE-MRA with time-resolved CE-MRA)	• Short examination times • Provides consistently high vascular contrast-to-noise ratio for reliable depiction of arterial segments and stenoses • Less susceptible to flow-related artifacts • Provides dynamic assessment of vascular territories (time-resolved CE-MRA)	• Requires intravenous contrast media administration

2D indicates 2-dimensional; CE-MRA, contrast-enhanced magnetic resonance angiography; CMR, cardiovascular magnetic resonance; and TOF, time of flight.

quirement results principally from the high incidence of synchronous and tandem lesions.

Several CMR techniques have evolved over time for the assessment of peripheral arterial disease, notably 2D time of flight (TOF) (72,307,308), and 3D CE-MRA (72). The strengths and limitations of the techniques are shown in Table 7.

Two meta-analyses of the diagnostic performance of CE-MRA for lower extremity arterial evaluation in patients with suspected or known PAD (Table 8) demonstrated heightened accuracy of CE-MRA over noncontrast 2D MRA for detecting and grading the severity of stenoses in patients with PAD.

The current preferred method for performing peripheral CE-MRA is a multistation ("bolus chase") 3D CE-MRA that provides an extended field of view coverage (e.g., 1 m) for a single contrast media injection (309–311). For improved visualization of the distal extremity (i.e., infrapopliteal and/or pedal) arteries, the bolus chase MRA can be supplemented by a dedicated separate contrast-enhanced 3D MRA using traditional timed arterial-phase CE-MRA (312) or multiphase, time-resolved CE-MRA methods (313,314). The supplement of bolus chase MRA with dedicated distal lower extremity MRA (Figure 15), also called "the hybrid" technique (312), has the advantage of improved arterial depiction of the infrapopliteal arteries in which arterial enhancement can often be variable or fast (diabetic patients [315]), and suboptimally depicted using bolus chase MRA alone (316).

3.12.1. Potential Advantages of CMR Relative to Other Imaging Modalities

In prospective studies comparing color duplex ultrasound to peripheral CE-MRA, CE-MRA was found to be more sensitive and more specific for the detection of arterial luminal narrowings of greater than 50% (317). A prospective multicenter trial of patients (318) randomized to either CE-MRA or duplex ultrasound for PAD evaluation found the results of both studied to have similar ability to predict changes in disease severity and quality of life. Importantly, patients that received peripheral CE-MRA experienced a reduction of additional vascular imaging procedures by 42%.

In a prospective study of consecutive patients (319) randomized to either peripheral CE-MRA or 16-detector row cardiac computed tomographic angiography (CTA), CTA was found to be less expensive ($438 per patient) but with no statistically significant differences in patient outcomes (i.e., quality of life). Mean therapeutic confidence for CE-MRA and CTA were similar and comparable to that for digital subtraction angiography. CTA exposed participants to ionizing radiation and ionic contrast.

A final consideration for comparison of CMR to CTA and ultrasound relates to the utility of CMR for characterizing the components of atherosclerotic plaques (Figure 16). CMR is able to differentiate proton spin characteristics associated with water, fibrosis, and fat, and thereby distinguish lipid relative to non-lipid plaque components.

Table 8. Meta-Analysis of Contrast-Enhanced Magnetic Resonance Angiography Versus Noncontrast 2D Magnetic Resonance Angiography for Assessment of Peripheral Arterial Disease

Meta-Analysis Study (Reference)	Technique	No. of Patients and Studies*	Sensitivity (%)	Specificity (%)	Diagnostic Odds Ratio
Nelemans et al. (2000) (71) gold standard = DSA	CE-MRA	2 patients/10 studies	92–100	91–99	7.5
	2D TOF MRA	344 patients/13 studies	64–100	68–96	4.5
Koelemay et al. (2001) (70) gold standard = DSA	CE-MRA†	495 patients/17 studies	83–100	64–100	2.8
	2D TOF or 2D proximal compression MRA	679 patients/20 studies	69–100	23–100	1.0

2D indicates 2-dimensional; CE-MRA, contrast-enhanced magnetic resonance angiography; DSA, digital subtraction angiography; MRA, magnetic resonance angiography; and TOF, time of flight.
*In some studies, patients underwent both CE-MRA and noncontrast 2D MRA. †Single study on 20 subjects evaluated 2D CE-MRA.
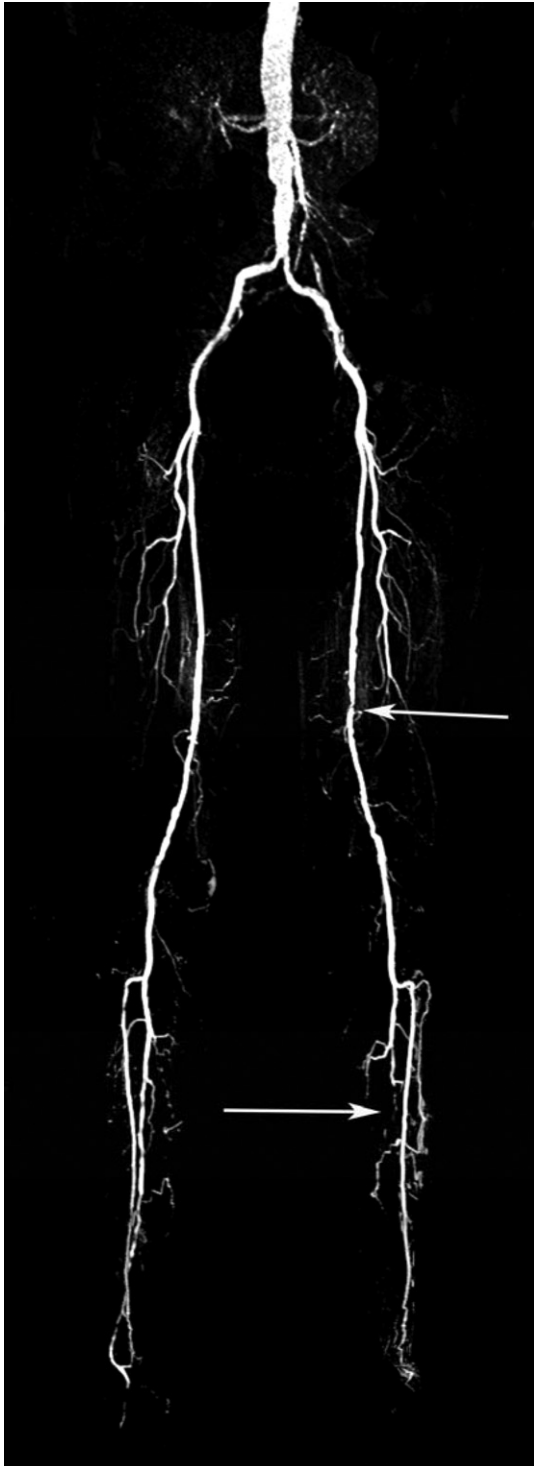
Figure 15. Bolus Chase Contrast-Enhanced Magnetic Resonance Angiography

Bolus chase CE-MRA of the aorta and lower extremity arteries obtained with a 3–stage table-stepping protocol during infusion of 0.2 mM/kg of gadolinium chelate in a patient with peripheral arterial disease. There is evidence of sequential moderate stenoses in the left superficial femoral artery (upper arrow), as well as runoff disease in the left calf (lower arrow). CE-MRA indicates contrast-enhanced magnetic resonance angiography; and mM, millimolar.

3.12.2. Summary of Existing Guidelines and Appropriate Use Criteria

The ACC/AHA 2005 Practice Guidelines for the Management of Patients With Peripheral Arterial Disease recommends MRA of the extremities: 1) as useful to diagnose anatomic location and degree of stenosis of PAD (Class I, *Level of Evidence: A*); 2) should be performed with Gd enhancement (Class I, *Level of Evidence: B*); and 3) useful in selecting patients with lower extremity PAD as candidates for endovascular intervention (Class I, *Level of Evidence: A*). The guidelines also indicate that MRA of the extremities may be considered: 1) to select patients with lower extremity PAD as candidates for surgical bypass and to select the sites of surgical anastomosis (Class IIb, *Level of Evidence: B*); and 2) for post-revascularization (endovascular and surgical bypass) surveillance in patients with lower extremity PAD (Class IIb, *Level of Evidence: B*) (305).

In regard to the presentation of claudication, the American College of Radiology Appropriateness Criteria 2005 ranks MRA of the lower extremities as highly appropriate with a ranking of 8 on a scale from 1 (least appropriate) to 9 (most appropriate) for patients with claudication (320).

3.13. Carotid Arterial Disease

CMR may be used for defining the location and extent of carotid arterial stenoses.

Arterial stenosis, occlusion, dissection, or aneurysm may occur anywhere from the aortic arch to the intracranial circulation, in 1 or several sites. Current recommendations state that endarterectomy, when performed in the presence of severe and symptomatic stenosis (i.e., 70% to 99%), can be expected to prevent 1 stroke in 10 cases performed (321). As with peripheral angiography, MRA has in recent years made advances for the study of the carotid and vertebrobasilar circulation. Various implementations of 2D or 3D TOF MRA with or without CE-MRA have met with intense interest for rapid, flow-independent evaluation of the extracranial carotids (322) and vertebrobasilar circulation (323). CE-MRA, however, is demanding machine hardware to generate sufficiently high spatial resolution during the first pass of a contrast agent, and some results in the intracranial circulation were disappointing (324).

With the more recent dissemination of 3.0-T CMR units and the development of multichannel radiofrequency (RF) subsystems that support parallel imaging, the performance of CE-MRA in the carotids has been greatly improved such that it rivals CTA and conventional angiography for assessment of carotid stenosis (325) and intracranial aneurysms (326,327) with a significant degree of intermodality agreement between MRA and both CTA and digital subtraction angiography (325).

A unique attribute of CMR is the ability to quantify blood flow. CMR allows for reproducible quantification of carotid arterial flow, using PC cine imaging. This technique has previously been shown to represent a reliable estimation

Figure 16. Atherosclerotic Plaques in Cardiovascular Magnetic Resonance

Multispectral atherosclerotic plaque imaging of the SFA in the same patient as Figure 10 with a T1-W image on the left, PDW image in the middle, and T2-W image on the right. The lumen is preserved (long white arrows), yet there is significant atherosclerotic plaque in the wall. The black arrows on the T1-W image point to areas of low signal consistent with calcification (seen on all 3 image weightings). The large white arrowheads point to areas of low signal on the PDW and T2-W images that are consistent with lipid-rich necrotic core. The brighter areas around the lumen on PDW and T2-W images represent fibrous tissue. PDW indicates proton density–weighted; SFA, superficial femoral artery; T1-W, T1-weighted; and T2-W, T2-weighted.

of cerebral blood flow (328,329). Furthermore, flow quantification of the immediate poststenotic region may be of value in the determination of peak blood velocity through this stenosis, an indicator of the hemodynamic significance of the luminal compromise seen. PC-CMR may also be used to assess vertebral artery flow in subclavian steal syndrome.

CMR can be used to address certain questions about plaque composition (330,331). However, at the time of writing, imaging of plaque remains a focus of research, not yet having found a defined role in clinical decision making.

3.13.1. Potential Advantages of CMR Relative to Other Imaging Modalities

CMR provides the capability to visualize carotid arterial segments and the intracranial carotid system, the vertebrobasilar system, and the aortic arch—important for the identification of coexistent or primary disease. This is accomplished noninvasively, without exposure to ionizing radiation. During the same examination, quantitative flow measurements may be acquired.

3.13.2. Summary of Existing Guidelines and Appropriate Use Criteria

The writing committee recognizes that few guidelines or appropriate use criteria are available for the use of CMR for assessing the carotid arteries.

3.14. CMR of Thoracic Aortic Disease

CMR may be used for defining the location and extent of aortic aneurysms, erosions, ulcers, dissections; evaluating post-surgical processes involving the aorta and surrounding structures, and aortic size blood flow and cardiac cycle–dependent changes in area.

CMR imaging techniques (e.g., spin echo, GRE, and cine PC; and 3D CE-MRA) permit the assessment of both the characteristic anatomic abnormalities and the predisposing or resulting pathophysiologic changes (332–335) associated with diseases of the aorta, including: aortic diameters, aortic root visualization, supra-aortic branch assessment, and recognition of aortic pathologies (e.g., aneurysm, communicating dissection, ulcers, noncommunicating dissection) (336). If surgical repair for thoracic aortic disease has been performed, CE-MRA can be used to assess progres-

sion or regression of the responsible disease process or detection of complications of the surgery (e.g., graft infection) (332,337–339). The utility of CMR for providing information regarding diseases of the aorta is provided in Table 9.

3.14.1. Potential Advantages of CMR Relative to Other Imaging Modalities

CMR can visualize the arterial lumen, assess the aortic wall, and measure flow in the aorta without ionizing radiation.

3.14.2. Summary of Existing Guidelines and Appropriate Use Criteria

The writing committee recognizes that few guidelines or appropriate use criteria are available for the use of CMR for assessing the aorta.

3.15. Renal Arterial Disease

CMR may be used for evaluating renal arterial stenoses and quantifying renal arterial blood flow.

Table 9. Cardiovascular Magnetic Resonance of Thoracic Aortic Diseases

Disease of Aorta	Unique Contributions of Cardiovascular Magnetic Resonance (Reference)
Atherosclerosis and penetrating ulcer	• Identify aortic wall pseudoaneurysm, noncommunicating dissection, aortic rupture (340–342)
Aneurysm	• Etiology (e.g., atherosclerosis, annuloaortic ectasia) (332–334)
	• Assess associated changes in aortic valve (i.e., regurgitation) (343)
	• Presurgical planning and postsurgical follow-up
Traumatic injury	• Identify hemorrhage within aortic wall
	• Differentiate partial versus circumferential tears
Dissection	• Identify acute versus chronic
	• Locate entry and exit flaps and extent of dissection
	• Measure flow in true and false lumen
	• Identify and assess severity of aortic valve pathology (344,345)
	• Differentiate intramural hematoma (323,346,347)
Aortitis	• Measure aortic wall thickness in response to treatment
	• Detection of wall inflammation (348–350)

CMR is well suited to assess several aspects of renal arterial disease (any condition which results in irregularity, stenosis, dissection, or aneurysmal dilatation of the renal arteries). Specifically, CMR can be used to determine the following:

1. The number and location of renal arteries. Multiple renal arteries are common and occur in approximately 24% of cases with bilateral multiple renal arteries in 5% of the population (351).
2. The severity of renal artery stenosis, including the presence of fibromuscular dysplasia.
3. The configuration of the renal blood supply. The incidence of horseshoe kidney at necropsy is estimated at 1:666 (352). Furthermore, only in 30% of cases is the horseshoe kidney supplied by a single renal artery to each side, the majority of cases receiving multiple renal arteries bilaterally, as well as variable arterial supply of the midline isthmus (353).
4. The presence of renal or adrenal parenchymal mass lesions.

Recent studies have estimated the sensitivity and specificity of 3.0-T MRA in the detection of intra-abdominal arterial stenosis as 100% and greater than 92%, respectively (354,355).

3.15.1. Potential Advantages of CMR Relative to Other Imaging Modalities

The absence of associated ionizing radiation and noniodinated contrast medium injection reduces potential toxicities related to ionic contrast materials, particularly in patients with renal insufficiency (356). CMR offers the opportunity to perform both morphological renal arterial assessment as well as derive complementary flow-related data by means of PC flow quantification of individual renal arteries. This combined approach to renal imaging may provide insight into which patients would most benefit from endovascular intervention (357,358). In addition to high-resolution 3D large field-of-view data acquisition, renal arterial MRA also allows assessment of the renal and adrenal parenchymal tissue for the presence of congenital anomalies or potentially causative occult tumors. Time-resolved first-pass perfusion imaging of the kidneys may be valuable in identifying significant renovascular lesions (359).

3.15.2. Summary of Existing Guidelines and Appropriate Use Criteria

The writing committee recognizes that few guidelines for appropriate use criteria are available for the use of CMR for assessing the renal arteries. The ACC/AHA 2005 Practice Guidelines for the Management of Patients With Peripheral Arterial Disease (lower extremity, renal, mesenteric, and abdominal aortic) designates CMR a Class I recommendation as a screening test to establish

the diagnosis of renal arterial stenosis *(Level of Evidence: B)* (305).

4. CMR Safety

4.1. Introduction

CMR is generally considered safe, but there are important safety concerns that fall into 3 general categories: potential projectiles in the MR scanner room, implanted cardiovascular devices, and issues related to contrast administration. In regard to potential projectiles, it is important to remember that the magnet is always "on." Therefore, ferromagnetic materials entering the MR room are a hazard and can be drawn into the bore of the scanner with unopposable and unstoppable force. This produces an immediate lethal danger to anyone in the scanner or in the path of ferromagnetic material attracted to the scanner bore. For this reason, local guidelines and safety policies are developed to guard against ferromagnetic material entering the MR environment.

This section will explore the issues related to implanted devices and MR contrast and present an overview of the types of devices that are of concern, as well as the underlying safety considerations for patients with these devices. Since device specifications change frequently, a comprehensive list of CMR compatible or incompatible devices is not possible, and information on specific devices will need to be obtained either from the manufacturer's package inserts or CMR safety Web sites or handbooks. After reviewing devices, issues related to Gd contrast will be presented.

4.2. General Safety Considerations for Implanted Devices

There are several reasons that implanted devices may pose safety considerations for patients undergoing CMR. First, the CMR scanner generates a very powerful static magnetic field. Ferromagnetic objects (i.e., those that contain iron) will interact with the static field and may move in the patient's body. Nearly all implanted devices, however, are nonferromagnetic or only weakly ferromagnetic. Each device must undergo separate testing to determine whether it is likely to translate or rotate in the magnetic field. Besides the static magnetic field, additional smaller and changing magnetic fields, termed *gradients*, are generated during CMR scanning. These gradient fields may change very rapidly during CMR scanning. Gradient fields can produce electric currents in wires or leads that can potentially result in arrhythmia.

In addition to magnetic fields, radiofrequency waves are transmitted into the patient by the CMR scanner. These radiofrequency waves are absorbed by the body and can produce slight (less than 1°C) heating of the patient. With respect to implanted devices, these radiowaves may potentially interfere with certain electronic components as well as cause heating at the tips of implanted wires.

Table 10. Safety Terminology for Implanted Devices

MR safe	A device that poses no hazards in the MR environment.
MR conditional	A device that poses no known hazards in a specific MR imaging environment with constraints on the conditions of use. These constraints may include, e.g., the magnetic field strength or specific absorption rate.
MR unsafe	An item that is known to pose hazards in all MR environments.

MR indicates magnetic resonance.

Besides the type of devices, there are many variables that affect the likelihood that a CMR device could be affected by the CMR scanner. These include the location of the device, the strength of the CMR scanner and, potentially, whether the device has been acutely placed or is firmly fixed in position. Because of these factors, experts in CMR safety and physics should be consulted when presented with an unfamiliar device prior to undergoing CMR. This applies to individuals with implanted devices receiving any type of magnetic resonance procedure including the heart, brain, extremities, or other body/organ/structure/part. If the type of device is unknown, alternatives to performing CMR should be evaluated. In general, the benefits of undergoing CMR must be weighed against the potential risk of injury to the patient or device failure.

Prior to undergoing CMR, patients are screened for both implanted cardiovascular devices as well as other types of implants. Patients are screened by licensed MR technologists with supervision by a CMR-knowledgeable physician. Standardized screen forms are available (360–362) that should be completed prior to undergoing CMR.

Medical devices are classified by the American Society for Testing and Materials as "MR safe," "MR conditional," and "MR unsafe" (Table 10) (363).

4.3. CMR Scanning Post Device Implantation

Devices that are manufactured from nonferromagnetic material (300 series stainless steel, titanium, titanium alloy, nitinol) that have no electrical or magnetic components and that have no concern for heating due to CMR may undergo CMR scanning immediately after implantation.

For devices that are weakly ferromagnetic, CMR safety has not been established for every device, and in some cases, the CMR scanner could potentially dislodge or move such a device immediately after implantation. Devices that are firmly implanted into a vessel wall or adjacent tissues are less likely to undergo motion. In the case of heart valves in particular, the forces of the heart on the valve are often much greater than the CMR forces due to weak ferromagnetism. In general, waiting after implantation (e.g., for 6 weeks) may be considered if this is an option for the patient. For weakly ferromagnetic devices, the risks and benefits of CMR immediately after implantation need to be considered to determine whether it is necessary or possible to defer the CMR scan.

4.4. Coronary Artery and Peripheral Vascular Stents

Most coronary artery and peripheral vascular stents exhibit weak ferromagnetism or are nonferromagnetic. Anchoring in the vascular wall likely provides protection against movement, and further anchoring of the stent may occur due to tissue ingrowth at 6 to 8 weeks after implantation. However, for nonferromagnetic coronary stents, there is no good rationale or clinical data to suggest that a delay is necessary after implantation. Data on specific coronary stents suggest that many of these could be considered CMR safe (364–367) but not necessarily at the highest (3.0-T) magnetic fields (366,368,369). There have been no reports of increased risk of stent subacute or late thrombosis following CMR scans (367,370–373).

Drug-eluting stents have the same considerations as conventional stents regarding ferromagnetism (374). Slight heating of the stent (less than 1°C or less than 2°C for overlapping stents) has been reported, but the effect of this on the drug-eluting properties of the stent is unknown. It is possible that stent heating may be mitigated by a heat-sink effect of flowing blood in the vessel. A small study of patients after myocardial infarction who underwent MR within 2 weeks of stent implantation detected no increased incidence of adverse events at 30 days and 6-month follow-up compared with patients who did not undergo CMR (375).

4.5. Aortic Stent Grafts

Most aortic stent grafts that have been tested have been labeled as MR safe with the exception of the Zenith AAA Endovascular Graft Stent, which has been labeled as MR unsafe (362,376). The Zenith stent has significant deflection and torque of the stainless steel component of the graft in the magnetic field. Although no adverse events have been reported with the Zenith stent, there remains a potential for device migration or vessel damage so that the risks and benefits of CMR examination should be considered in these patients (377). With other aortic stent grafts (e.g., Endologic AAA or Lifepath AA), there may be significant associated artifact around the stent or obscuring of the vascular lumen due to the metallic components.

4.6. Intracardiac Devices

The majority of prosthetic heart valves and annuloplasty rings that have been tested have been labeled as MR safe, with a lesser number labeled as MR conditional. In general, the presence of a prosthetic heart valve or annuloplasty ring is not considered a contraindication to CMR examination up to 3.0-T at any time after implantation (376,378–382). The forces exerted on valve prosthesis are substantially less than those exerted by the beating heart and pulsatile flow (383). The forces required to pull a suture through the valve annulus tissue have been shown to be greater than magnetically induced forces up to a field strength of 4.7-T (384). Thus, patients with valve prosthesis are unlikely to be at risk for valve dehiscence during clinical

CMR examinations. Associated CMR-related heating has been determined to be less than 1°C in ex vivo studies (378,380,381,385,386); this is likely to be less due to the heat-sink effect of flowing blood. Valve dysfunction due to interaction with the magnetic field has not been reported.

Cardiac closure and left atrial appendage occluder devices are either weakly ferromagnetic or nonferromagnetic depending on the materials used (376,387,388). The majority of cardiac closure and occluder devices that have been tested have been labeled as MR safe; several that have been tested are labeled as MR conditional (362). Patients with nonferromagnetic cardiac closure and occluder devices may undergo CMR procedures at any time after implantation. The timing of CMR examination at 3.0-T or less in patients with cardiac closure or occluder devices that are weakly ferromagnetic should be weighed on a case-by-case basis. For cases in which there is a clear potential clinical benefit of scanning in the days to weeks after implantation, the benefits of the MR examination will likely outweigh the risks of the examination.

Sternal wires associated with cardiac surgery/valve replacement are not considered to be a contraindication to CMR examination.

4.7. Inferior Vena Cava Filters

CMR examinations of both animals and humans with implanted inferior vena cava (IVC) filters have thus far not reported complications or symptomatic filter displacement (389–394). Most IVC filters that have been tested have been labeled as MR safe; the remainder of IVC filters that have been tested are classified as MR conditional (362). In patients who have a weakly ferromagnetic IVC filter (Gianturco bird nest IVC filter [Cook, Bloomington, Ind], stainless steel Greenfield vena cava filter [Boston Scientific, Watertown, Mass]), consideration should be made to wait at least 6 weeks before performing CMR examination to allow firm implantation of the device. In cases where there is a strong clinical indication for CMR and the device is firmly anchored, the benefits of performing the CMR prior to 6 weeks may outweigh the potential risks.

4.8. Embolization Coils

Commonly utilized embolization coils are either nonferromagnetic or weakly ferromagnetic. Although there is theoretical potential for coil heating during a CMR examination, no significant effects were found on the Guglielmi detachable coil (GDC) (Boston Scientific) ex vivo (395) or in patient studies (396). Embolization coils made from nitinol, platinum, or platinum and iridium have been evaluated and found to be safe for CMR performed at magnetic field strengths of 3.0-T or less (376,397–400). Platinum coils implanted in the CNS have not been reported to cause complications for patients undergoing MR. Most embolization coils that have been tested have been labeled as MR safe; the remainder of embolization coils that have been tested have been labeled as MR conditional (362). For weakly ferromagnetic devices, the

risks of performing CMR prior to 6 weeks after coil placement must be considered relative to the benefits of CMR on a case-by-case basis.

4.9. Hemodynamic Monitoring and Temporary Pacing Devices

Retained temporary epicardial pacing leads are relatively short in length without large loops. These are felt not to pose a significant risk during CMR. No complications have been reported as a result of MR scanning for a patient with retained leads (401).

Hemodynamic catheters that contain conducting wires and those few temporary transvenous pacing wires that have been tested have been labeled as MR unsafe (362). Patients with pulmonary artery hemodynamic monitoring/ thermodilution catheters (such as the Swan-Ganz catheter) should not undergo CMR examinations because of the possible associated risks unless labeling information or instructions for use are provided that permit CMR examinations to be performed safely. Nonferromagnetic pulmonary artery catheters without electrically conductive pathways in the catheter are safe for CMR examination.

CMR of patients with temporary pacemaker external pulse generators is not recommended as CMR can alter the operation of an external pulse generator or damage it. Pacing of the patient during the CMR may also be unreliable with a temporary transvenous lead.

4.10. Permanent Cardiac Pacemakers and Implantable Cardioverter Defibrillators

Due to the wide prevalence of cardiovascular diseases, a significant proportion of patients who would normally be referred for CMR examinations will have permanent cardiac pacemakers or implantable cardioverter defibrillators (ICDs). Pacemakers and ICDs contain metal with ferromagnetic properties, as well as complex electrical systems with 1 or several leads implanted into the myocardium. Potential complications of CMR under these circumstances include damage or movement of the device, inhibition of the pacing output, activation of the tachyarrhythmia therapy of the device, cardiac stimulation, and heating of the electrode tips (402–408). These factors may lead to clinical sequelae including changes in pacing/defibrillation thresholds, pacemaker ICD dysfunction or damage (including battery depletion), arrhythmia, or death (404,409,410).

A few small clinical trials have been conducted to assess conditions under which MR examination with these devices could be conducted safely. Pacemaker-dependent patients were excluded from these studies, and the heart rhythm was monitored during the exam. No episodes of pacing above the upper rate limit or arrhythmias were noted (410), though 1 patient had a change in device programming (411). Another study suggested that ICDs and pacemakers manufactured after the year 2000 are more resistant to the electrical and magnetic fields associated with MR examination at 1.5-T (412). To date, it is likely that several hundred

patients have undergone MR examination with either pacemakers or ICDs (413–419), and strategies and protocols for safe pacemaker/ICD scanning during CMR have been proposed (420,421). As of this writing, no deaths have been reported under conditions in which patients were deliberately scanned and monitored during the MR examination, although changes in pacing threshold, programming changes, need for device reprogramming, and possibly battery depletion have been reported.

Currently, pacemakers available in the United States are labeled as MR unsafe (362). At present, CMR examination of patients with pacemakers is discouraged and should only be considered at highly experienced centers in cases in which there is a strong clinical indication and where the benefits clearly outweigh the risks. CMR examination of patients with ICDs should not be performed unless the center is highly experienced in both the operation of these devices and in complex CMR procedures in the setting of highly compelling circumstances where the benefits clearly outweigh the risks.

4.11. Retained Transvenous Pacemaker and Defibrillator Leads

There are no clinical studies that have specifically addressed the risk for CMR associated with retained pacemaker or ICD leads. Since no radiofrequency chokes are present on these leads, significant heating of the lead tips may occur. CMR in these circumstances is discouraged, and CMR examination should only be considered in centers with expertise in electrophysiology and CMR when there are no alternatives to the CMR examination under compelling clinical circumstances. Similarly, CMR examination should not be performed in patients with known retained transvenous leads that have fractures.

4.12. Hemodynamic Support Devices

Hemodynamic support devices such as ventricular assist devices and intra-aortic balloon pumps are complex electromagnetic devices containing ferromagnetic materials. Formal CMR testing of these devices has not been conducted. However, it is believed that these hemodynamic support devices represent absolute contraindications to CMR examination.

4.13. Gadolinium Contrast Agents

Gadolinium contrast agents are frequently used for CE-MRA as well as for imaging the heart for LGE, perfusion, or masses. Currently the use of Gd contrast agents for these purposes is off-label in the United States. Unlike iodinated contrast materials used with radiographic techniques, there are different safety issues relating to underlying renal function that need to be considered prior to their administration.

Mild-to-moderate reactions to Gd contrast agents (e.g., hives, shortness of breath) have been reported to occur in approximately 1 in 5000 patients. Severe anaphylactic reactions occur in 1 in 250 000 to 300 000 patients. Nephrogenic systemic fibrosis (NSF) is an extremely rare but important complication of Gd administration associated with acute renal failure or severe renal failure due to advanced chronic kidney disease (National Kidney Foundation Stage 4 or 5 renal failure). NSF is a scleroderma-like fibrosing entity of the skin (422). The disease has systemic features that include involvement of pleura, pericardium, lungs, joints, and striated muscle (including diaphragm and myocardium) (359,423). Besides acute renal failure or severe renal failure due to advanced chronic kidney disease (glomerular filtration rate less than 30 mL/min/1.73 m^2), other characteristics that have been implicated with an increased risk for NSF include severe liver failure or liver transplant, kidney transplant, hypercoagulability, deep vein thrombosis, and tissue injury secondary to surgical procedures (424). The 1-year incidence of NSF in the presence of all recognized risk factors (end-stage renal disease [ESRD], use of Gd contrast, dialysis, and proinflammatory events) has been estimated to be between 1% (unpublished data, Mayo Clinic Experience; ISMRM proceedings, Toronto, 2008) and 4.6% (425). Over 200 cases have been reported to the Food and Drug Administration as of May 2007, but not all are confirmed. Given the total number of Gd contrast applications, the overall risk of NSF in other groups is considered very low. Because of the risk of NSF, screening for reduced renal function prior to CMR should be considered in most individuals and particularly in at-risk groups, for example, older patients, individuals with history of renal disease or dysfunction, or patients with a prior renal transplant. Patients with hepatorenal syndrome in association with severe liver disease, periliver transplant patients, and patients with acute renal failure are typically poor candidates for Gd contrast administration. Patients undergoing peritoneal dialysis have prolonged retention of Gd contrast agents and their use is discouraged. The use of Gd in patients with ESRD must be balanced by the significant risk of NSF (3% to 5%). Once informed consent is obtained, using a macrocyclic chelate (like gadoteridol) in the lowest possible dose and avoiding repeat exposure appear reasonable measures, based on available evidence (426). Postprocedure hemodialysis of all patients with ESRD should be considered.

5. Summary

With its advantages in studying patients with cardiovascular disease and ability to provide high-resolution images, CMR offers a suitable mechanism for assessment in various clinical and research applications. Table 11 summarizes the writing committee's potential indications for the use of CMR in clinical practice situations.

Table 11. Summary of Potential Indications for the Use of Cardiovascular Magnetic Resonance

Disease/Condition	Recommendations for Use in Clinical Practice
Heart failure	CMR may be used for assessment of LV and RV size and morphology, systolic and diastolic function, and for characterizing myocardial tissue for the purpose of understanding the etiology of LV systolic or diastolic dysfunction. The writing committee recognizes the potential capabilities of spectroscopic techniques for acquiring metabolic information of the heart when evaluating individuals with heart failure.
Coronary artery disease	CMR may be used for identifying coronary artery anomalies and aneurysms and for determining coronary artery patency. In specialized centers, CMR may be uniquely useful in identifying patients with multivessel coronary artery disease without exposure to ionizing radiation or iodinated contrast medium.
Ischemic heart disease	The combination of CMR stress perfusion, function, and LGE allows the use of CMR as a primary form of testing for • identifying patients with ischemic heart disease when there are resting ECG abnormalities or an inability to exercise, • defining patients with large vessel coronary artery disease and its distribution who are candidates for interventional procedures, or • determining patients who are appropriate candidates for interventional procedures. Assessment of LV wall motion after low-dose dobutamine in patients with resting akinetic LV wall segments is useful for identifying patients who will develop improvement in LV systolic function after coronary arterial revascularization. The writing committee recognizes the potential advantages of spectroscopic techniques for identifying early evidence of myocardial ischemia that may or may not be evident using existing non-CMR methods.
Myocardial infarction/scar	LGE-CMR may be used for identifying the extent and location of myocardial necrosis in individuals suspected of having or possessing chronic or acute ischemic heart disease.
Nonischemic cardiomyopathy/ myocarditis	CMR may be used for assessment of patients with LV dysfunction or hypertrophy or suspected forms of cardiac injury not related to ischemic heart disease. When the diagnosis is unclear, CMR may be considered to identify the etiology of cardiac dysfunction in patients presenting with heart failure including • evaluation of dilated cardiomyopathy in the setting of normal coronary arteries, • patients with positive cardiac enzymes without obstructive atherosclerosis on angiography, • patients suspected of amyloidosis or other infiltrative diseases, • hypertrophic cardiomyopathy, • arrhythmogenic right ventricular dysplasia, or • syncope or ventricular arrhythmia.
Assessment of valvular heart disease	CMR may be used for assessing individuals with valvular heart disease in which evaluation of valvular stenosis, regurgitation, para- or perivalvular masses, perivalvular complications of infectious processes, or prosthetic valve disease are needed. CMR may be useful in identifying serial changes in LV volumes or mass in patients with valvular dysfunction.
Cardiac masses	CMR may be used for clinical evaluation of cardiac masses, extracardiac structures, and involvement and characterization of masses in the differentiation of tumors from thrombi.
Pericardial disease (constrictive pericarditis)	CMR may be used as a noninvasive imaging modality to diagnose patients with suspected pericardial disease. CMR can provide a comprehensive structural and functional assessment of the pericardium as well as evaluate the physiological consequences of pericardial constriction.
Congenital heart disease	CMR may be used for assessing cardiac structure and function, blood flow, and cardiac and extracardiac conduits in individuals with simple and complex congenital heart disease. Specifically, CMR can be used to identify and characterize congenital heart disease, to assess the magnitude or quantify the severity of intracardiac shunts or extracardiac conduit blood flow to evaluate the aorta, and to assess the pathological and physiologic consequences of congenital heart disease on left and right atrial and ventricular function and anatomy.
Pulmonary angiography	CE-MRA may be used in patients with a strong suspicion of pulmonary embolism in whom the results of other tests are equivocal or for whom iodinated contrast material or ionizing radiation are relatively contraindicated (255). The writing committee agrees that data in the literature are insufficient to recommend where pulmonary CE-MRA should fit into a diagnostic pathway for pulmonary embolism.
Atrial fibrillation	CMR may be used for assessing left atrial structure and function in patients with atrial fibrillation. The writing committee recognizes that evolving techniques utilizing LGE may have high utility for identifying evidence of fibrotic tissue within the atrial wall or an adjoining structure. Standardization of protocols and further studies are needed to determine if CMR provides a reliable effective method for detecting thrombi in the left atrial appendage in patients with atrial fibrillation. CMR is recommended for identifying pulmonary vein anatomy prior to or after electrophysiology procedures without need for patient exposure to ionizing radiation.
Peripheral arterial disease	CMR recommendations for PAD are in agreement with current guidelines and appropriate use criteria. CMR for PAD 1. is recommended to diagnose anatomic location and degree of stenosis of PAD (Class I, *Level of Evidence: A*); 2. should be performed with gadolinium enhancement (Class I, *Level of Evidence: B*); and 3. is useful in selecting patients with lower extremity PAD as candidates for endovascular intervention (Class I, *Level of Evidence: A*). CMR of the extremities may be considered 1. to select patients with lower extremity PAD as candidates for surgical bypass and to select the sites of surgical anastomosis (Class IIb, *Level of Evidence: B*); and 2. for post-revascularization (endovascular and surgical bypass) surveillance in patients with lower extremity PAD (Class IIb, *Level of Evidence: B*) (288). Additionally, MRA of the lower extremities is appropriate for patients with claudication.
Carotid arterial disease	CMR may be used for defining the location and extent of carotid arterial stenoses.
CMR of thoracic aortic disease	CMR may be used for defining the location and extent of aortic aneurysms, erosions, ulcers, dissections; evaluating postsurgical processes involving the aorta and surrounding structures, and aortic size blood flow and cardiac cycle–dependent changes in area.
Renal arterial disease	CMR may be used for evaluating renal arterial stenoses and quantifying renal arterial blood flow.

CE-MRA indicates contrast-enhanced magnetic resonance angiography; CMR, cardiovascular magnetic resonance; ECG, electrocardiogram; LGE, late gadolinium enhancement; LV, left ventricular; RV, right ventricular; MRA, magnetic resonance angiography; and PAD, peripheral arterial disease.

Staff

American College of Cardiology Foundation

John C. Lewin, MD, Chief Executive Officer

Charlene May, Senior Director, Science and Clinical Policy

Dawn R. Phoubandith, MSW, Director, ACCF Clinical Documents

Tanja Kharlamova, Associate Director, Science and Clinical Policy

Fareen Pourhamidi, MS, MPH, Senior Specialist, Evidence-Based Medicine

María Velásquez, Specialist, Science and Clinical Policy

Erin A. Barrett, Senior Specialist, Science and Clinical Policy

REFERENCES

1. Saini S, Frankel RB, Stark DD, et al. Magnetism: a primer and review. AJR Am J Roentgenol. 1988;150:735–43.
2. Pettigrew RI. Dynamic cardiac MR imaging: techniques and applications. Radiol Clin North Am. 1989;27:1183–203.
3. Hundley WG, Li HF, Willard JE, et al. Magnetic resonance imaging assessment of the severity of mitral regurgitation: comparison with invasive techniques. Circulation. 1995;92:1151–8.
4. Gandy SJ, Waugh SA, Nicholas RS, et al. Comparison of the reproducibility of quantitative cardiac left ventricular assessments in healthy volunteers using different MRI scanners: a multicenter simulation. J Magn Reson Imaging. 2008;28:359–65.
5. Edelman RR, Chien D, Kim D. Fast selective black blood MR imaging. Radiology. 1991;181:655–60.
6. Haddad JL, Rofsky NM, Ambrosino MM, et al. T2-weighted MR imaging of the chest: comparison of electrocardiograph-triggered conventional and turbo spin-echo and nontriggered turbo spin-echo sequences. J Magn Reson Imaging. 1995;5:325–9.
7. Simonetti OP, Finn JP, White RD, et al. "Black blood" T2-weighted inversion-recovery MR imaging of the heart. Radiology. 1996;199:49–57.
8. Stark DD, Higgins CB, Lanzer P, et al. Magnetic resonance imaging of the pericardium: normal and pathologic findings. Radiology. 1984;150:469–74.
9. Didier D, Saint-Martin C, Lapierre C, et al. Coarctation of the aorta: pre and postoperative evaluation with MRI and MR angiography; correlation with echocardiography and surgery. Int J Cardiovasc Imaging. 2006;22:457–75.
10. Duerinckx AJ, Wexler L, Banerjee A, et al. Postoperative evaluation of pulmonary arteries in congenital heart surgery by magnetic resonance imaging: comparison with echocardiography. Am Heart J. 1994;128:1139–46.
11. Nienaber CA, Rehders TC, Fratz S. Detection and assessment of congenital heart disease with magnetic resonance techniques. J Cardiovasc Magn Reson. 1999;1:169–84.
12. Nienaber CA, Spielmann RP, von Kodolitsch Y, et al. Diagnosis of thoracic aortic dissection: magnetic resonance imaging versus transesophageal echocardiography. Circulation. 1992;85:434–47.
13. Nienaber CA, von Kodolitsch Y, Brockhoff CJ, et al. Comparison of conventional and transesophageal echocardiography with magnetic resonance imaging for anatomical mapping of thoracic aortic dissection: a dual noninvasive imaging study with anatomical and/or angiographic validation. Int J Card Imaging. 1994;10:1–14.
14. von Kodolitsch Y, Csosz SK, Koschyk DH, et al. Intramural hematoma of the aorta: predictors of progression to dissection and rupture. Circulation. 2003;107:1158–63.
15. Utz JA, Herfkens RJ, Heinsimer JA, et al. Valvular regurgitation: dynamic MR imaging. Radiology. 1988;168:91–4.
16. Natori S, Lai S, Finn JP, et al. Cardiovascular function in multi-ethnic study of atherosclerosis: normal values by age, sex, and ethnicity. AJR Am J Roentgenol. 2006;186:S357–65.
17. Sechtem U, Pflugfelder PW, Gould RG, et al. Measurement of right and left ventricular volumes in healthy individuals with cine MR imaging. Radiology. 1987;163:697–702.
18. Semelka RC, Tomei E, Wagner S, et al. Normal left ventricular dimensions and function: interstudy reproducibility of measurements with cine MR imaging. Radiology. 1990;174:763–8.
19. Semelka RC, Tomei E, Wagner S, et al. Interstudy reproducibility of dimensional and functional measurements between cine magnetic resonance studies in the morphologically abnormal left ventricle. Am Heart J. 1990;119:1367–73.
20. Barkhausen J, Ruehm SG, Goyen M, et al. MR evaluation of ventricular function: true fast imaging with steady-state precession versus fast low-angle shot cine MR imaging: feasibility study. Radiology. 2001;219:264–9.
21. Moon JC, Lorenz CH, Francis JM, et al. Breath-hold FLASH and FISP cardiovascular MR imaging: left ventricular volume differences and reproducibility. Radiology. 2002;223:789–97.
22. Malayeri AA, Johnson WC, Macedo R, et al. Cardiac cine MRI: quantification of the relationship between fast gradient echo and steady-state free precession for determination of myocardial mass and volumes. J Magn Reson Imaging. 2008;28:60–6.
23. Bloomer TN, Plein S, Radjenovic A, et al. Cine MRI using steady state free precession in the radial long axis orientation is a fast accurate method for obtaining volumetric data of the left ventricle. J Magn Reson Imaging. 2001;14:685–92.
24. Bloomgarden DC, Fayad ZA, Ferrari VA, et al. Global cardiac function using fast breath-hold MRI: validation of new acquisition and analysis techniques. Magn Reson Med. 1997;37:683–92.
25. Friedrich MG, Schulz-Menger J, Strohm O, et al. The diagnostic impact of 2D- versus 3D-left ventricular volumetry by MRI in patients with suspected heart failure. MAGMA. 2000;11:16–9.
26. Bellenger NG, Davies LC, Francis JM, et al. Reduction in sample size for studies of remodeling in heart failure by the use of cardiovascular magnetic resonance. J Cardiovasc Magn Reson. 2000;2:271–8.
27. Bellenger NG, Burgess MI, Ray SG, et al. Comparison of left ventricular ejection fraction and volumes in heart failure by echocardiography, radionuclide ventriculography and cardiovascular magnetic resonance; are they interchangeable? Eur Heart J. 2000;21:1387–96.
28. Grothues F, Smith GC, Moon JC, et al. Comparison of interstudy reproducibility of cardiovascular magnetic resonance with 2-dimensional echocardiography in normal subjects and in patients with heart failure or left ventricular hypertrophy. Am J Cardiol. 2002;90:29–34.
29. Grothues F, Moon JC, Bellenger NG, et al. Interstudy reproducibility of right ventricular volumes, function, and mass with cardiovascular magnetic resonance. Am Heart J. 2004;147:218–23.
30. Pattynama PM, Lamb HJ, van der Velde EA, et al. Left ventricular measurements with cine and spin-echo MR imaging: a study of reproducibility with variance component analysis. Radiology. 1993;187:261–8.
31. Axel L, Dougherty L. MR imaging of motion with spatial modulation of magnetization. Radiology. 1989;171:841–5.
32. Zerhouni EA, Parish DM, Rogers WJ, et al. Human heart: tagging with MR imaging—a method for noninvasive assessment of myocardial motion. Radiology. 1988;169:59–63.
33. Edvardsen T, Rosen BD, Pan L, et al. Regional diastolic dysfunction in individuals with left ventricular hypertrophy measured by tagged magnetic resonance imaging—the Multi-Ethnic Study of Atherosclerosis (MESA). Am Heart J. 2006;151:109–14.
34. Fernandes VR, Polak JF, Edvardsen T, et al. Subclinical atherosclerosis and incipient regional myocardial dysfunction in asymptomatic individuals: the Multi-Ethnic Study of Atherosclerosis (MESA). J Am Coll Cardiol. 2006;47:2420–8.
35. Reichek N. MRI myocardial tagging. J Magn Reson Imaging. 1999;10:609–16.
36. Rosen BD, Lima JA, Nasir K, et al. Lower myocardial perfusion reserve is associated with decreased regional left ventricular function in asymptomatic participants of the multi-ethnic study of atherosclerosis. Circulation. 2006;114:289–97.
37. Aletras AH, Ding S, Balaban RS, et al. DENSE: displacement encoding with stimulated echoes in cardiac functional MRI. J Magn Reson. 1999;137:247–52.
38. Osman NF, Kerwin WS, McVeigh ER, et al. Cardiac motion tracking using CINE harmonic phase (HARP) magnetic resonance imaging. Magn Reson Med. 1999;42:1048–60.
39. Ingwall J. ATP and the Heart (Basic Science for the Cardiologist). Norwell, Mass: Kluwer Academic Publishers, 2002.

40. Firmin DN, Nayler GL, Kilner PJ, et al. The application of phase shifts in NMR for flow measurement. Magn Reson Med. 1990;14:230–41.

41. Moran PR. A flow velocity zeugmatographic interlace for NMR imaging in humans. Magn Reson Imaging. 1982;1:197–203.

42. Hangiandreou NJ, Rossman PJ, Riederer SJ. Analysis of MR phase-contrast measurements of pulsatile velocity waveforms. J Magn Reson Imaging. 1993;3:387–94.

43. Hundley WG, Li HF, Hillis LD, et al. Quantitation of cardiac output with velocity-encoded, phase-difference magnetic resonance imaging. Am J Cardiol. 1995;75:1250–5.

44. Markl M, Harloff A, Bley TA, et al. Time-resolved 3D MR velocity mapping at 3T: improved navigator-gated assessment of vascular anatomy and blood flow. J Magn Reson Imaging. 2007;25:824–31.

45. Kuehne T, Yilmaz S, Steendijk P, et al. Magnetic resonance imaging analysis of right ventricular pressure-volume loops: in vivo validation and clinical application in patients with pulmonary hypertension. Circulation. 2004;110:2010–6.

46. Bogren HG, Buonocore MH, Follette DM. Four-dimensional aortic blood flow patterns in thoracic aortic grafts. J Cardiovasc Magn Reson. 2000;2:201–8.

47. Caruthers SD, Lin SJ, Brown P, et al. Practical value of cardiac magnetic resonance imaging for clinical quantification of aortic valve stenosis: comparison with echocardiography. Circulation. 2003;108:2236–43.

48. Hundley WG, Li HF, Lange RA, et al. Assessment of left-to-right intracardiac shunting by velocity-encoded, phase-difference magnetic resonance imaging: a comparison with oximetric and indicator dilution techniques. Circulation. 1995;91:2955–60.

49. Weber OM, Higgins CB. MR evaluation of cardiovascular physiology in congenital heart disease: flow and function. J Cardiovasc Magn Reson. 2006;8:607–17.

50. Kwong RY, Schussheim AE, Rekhraj S, et al. Detecting acute coronary syndrome in the emergency department with cardiac magnetic resonance imaging. Circulation. 2003;107:531–7.

51. Pérez-Mayoral E, Negri V, Soler-Padrós J, et al. Chemistry of paramagnetic and diamagnetic contrast agents for Magnetic Resonance Imaging and Spectroscopy pH responsive contrast agents. Eur J Radiol. 2008;67:453–8.

52. Jahnke C, Nagel E, Gebker R, et al. Prognostic value of cardiac magnetic resonance stress tests: adenosine stress perfusion and dobutamine stress wall motion imaging. Circulation. 2007;115:1769–76.

53. Al-Saadi N, Nagel E, Gross M, et al. Noninvasive detection of myocardial ischemia from perfusion reserve based on cardiovascular magnetic resonance. Circulation. 2000;101:1379–83.

54. Cullen JH, Horsfield MA, Reek CR, et al. A myocardial perfusion reserve index in humans using first-pass contrast-enhanced magnetic resonance imaging. J Am Coll Cardiol. 1999;33:1386–94.

55. Nagel E, Klein C, Paetsch I, et al. Magnetic resonance perfusion measurements for the noninvasive detection of coronary artery disease. Circulation. 2003;108:432–7.

56. Al-Saadi N, Nagel E, Gross M, et al. Improvement of myocardial perfusion reserve early after coronary intervention: assessment with cardiac magnetic resonance imaging. J Am Coll Cardiol. 2000;36:1557–64.

57. Fenchel M, Franow A, Stauder NI, et al. Myocardial perfusion after angioplasty in patients suspected of having single-vessel coronary artery disease: improvement detected at rest-stress first-pass perfusion MR imaging—initial experience. Radiology. 2005;237:67–74.

58. Lauerma K, Virtanen KS, Sipila LM, et al. Multislice MRI in assessment of myocardial perfusion in patients with single-vessel proximal left anterior descending coronary artery disease before and after revascularization. Circulation. 1997;96:2859–67.

59. Wu KC, Kim RJ, Bluemke DA, et al. Quantification and time course of microvascular obstruction by contrast-enhanced echocardiography and magnetic resonance imaging following acute myocardial infarction and reperfusion. J Am Coll Cardiol. 1998;32:1756–64.

60. Yan AT, Gibson CM, Larose E, et al. Characterization of microvascular dysfunction after acute myocardial infarction by cardiovascular magnetic resonance first-pass perfusion and late gadolinium enhancement imaging. J Cardiovasc Magn Reson. 2006;8:831–7.

61. Bogaert J, Kalantzi M, Rademakers FE, et al. Determinants and impact of microvascular obstruction in successfully reperfused ST-segment elevation myocardial infarction: assessment by magnetic resonance imaging. Eur Radiol. 2007;17:2572–80.

62. Hombach V, Grebe O, Merkle N, et al. Sequelae of acute myocardial infarction regarding cardiac structure and function and their prognostic significance as assessed by magnetic resonance imaging. Eur Heart J. 2005;26:549–57.

63. Wu KC, Zerhouni EA, Judd RM, et al. Prognostic significance of microvascular obstruction by magnetic resonance imaging in patients with acute myocardial infarction. Circulation. 1998;97:765–72.

64. Tarantini G, Cacciavillani L, Corbetti F, et al. Duration of ischemia is a major determinant of transmurality and severe microvascular obstruction after primary angioplasty: a study performed with contrast-enhanced magnetic resonance. J Am Coll Cardiol. 2005;46:1229–35.

65. Schwitter J, Wacker CM, van Rossum AC, et al. MR-IMPACT: comparison of perfusion-cardiac magnetic resonance with single-photon emission computed tomography for the detection of coronary artery disease in a multicentre, multivendor, randomized trial. Eur Heart J. 2008;29:480–9.

66. Sakuma H, Suzawa N, Ichikawa Y, et al. Diagnostic accuracy of stress first-pass contrast-enhanced myocardial perfusion MRI compared with stress myocardial perfusion scintigraphy. AJR Am J Roentgenol. 2005;185:95–102.

67. Schwitter J, Nanz D, Kneifel S, et al. Assessment of myocardial perfusion in coronary artery disease by magnetic resonance: a comparison with positron emission tomography and coronary angiography. Circulation. 2001;103:2230–5.

68. Wagner A, Mahrholdt H, Holly TA, et al. Contrast-enhanced MRI and routine single-photon emission computed tomography (SPECT) perfusion imaging for detection of subendocardial myocardial infarcts: an imaging study. Lancet. 2003;361:374–9.

69. Prakash A, Powell AJ, Krishnamurthy R, et al. Magnetic resonance imaging evaluation of myocardial perfusion and viability in congenital and acquired pediatric heart disease. Am J Cardiol. 2004;93:657–61.

70. Koelemay MJ, Lijmer JG, Stoker J, et al. Magnetic resonance angiography for the evaluation of lower extremity arterial disease: a meta-analysis. JAMA. 2001;285:1338–45.

71. Nelemans PJ, Leiner T, de Vet HC, et al. Peripheral arterial disease: meta-analysis of the diagnostic performance of MR angiography. Radiology. 2000;217:105–14.

72. Yucel EK, Anderson CM, Edelman RR, et al. AHA scientific statement: magnetic resonance angiography: update on applications for extracranial arteries. Circulation. 1999;100:2284–301.

73. Krinsky GA, Rofsky NM, DeCorato DR, et al. Thoracic aorta: comparison of gadolinium-enhanced three-dimensional MR angiography with conventional MR imaging. Radiology. 1997;202:183–93.

74. Willerson JT, Scales F, Mukherjee A, et al. Abnormal myocardial fluid retention as an early manifestation of ischemic injury. Am J Pathol. 1977;87:159–88.

75. Ingkanisorn WP, Kwong RY, Bohme NS, et al. Prognosis of negative adenosine stress magnetic resonance in patients presenting to an emergency department with chest pain. J Am Coll Cardiol. 2006;47:1427–32.

76. Rehwald WG, Fieno DS, Chen EL, et al. Myocardial magnetic resonance imaging contrast agent concentrations after reversible and irreversible ischemic injury. Circulation. 2002;105:224–9.

77. Kim RJ, Wu E, Rafael A, et al. The use of contrast-enhanced magnetic resonance imaging to identify reversible myocardial dysfunction. N Engl J Med. 2000;343:1445–53.

78. Kwong RY, Chan AK, Brown KA, et al. Impact of unrecognized myocardial scar detected by cardiac magnetic resonance imaging on event-free survival in patients presenting with signs or symptoms of coronary artery disease. Circulation. 2006;113:2733–43.

79. Maceira AM, Joshi J, Prasad SK, et al. Cardiovascular magnetic resonance in cardiac amyloidosis. Circulation. 2005;111:186–93.

80. Colucci WS, Braunwald E. Pathophysiology of heart failure. In: Zipes DP, Libby P, Bonow R, eds. Braunwald's Heart Disease: A Textbook of Cardiovascular Medicine. Philadelphia, Pa: Elsevier Saunders, 2005:509–38.

81. Hudsmith LE, Petersen SE, Francis JM, et al. Normal human left and right ventricular and left atrial dimensions using steady state free precession magnetic resonance imaging. J Cardiovasc Magn Reson. 2005;7:775–82.

82. Gotte MJ, Germans T, Russel IK, et al. Myocardial strain and torsion quantified by cardiovascular magnetic resonance tissue tagging: studies in normal and impaired left ventricular function. J Am Coll Cardiol. 2006;48:2002–11.

83. Paelinck BP, de Roos A, Bax JJ, et al. Feasibility of tissue magnetic resonance imaging: a pilot study in comparison with tissue Doppler imaging and invasive measurement. J Am Coll Cardiol. 2005; 45:1109–16.

84. Abdel-Aty H, Zagrosek A, Schulz-Menger J, et al. Delayed enhancement and T2-weighted cardiovascular magnetic resonance imaging differentiate acute from chronic myocardial infarction. Circulation. 2004;109:2411–6.

85. Assomull RG, Prasad SK, Lyne J, et al. Cardiovascular magnetic resonance, fibrosis, and prognosis in dilated cardiomyopathy. J Am Coll Cardiol. 2006;48:1977–85.

86. Maceira AM, Prasad SK, Khan M, et al. Normalized left ventricular systolic and diastolic function by steady state free precession cardiovascular magnetic resonance. J Cardiovasc Magn Reson. 2006; 8:417–26.

87. Castillo E, Osman NF, Rosen BD, et al. Quantitative assessment of regional myocardial function with MR-tagging in a multi-center study: interobserver and intraobserver agreement of fast strain analysis with Harmonic Phase (HARP) MRI. J Cardiovasc Magn Reson. 2005;7:783–91.

88. McCrohon JA, Moon JC, Prasad SK, et al. Differentiation of heart failure related to dilated cardiomyopathy and coronary artery disease using gadolinium-enhanced cardiovascular magnetic resonance. Circulation. 2003;108:54–9.

89. Adabag AS, Maron BJ, Appelbaum E, et al. Occurrence and frequency of arrhythmias in hypertrophic cardiomyopathy in relation to delayed enhancement on cardiovascular magnetic resonance. J Am Coll Cardiol. 2008;51:1369–74.

90. Mahrholdt H, Goedecke C, Wagner A, et al. Cardiovascular magnetic resonance assessment of human myocarditis: a comparison to histology and molecular pathology. Circulation. 2004;109:1250–8.

91. Skouri HN, Dec GW, Friedrich MG, et al. Noninvasive imaging in myocarditis. J Am Coll Cardiol. 2006;48:2085–93.

92. Anderson LJ, Westwood MA, Prescott E, et al. Development of thalassaemic iron overload cardiomyopathy despite low liver iron levels and meticulous compliance to desferrioxamine. Acta Haematol. 2006;115:106–8.

93. Neubauer S, Horn M, Cramer M, et al. Myocardial phosphocreatine-to-ATP ratio is a predictor of mortality in patients with dilated cardiomyopathy. Circulation. 1997;96:2190–6.

94. Jung WI, Sieverding L, Breuer J, et al. 31P NMR spectroscopy detects metabolic abnormalities in asymptomatic patients with hypertrophic cardiomyopathy. Circulation. 1998;97:2536–42.

95. Strohm O, Schulz-Menger J, Pilz B, et al. Measurement of left ventricular dimensions and function in patients with dilated cardiomyopathy. J Magn Reson Imaging. 2001;13:367–71.

96. Hunt SA, Abraham W, Chin M, et al. ACC/AHA 2005 guideline update for the diagnosis and management of chronic heart failure in the adult: a report of the American College of Cardiology/American Heart Association Task Force on Practice Guidelines (Writing Committee to Update the 2001 Guidelines for the Evaluation and Management of Heart Failure). J Am Coll Cardiol. 2005;46:e1–82.

97. Hendel RC, Patel MR, Kramer CM, et al. ACCF/ACR/SCCT/SCMR/ASNC/NASCI/SCAI/SIR 2006 appropriateness criteria for cardiac computed tomography and cardiac magnetic resonance imaging: a report of the American College of Cardiology Foundation Quality Strategic Directions Committee Appropriateness Criteria Working Group, American College of Radiology, Society of Cardiovascular Computed Tomography, Society for Cardiovascular Magnetic Resonance, American Society of Nuclear Cardiology, North American Society for Cardiac Imaging, Society for Cardiovascular Angiography and Interventions, and Society of Interventional Radiology. J Am Coll Cardiol. 2006;48:1475–97.

98. Bunce NH, Lorenz CH, Keegan J, et al. Coronary artery anomalies: assessment with free-breathing three-dimensional coronary MR angiography. Radiology. 2003;227:201–8.

99. Cheitlin MD, De Castro CM, McAllister HA. Sudden death as a complication of anomalous left coronary origin from the anterior sinus of Valsalva, a not-so-minor congenital anomaly. Circulation. 1974;50:780–7.

100. Gharib A, Ho V, Rosing D, et al. Coronary artery anomalies and variants: technical feasibility of assessment with coronary MR angiography at 3T. Radiology 2008;247:220–227. Abstract.

101. McConnell MV, Ganz P, Selwyn AP, et al. Identification of anomalous coronary arteries and their anatomic course by magnetic resonance coronary angiography. Circulation. 1995;92:3158–62.

102. Post JC, van Rossum AC, Bronzwaer JG, et al. Magnetic resonance angiography of anomalous coronary arteries. A new gold standard for delineating the proximal course? Circulation. 1995;92:3163–71.

103. Setser R, Arruda J, Weaver JA, et al. Exclusion of coronary artery anomalies in patients with congenital cardiovascular abnormalities using whole heart approach. J Cardiovasc Magn Reson 2007;9: 128–9. Abstract.

104. Taylor AM, Thorne SA, Rubens MB, et al. Coronary artery imaging in grown up congenital heart disease: complementary role of magnetic resonance and X-ray coronary angiography. Circulation. 2000; 101:1670–8.

105. Vliegen HW, Doornbos J, de Roos A, et al. Value of fast gradient echo magnetic resonance angiography as an adjunct to coronary arteriography in detecting and confirming the course of clinically significant coronary artery anomalies. Am J Cardiol. 1997;79:773–6.

106. Engel HJ, Torres C, Page HL Jr. Major variations in anatomical origin of the coronary arteries: angiographic observations in 4,250 patients without associated congenital heart disease. Cathet Cardiovasc Diagn. 1975;1:157–69.

107. Pennell DJ, Sechtem U, Higgins C, et al. Clinical indications for cardiovascular magnetic resonance: consensus panel report 1. J Cardiovasc Magn Reson. 2004;6:727–65.

108. Akagi T, Rose V, Benson LN, et al. Outcome of coronary artery aneurysms after Kawasaki disease. J Pediatr. 1992;121:689–94.

109. Greil GF, Stuber M, Botnar RM, et al. Coronary magnetic resonance angiography in adolescents and young adults with Kawasaki disease. Circulation. 2002;105:908–11.

110. Mavrogeni S, Papadopoulos G, Douskou M, et al. Magnetic resonance angiography is equivalent to X-ray coronary angiography for the evaluation of coronary arteries in Kawasaki disease. J Am Coll Cardiol. 2004;43:649–52.

111. Mavrogeni S, Papadopoulos G, Douskou M, et al. Magnetic resonance angiography, function and viability evaluation in patients with Kawasaki disease. J Cardiovasc Magn Reson. 2006;8:493–8.

112. Mavrogeni S, Manginas A, Papadakis E, et al. Correlation between magnetic resonance angiography (MRA) and quantitative coronary angiography (QCA) in ectatic coronary vessels. J Cardiovasc Magn Reson. 2004;6:17–23.

113. Bogaert J, Kuzo R, Dymarkowski S, et al. Coronary artery imaging with real-time navigator three-dimensional turbo-field-echo MR coronary angiography: initial experience. Radiology. 2003;226: 707–16.

114. Botnar RM, Stuber M, Danias PG, et al. Improved coronary artery definition with T2-weighted, free-breathing, three-dimensional coronary MRA. Circulation. 1999;99:3139–48.

115. Dewey M, Teige F, Schnapauff D, et al. Combination of free-breathing and breathhold steady-state free precession magnetic resonance angiography for detection of coronary artery stenoses. J Magn Reson Imaging. 2006;23:674–81.

116. Jahnke C, Paetsch I, Schnackenburg B, et al. Coronary MR angiography with steady-state free precession: individually adapted breathhold technique versus free-breathing technique. Radiology. 2004; 232:669–76.

117. Jahnke C, Paetsch I, Nehrke K, et al. Rapid and complete coronary arterial tree visualization with magnetic resonance imaging: feasibility and diagnostic performance. Eur Heart J. 2005;26:2313–9.

118. Kim WY, Danias PG, Stuber M, et al. Coronary magnetic resonance angiography for the detection of coronary stenoses. N Engl J Med. 2001;345:1863–9.

119. Maintz D, Aepfelbacher FC, Kissinger KV, et al. Coronary MR angiography: comparison of quantitative and qualitative data from four techniques. AJR Am J Roentgenol. 2004;182:515–21.

120. Ozgun M, Hoffmeier A, Kouwenhoven M, et al. Comparison of 3D segmented gradient-echo and steady-state free precession coronary MRI sequences in patients with coronary artery disease. AJR Am J Roentgenol. 2005;185:103–9.

121. Sakuma H, Ichikawa Y, Suzawa N, et al. Assessment of coronary arteries with total study time of less than 30 minutes by using whole-heart coronary MR angiography. Radiology. 2005;237:316–21.

122. Sakuma H, Ichikawa Y, Chino S, et al. Detection of coronary artery stenosis with whole-heart coronary magnetic resonance angiography. J Am Coll Cardiol. 2006;48:1946–50.

123. Sommer T, Hofer U, Meyer C, et al. Submillimeter 3D coronary MR angiography with real-time navigator correction in 107 patients with suspected coronary artery disease. Rofo. 2002;174:459–66.

124. Hauser T, Yeon SB, Appelbaum E, et al. Multimodality CMR detection of coronary artery disease in patients with heart failure and depressed systolic function: superiority of coronary MRI compared to late gadolinium enhancement. J Cardiovasc Magn Reson. 2009. Abstract in press.

125. Liu X, Zhao X, Huang J, et al. Comparison of 3D free-breathing coronary MR angiography and 64–MDCT angiography for detection of coronary stenosis in patients with high calcium scores. AJR Am J Roentgenol. 2007;189:1326–32.

126. Aurigemma GP, Reichek N, Axel L, et al. Noninvasive determination of coronary artery bypass graft patency by cine magnetic resonance imaging. Circulation. 1989;80:1595–602.

127. Engelmann MG, Knez A, von Smekal A, et al. Noninvasive coronary bypass graft imaging after multivessel revascularisation. Int J Cardiol. 2000;76:65–74.

128. Fitzgibbon GM, Kafka HP, Leach AJ, et al. Coronary bypass graft fate and patient outcome: angiographic follow-up of 5,065 grafts related to survival and reoperation in 1,388 patients during 25 years. J Am Coll Cardiol. 1996;28:616–26.

129. Goldman S, Copeland J, Moritz T, et al. Saphenous vein graft patency 1 year after coronary artery bypass surgery and effects of antiplatelet therapy: results of a Veterans Administration Cooperative Study. Circulation. 1989;80:1190–7.

130. van Geuns RJ, Wielopolski PA, de Bruin HG, et al. MR coronary angiography with breath-hold targeted volumes: preliminary clinical results. Radiology. 2000;217:270–7.

131. White RD, Caputo GR, Mark AS, et al. Coronary artery bypass graft patency: noninvasive evaluation with MR imaging. Radiology. 1987;164:681–6.

132. Langerak SE, Kunz P, Vliegen HW, et al. MR flow mapping in coronary artery bypass grafts: a validation study with Doppler flow measurements. Radiology. 2002;222:127–35.

133. Langerak SE, Vliegen HW, Jukema JW, et al. Value of magnetic resonance imaging for the noninvasive detection of stenosis in coronary artery bypass grafts and recipient coronary arteries. Circulation. 2003;107:1502–8.

134. Gibbons RJ, Abrams J, Chatterjee K, et al. ACC/AHA 2002 guideline update for the management of patients with chronic stable angina—summary article: a report of the American College of Cardiology/American Heart Association Task Force on Practice Guidelines (Committee on the Management of Patients With Chronic Stable Angina). J Am Coll Cardiol. 2003;41:159–68.

135. Wilke N, Jerosch-Herold M, Wang Y, et al. Myocardial perfusion reserve: assessment with multisection, quantitative, first-pass MR imaging. Radiology. 1997;204:373–84.

136. Schaefer S, van Tyen R, Saloner D. Evaluation of myocardial perfusion abnormalities with gadolinium-enhanced snapshot MR imaging in humans. Work in progress. Radiology. 1992;185:795–801.

137. Cury RC, Cattani CA, Gabure LA, et al. Diagnostic performance of stress perfusion and delayed-enhancement MR imaging in patients with coronary artery disease. Radiology. 2006;240:39–45.

138. Doyle M, Fuisz A, Kortright E, et al. The impact of myocardial flow reserve on the detection of coronary artery disease by perfusion imaging methods: an NHLBI WISE study. J Cardiovasc Magn Reson. 2003;5:475–85.

139. Giang TH, Nanz D, Coulden R, et al. Detection of coronary artery disease by magnetic resonance myocardial perfusion imaging with various contrast medium doses: first European multi-centre experience. Eur Heart J. 2004;25:1657–65.

140. Ishida N, Sakuma H, Motoyasu M, et al. Noninfarcted myocardium: correlation between dynamic first-pass contrast-enhanced myocardial MR imaging and quantitative coronary angiography. Radiology. 2003;229:209–16.

141. Kawase Y, Nishimoto M, Hato K, et al. Assessment of coronary artery disease with nicorandil stress magnetic resonance imaging. Osaka City Med J. 2004;50:87–94.

142. Klem I, Heitner JF, Shah DJ, et al. Improved detection of coronary artery disease by stress perfusion cardiovascular magnetic resonance with the use of delayed enhancement infarction imaging. J Am Coll Cardiol. 2006;47:1630–8.

143. Pilz G, Bernhardt P, Klos M, et al. Clinical implication of adenosine-stress cardiac magnetic resonance imaging as potential gatekeeper prior to invasive examination in patients with AHA/ACC class II indication for coronary angiography. Clin Res Cardiol. 2006;95:531–8.

144. Plein S, Radjenovic A, Ridgway JP, et al. Coronary artery disease: myocardial perfusion MR imaging with sensitivity encoding versus conventional angiography. Radiology. 2005;235:423–30.

145. Takase B, Nagata M, Kihara T, et al. Whole-heart dipyridamole stress first-pass myocardial perfusion MRI for the detection of coronary artery disease. Jpn Heart J. 2004;45:475–86.

146. Nandalur KR, Dwamena BA, Choudhri AF, et al. Diagnostic performance of stress cardiac magnetic resonance imaging in the detection of coronary artery disease: a meta-analysis. J Am Coll Cardiol. 2007;50:1343–53.

147. Wahl A, Paetsch I, Gollesch A, et al. Safety and feasibility of high-dose dobutamine-atropine stress cardiovascular magnetic resonance for diagnosis of myocardial ischaemia: experience in 1000 consecutive cases. Eur Heart J. 2004;25:1230–6.

148. Nagel E, Lehmkuhl HB, Bocksch W, et al. Noninvasive diagnosis of ischemia-induced wall motion abnormalities with the use of high-dose dobutamine stress MRI: comparison with dobutamine stress echocardiography. Circulation. 1999;99:763–70.

149. Hundley WG, Hamilton CA, Thomas MS, et al. Utility of fast cine magnetic resonance imaging and display for the detection of myocardial ischemia in patients not well suited for second harmonic stress echocardiography. Circulation. 1999;100:1697–702.

150. Baer FM, Smolarz K, Jungehulsing M, et al. Feasibility of high-dose dipyridamole-magnetic resonance imaging for detection of coronary artery disease and comparison with coronary angiography. Am J Cardiol. 1992;69:51–6.

151. Baer FM, Voth E, Theissen P, et al. Coronary artery disease: findings with GRE MR imaging and Tc-99m-methoxyisobutyl-isonitrile SPECT during simultaneous dobutamine stress. Radiology. 1994;193:203–9.

152. Jahnke C, Paetsch I, Gebker R, et al. Accelerated 4D dobutamine stress MR imaging with k-t BLAST: feasibility and diagnostic performance. Radiology. 2006;241:718–28.

153. Paetsch I, Jahnke C, Wahl A, et al. Comparison of dobutamine stress magnetic resonance, adenosine stress magnetic resonance, and adenosine stress magnetic resonance perfusion. Circulation. 2004;110:835–42.

154. Paetsch I, Jahnke C, Ferrari VA, et al. Determination of interobserver variability for identifying inducible left ventricular wall motion abnormalities during dobutamine stress magnetic resonance imaging. Eur Heart J. 2006;27:1459–64.

155. Pennell DJ, Underwood SR, Ell PJ, et al. Dipyridamole magnetic resonance imaging: a comparison with thallium-201 emission tomography. Br Heart J. 1990;64:362–9.

156. Pennell DJ, Underwood SR, Manzara CC, et al. Magnetic resonance imaging during dobutamine stress in coronary artery disease. Am J Cardiol. 1992;70:34–40.

157. Rerkpattanapipat P, Gandhi SK, Darty SN, et al. Feasibility to detect severe coronary artery stenoses with upright treadmill exercise magnetic resonance imaging. Am J Cardiol. 2003;92:603–6.

158. Schalla S, Klein C, Paetsch I, et al. Real-time MR image acquisition during high-dose dobutamine hydrochloride stress for detecting left ventricular wall-motion abnormalities in patients with coronary arterial disease. Radiology. 2002;224:845–51.

159. van Rugge FP, van der Wall EE, de Roos A, et al. Dobutamine stress magnetic resonance imaging for detection of coronary artery disease. J Am Coll Cardiol. 1993;22:431–9.

160. van Rugge FP, van der Wall EE, Spanjersberg SJ, et al. Magnetic resonance imaging during dobutamine stress for detection and localization of coronary artery disease. Quantitative wall motion analysis using a modification of the centerline method. Circulation. 1994;90:127–38.

161. Kuijpers D, Ho KY, van Dijkman PR, et al. Dobutamine cardiovascular magnetic resonance for the detection of myocardial ischemia with the use of myocardial tagging. Circulation. 2003;107:1592–7.

162. Sayad DE, Willett DL, Hundley WG, et al. Dobutamine magnetic resonance imaging with myocardial tagging quantitatively predicts

improvement in regional function after revascularization. Am J Cardiol. 1998;82:1149–51.

163. Buchthal SD, den Hollander JA, Merz CN, et al. Abnormal myocardial phosphorus-31 nuclear magnetic resonance spectroscopy in women with chest pain but normal coronary angiograms. N Engl J Med. 2000;342:829–35.

164. Weiss RG, Bottomley PA, Hardy CJ, et al. Regional myocardial metabolism of high-energy phosphates during isometric exercise in patients with coronary artery disease. N Engl J Med. 1990;323:1593–600.

165. Johnson BD, Shaw LJ, Buchthal SD, et al. Prognosis in women with myocardial ischemia in the absence of obstructive coronary disease: results from the National Institutes of Health-National Heart, Lung, and Blood Institute-Sponsored Women's Ischemia Syndrome Evaluation (WISE). Circulation. 2004;109:2993–9.

166. Antman EM, Anbe DT, Armstrong PW, et al. ACC/AHA guidelines for the management of patients with ST-elevation myocardial infarction: a report of the American College of Cardiology/American Heart Association Task Force on Practice Guidelines (Committee to Revise the 1999 Guidelines for the Management of Patients with Acute Myocardial Infarction). J Am Coll Cardiol. 2004;44:e1–211.

167. Zipes DP, Camm AJ, Borggrefe M, et al. ACC/AHA/ESC 2006 guidelines for management of patients with ventricular arrhythmias and the prevention of sudden cardiac death: a report of the American College of Cardiology/American Heart Association Task Force on Practice Guidelines and the European Society of Cardiology Committee for Practice Guidelines (Writing Committee to Develop Guidelines for Management of Patients With Ventricular Arrhythmias and the Prevention of Sudden Cardiac Death). J Am Coll Cardiol. 2006;48:e247–346.

168. Kim RJ, Lima JA, Chen EL, et al. Fast 23Na magnetic resonance imaging of acute reperfused myocardial infarction. Potential to assess myocardial viability. Circulation. 1997;95:1877–85.

169. Fieno DS, Kim RJ, Chen EL, et al. Contrast-enhanced magnetic resonance imaging of myocardium at risk: distinction between reversible and irreversible injury throughout infarct healing. J Am Coll Cardiol. 2000;36:1985–91.

170. Ibrahim T, Bulow HP, Hackl T, et al. Diagnostic value of contrast-enhanced magnetic resonance imaging and single-photon emission computed tomography for detection of myocardial necrosis early after acute myocardial infarction. J Am Coll Cardiol. 2007;49:208–16.

171. Kumar A, Abdel-Aty H, Kriedemann I, et al. Contrast-enhanced cardiovascular magnetic resonance imaging of right ventricular infarction. J Am Coll Cardiol. 2006;48:1969–76.

172. Choi KM, Kim RJ, Gubernikoff G, et al. Transmural extent of acute myocardial infarction predicts long-term improvement in contractile function. Circulation. 2001;104:1101–7.

173. Choi JW, Gibson CM, Murphy SA, et al. Myonecrosis following stent placement: association between impaired TIMI myocardial perfusion grade and MRI visualization of microinfarction. Catheter Cardiovasc Interv. 2004;61:472–6.

174. Ricciardi MJ, Wu E, Davidson CJ, et al. Visualization of discrete microinfarction after percutaneous coronary intervention associated with mild creatine kinase-MB elevation. Circulation. 2001;103:2780–3.

175. Steuer J, Bjerner T, Duvernoy O, et al. Visualisation and quantification of perioperative myocardial infarction after coronary artery bypass surgery with contrast-enhanced magnetic resonance imaging. Eur Heart J. 2004;25:1293–9.

176. Barbier CE, Bjerner T, Johansson L, et al. Myocardial scars more frequent than expected: magnetic resonance imaging detects potential risk group. J Am Coll Cardiol. 2006;48:765–71.

177. Yan AT, Shayne AJ, Brown KA, et al. Characterization of the peri-infarct zone by contrast-enhanced cardiac magnetic resonance imaging is a powerful predictor of post-myocardial infarction mortality. Circulation. 2006;114:32–9.

178. Kramer CM. The prognostic significance of microvascular obstruction after myocardial infarction as defined by cardiovascular magnetic resonance. Eur Heart J. 2005;26:532–3.

179. Reimer KA, Jennings RB. The changing anatomic reference base of evolving myocardial infarction: underestimation of myocardial collateral blood flow and overestimation of experimental anatomic infarct size due to tissue edema, hemorrhage and acute inflammation. Circulation. 1979;60:866–76.

180. Rahimtoola SH. The hibernating myocardium. Am Heart J. 1989;117:211–21.

181. Lieberman AN, Weiss JL, Jugdutt BI, et al. Two-dimensional echocardiography and infarct size: relationship of regional wall motion and thickening to the extent of myocardial infarction in the dog. Circulation. 1981;63:739–46.

182. Rogers WJ Jr., Kramer CM, Geskin G, et al. Early contrast-enhanced MRI predicts late functional recovery after reperfused myocardial infarction. Circulation. 1999;99:744–50.

183. Choi CJ, Haji-Momenian S, Dimaria JM, et al. Infarct involution and improved function during healing of acute myocardial infarction: the role of microvascular obstruction. J Cardiovasc Magn Reson. 2004;6:917–25.

184. Ingkanisorn WP, Rhoads KL, Aletras AH, et al. Gadolinium delayed enhancement cardiovascular magnetic resonance correlates with clinical measures of myocardial infarction. J Am Coll Cardiol. 2004;43:2253–9.

185. Schulz-Menger J, Abdel-Aty H, Busjahn A, et al. Left ventricular outflow tract planimetry by cardiovascular magnetic resonance differentiates obstructive from non-obstructive hypertrophic cardiomyopathy. J Cardiovasc Magn Reson. 2006;8:741–6.

186. Moon JC, McKenna WJ, McCrohon JA, et al. Toward clinical risk assessment in hypertrophic cardiomyopathy with gadolinium cardiovascular magnetic resonance. J Am Coll Cardiol. 2003;41:1561–7.

187. Matsunaka T, Hamada M, Matsumoto Y, et al. First-pass myocardial perfusion defect and delayed contrast enhancement in hypertrophic cardiomyopathy assessed with MRI. Magn Reson Med Sci. 2003;2:61–9.

188. Rickers C, Wilke NM, Jerosch-Herold M, et al. Utility of cardiac magnetic resonance imaging in the diagnosis of hypertrophic cardiomyopathy. Circulation. 2005;112:855–61.

189. Tandri H, Friedrich MG, Calkins H, et al. MRI of arrhythmogenic right ventricular cardiomyopathy/dysplasia. J Cardiovasc Magn Reson. 2004;6:557–63.

190. Tandri H, Macedo R, Calkins H, et al. Role of magnetic resonance imaging in arrhythmogenic right ventricular dysplasia: insights from the North American arrhythmogenic right ventricular dysplasia (ARVD/C) study. Am Heart J. 2008;155:147–53.

191. Jain A, Tandri H, Calkins H, et al. Role of cardiovascular magnetic resonance imaging in arrhythmogenic right ventricular dysplasia. J Cardiovasc Magn Reson. 2008;10:32.

192. Tandri H, Castillo E, Ferrari VA, et al. Magnetic resonance imaging of arrhythmogenic right ventricular dysplasia: sensitivity, specificity, and observer variability of fat detection versus functional analysis of the right ventricle. J Am Coll Cardiol. 2006;48:2277–84.

193. Tandri H, Saranathan M, Rodriguez ER, et al. Noninvasive detection of myocardial fibrosis in arrhythmogenic right ventricular cardiomyopathy using delayed-enhancement magnetic resonance imaging. J Am Coll Cardiol. 2005;45:98–103.

194. Sen-Chowdhry S, Prasad SK, Syrris P, et al. Cardiovascular magnetic resonance in arrhythmogenic right ventricular cardiomyopathy revisited: comparison with task force criteria and genotype. J Am Coll Cardiol. 2006;48:2132–40.

195. Sen-Chowdhry S, Syrris P, Ward D, et al. Clinical and genetic characterization of families with arrhythmogenic right ventricular dysplasia/cardiomyopathy provides novel insights into patterns of disease expression. Circulation. 2007;115:1710–20.

196. Petersen SE, Selvanayagam JB, Wiesmann F, et al. Left ventricular non-compaction: insights from cardiovascular magnetic resonance imaging. J Am Coll Cardiol. 2005;46:101–5.

197. Nazarian S, Bluemke DA, Lardo AC, et al. Magnetic resonance assessment of the substrate for inducible ventricular tachycardia in nonischemic cardiomyopathy. Circulation. 2005;112:2821–5.

198. Abdel-Aty H, Boye P, Zagrosek A, et al. Diagnostic performance of cardiovascular magnetic resonance in patients with suspected acute myocarditis: comparison of different approaches. J Am Coll Cardiol. 2005;45:1815–22.

199. Gutberlet M, Spors B, Thoma T, et al. Suspected chronic myocarditis at cardiac MR: diagnostic accuracy and association with immunohistologically detected inflammation and viral persistence. Radiology. 2008;246:401–9.

200. Liu PP, Yan AT. Cardiovascular magnetic resonance for the diagnosis of acute myocarditis: prospects for detecting myocardial inflammation. J Am Coll Cardiol. 2005;45:1823–5.

201. Friedrich M, Sechtem U, Schulz-Menger J, et al. Cardiovascular magnetic resonance in myocarditis: a JACC white paper. J Am Coll Cardiol. 2009;53:1475–87.

202. Schulz-Menger J, Wassmuth R, Abdel-Aty H, et al. Patterns of myocardial inflammation and scarring in sarcoidosis as assessed by cardiovascular magnetic resonance. Heart. 2006;92:399–400.

203. Pennell DJ. T2* magnetic resonance and myocardial iron in thalassemia. Ann N Y Acad Sci. 2005;1054:373–8.

204. Anderson LJ, Holden S, Davis B, et al. Cardiovascular T2-star (T2*) magnetic resonance for the early diagnosis of myocardial iron overload. Eur Heart J. 2001;22:2171–9.

205. Pereles FS, Kapoor V, Carr JC, et al. Usefulness of segmented TrueFISP cardiac pulse sequence in evaluation of congenital and acquired adult cardiac abnormalities. AJR Am J Roentgenol. 2001; 177:1155–60.

206. Suzuki J, Caputo GR, Kondo C, et al. Cine MR imaging of valvular heart disease: display and imaging parameters affect the size of the signal void caused by valvular regurgitation. AJR Am J Roentgenol. 1990;155:723–7.

207. Kupfahl C, Honold M, Meinhardt G, et al. Evaluation of aortic stenosis by cardiovascular magnetic resonance imaging: comparison with established routine clinical techniques. Heart. 2004;90:893–901.

208. Djavidani B, Debl K, Lenhart M, et al. Planimetry of mitral valve stenosis by magnetic resonance imaging. J Am Coll Cardiol. 2005; 45:2048–53.

209. Djavidani B, Debl K, Buchner S, et al. MRI planimetry for diagnosis and follow-up of valve area in mitral stenosis treated with valvuloplasty. Rofo. 2006;178:781–6.

210. Didier D, Ratib O, Lerch R, et al. Detection and quantification of valvular heart disease with dynamic cardiac MR imaging. Radiographics. 2000;20:1279–99.

211. Dall'Armellina E, Hamilton CA, Hundley WG. Assessment of blood flow and valvular heart disease using phase-contrast cardiovascular magnetic resonance. Echocardiography. 2007;24:207–16.

212. Eichenberger AC, Jenni R, von Schulthess GK. Aortic valve pressure gradients in patients with aortic valve stenosis: quantification with velocity-encoded cine MR imaging. AJR Am J Roentgenol. 1993; 160:971–7.

213. Friedrich M, Schulz-Menger J, Dietz R. Magnetic resonance to assess the aortic valve area in aortic stenosis. J Am Coll Cardiol. 2004;43:2148–9.

214. Fujita N, Chazouilleres AF, Hartiala JJ, et al. Quantification of mitral regurgitation by velocity-encoded cine nuclear magnetic resonance imaging. J Am Coll Cardiol. 1994;23:951–8.

215. Gelfand EV, Hughes S, Hauser TH, et al. Severity of mitral and aortic regurgitation as assessed by cardiovascular magnetic resonance: optimizing correlation with Doppler echocardiography. J Cardiovasc Magn Reson. 2006;8:503–7.

216. Sondergaard L, Lindvig K, Hildebrandt P, et al. Quantification of aortic regurgitation by magnetic resonance velocity mapping. Am Heart J. 1993;125:1081–90.

217. Helbing WA, Niezen RA, Le CS, et al. Right ventricular diastolic function in children with pulmonary regurgitation after repair of tetralogy of Fallot: volumetric evaluation by magnetic resonance velocity mapping. J Am Coll Cardiol. 1996;28:1827–35.

218. Akins EW, Slone RM, Wiechmann BN, et al. Perivalvular pseudoaneurysm complicating bacterial endocarditis: MR detection in five cases. AJR Am J Roentgenol. 1991;156:1155–8.

219. Araoz PA, Mulvagh SL, Tazelaar HD, et al. CT and MR imaging of benign primary cardiac neoplasms with echocardiographic correlation. Radiographics. 2000;20:1303–19.

220. Caduff JH, Hernandez RJ, Ludomirsky A. MR visualization of aortic valve vegetations. J Comput Assist Tomogr. 1996;20:613–5.

221. Syed IS, Feng D, Harris SR, et al. MR imaging of cardiac masses. Magn Reson Imaging Clin N Am. 2008;16:137–64.

222. Bonow RO, Carabello BA, Kanu C, et al. ACC/AHA 2006 guidelines for the management of patients with valvular heart disease: a report of the American College of Cardiology/American Heart Association Task Force on Practice Guidelines (Writing Committee to Revise the 1998 Guidelines for the Management of Patients With Valvular Heart Disease). J Am Coll Cardiol 2006;48:e1–148.

223. Lam KY, Dickens P, Chan AC. Tumors of the heart. A 20-year experience with a review of 12,485 consecutive autopsies. Arch Pathol Lab Med. 1993;117:1027–31.

224. Roberts WC. Primary and secondary neoplasms of the heart. Am J Cardiol. 1997;80:671–82.

225. Gulati G, Sharma S, Kothari SS, et al. Comparison of echo and MRI in the imaging evaluation of intracardiac masses. Cardiovasc Intervent Radiol. 2004;27:459–69.

226. Mollet NR, Dymarkowski S, Volders W, et al. Visualization of ventricular thrombi with contrast-enhanced magnetic resonance imaging in patients with ischemic heart disease. Circulation. 2002;106: 2873–6.

227. Srichai MB, Junor C, Rodriguez LL, et al. Clinical, imaging, and pathological characteristics of left ventricular thrombus: a comparison of contrast-enhanced magnetic resonance imaging, transthoracic echocardiography, and transesophageal echocardiography with surgical or pathological validation. Am Heart J. 2006;152:75–84.

228. Weinsaft JW, Kim HW, Shah DJ, et al. Detection of left ventricular thrombus by delayed-enhancement cardiovascular magnetic resonance prevalence and markers in patients with systolic dysfunction. J Am Coll Cardiol. 2008;52:148–57.

229. Simonetti OP, Kim RJ, Fieno DS, et al. An improved MR imaging technique for the visualization of myocardial infarction. Radiology. 2001;218:215–23.

230. Chiles C, Woodard PK, Gutierrez FR, et al. Metastatic involvement of the heart and pericardium: CT and MR imaging. Radiographics. 2001;21:439–49.

231. Sparrow PJ, Kurian JB, Jones TR, et al. MR imaging of cardiac tumors. Radiographics. 2005;25:1255–76.

232. Hoffmann U, Globits S, Schima W, et al. Usefulness of magnetic resonance imaging of cardiac and paracardiac masses. Am J Cardiol. 2003;92:890–5.

233. Myers RB, Spodick DH. Constrictive pericarditis: clinical and pathophysiologic characteristics. Am Heart J. 1999;138:219–32.

234. Sechtem U, Tscholakoff D, Higgins CB. MRI of the abnormal pericardium. AJR Am J Roentgenol. 1986;147:245–52.

235. Soulen RL, Stark DD, Higgins CB. Magnetic resonance imaging of constrictive pericardial disease. Am J Cardiol. 1985;55:480–4.

236. Talreja DR, Edwards WD, Danielson GK, et al. Constrictive pericarditis in 26 patients with histologically normal pericardial thickness. Circulation. 2003;108:1852–7.

237. Vaitkus PT, Kussmaul WG. Constrictive pericarditis versus restrictive cardiomyopathy: a reappraisal and update of diagnostic criteria. Am Heart J. 1991;122:1431–41.

238. Francone M, Dymarkowski S, Kalantzi M, et al. Real-time cine MRI of ventricular septal motion: a novel approach to assess ventricular coupling. J Magn Reson Imaging. 2005;21:305–9.

239. Francone M, Dymarkowski S, Kalantzi M, et al. Assessment of ventricular coupling with real-time cine MRI and its value to differentiate constrictive pericarditis from restrictive cardiomyopathy. Eur Radiol. 2006;16:944–51.

240. Santarone M, Corrado G, Belloni G. Effusive-constrictive pericarditis. Heart. 2000;83:551–6.

241. Kojima S, Yamada N, Goto Y. Diagnosis of constrictive pericarditis by tagged cine magnetic resonance imaging. N Engl J Med. 1999; 341:373–4.

242. Shabetai R, Fowler NO, Guntheroth WG. The hemodynamics of cardiac tamponade and constrictive pericarditis. Am J Cardiol. 1970;26:480–9.

243. Hurrell DG, Nishimura RA, Higano ST, et al. Value of dynamic respiratory changes in left and right ventricular pressures for the diagnosis of constrictive pericarditis. Circulation. 1996;93:2007–13.

244. Hatle LK, Appleton CP, Popp RL. Differentiation of constrictive pericarditis and restrictive cardiomyopathy by Doppler echocardiography. Circulation. 1989;79:357–70.

245. Fogel MA, Donofrio MT, Ramaciotti C, et al. Magnetic resonance and echocardiographic imaging of pulmonary artery size throughout stages of Fontan reconstruction. Circulation. 1994;90:2927–36.

246. Geva T, Vick GW 3rd, Wendt RE, et al. Role of spin echo and cine magnetic resonance imaging in presurgical planning of heterotaxy syndrome. Comparison with echocardiography and catheterization. Circulation. 1994;90:348–56.

247. Beerbaum P, Korperich H, Barth P, et al. Noninvasive quantification of left-to-right shunt in pediatric patients: phase-contrast cine magnetic resonance imaging compared with invasive oximetry. Circulation. 2001;103:2476–82.

248. Beerbaum P, Korperich H, Gieseke J, et al. Rapid left-to-right shunt quantification in children by phase-contrast magnetic resonance imaging combined with sensitivity encoding (SENSE). Circulation. 2003;108:1355–61.

249. Pujadas S, Reddy GP, Weber O, et al. Phase contrast MR imaging to measure changes in collateral blood flow after stenting of recurrent aortic coarctation: initial experience. J Magn Reson Imaging. 2006; 24:72–6.

250. Steffens JC, Bourne MW, Sakuma H, et al. Quantification of collateral blood flow in coarctation of the aorta by velocity encoded cine magnetic resonance imaging. Circulation. 1994;90:937–43.

251. Fogel MA, Weinberg PM, Rychik J, et al. Caval contribution to flow in the branch pulmonary arteries of Fontan patients with a novel application of magnetic resonance presaturation pulse. Circulation. 1999;99:1215–21.

252. Fogel MA, Durning S, Wernovsky G, et al. Brain versus lung: hierarchy of feedback loops in single ventricle patients with superior cavopulmonary connection. Circulation. 2004;110:II152.

253. Rebergen SA, Chin JG, Ottenkamp J, et al. Pulmonary regurgitation in the late postoperative follow-up of tetralogy of Fallot. Volumetric quantitation by nuclear magnetic resonance velocity mapping. Circulation. 1993;88:2257–66.

254. van den Berg J, Hop WC, Strengers JL, et al. Clinical condition at mid-to-late follow-up after transatrial-transpulmonary repair of tetralogy of Fallot. J Thorac Cardiovasc Surg. 2007;133:470–7.

255. Manning WJ, Wei JY, Fossel ET, et al. Measurement of left ventricular mass in rats using electrocardiogram-gated magnetic resonance imaging. Am J Physiol. 1990;258:H1181–6.

256. Markiewicz W, Sechtem U, Kirby R, et al. Measurement of ventricular volumes in the dog by nuclear magnetic resonance imaging. J Am Coll Cardiol. 1987;10:170–7.

257. Eicken A, Fratz S, Gutfried C, et al. Hearts late after Fontan operation have normal mass, normal volume, and reduced systolic function: a magnetic resonance imaging study. J Am Coll Cardiol. 2003;42:1061–5.

258. Fogel MA, Weinberg PM, Chin AJ, et al. Late ventricular geometry and performance changes of functional single ventricle throughout staged Fontan reconstruction assessed by magnetic resonance imaging. J Am Coll Cardiol. 1996;28:212–21.

259. Jenkins NP, Ward C. Coarctation of the aorta: natural history and outcome after surgical treatment. QJM. 1999;92:365–71.

260. Gerber BL, Coche E, Pasquet A, et al. Coronary artery stenosis: direct comparison of four-section multi-detector row CT and 3D navigator MR imaging for detection—initial results. Radiology. 2005;234:98–108.

261. Dewey M, Teige F, Schnapauff D, et al. Noninvasive detection of coronary artery stenoses with multislice computed tomography or magnetic resonance imaging. Ann Intern Med. 2006;145:407–15.

262. Galjee MA, van Rossum AC, Doesburg T, et al. Value of magnetic resonance imaging in assessing patency and function of coronary artery bypass grafts. An angiographically controlled study. Circulation. 1996;93:660–6.

263. Molinari G, Sardanelli F, Zandrino F, et al. Value of navigator echo magnetic resonance angiography in detecting occlusion/patency of arterial and venous, single and sequential coronary bypass grafts. Int J Card Imaging. 2000;16:149–60.

264. Wintersperger BJ, Engelmann MG, von Smekal A, et al. Patency of coronary bypass grafts: assessment with breath-hold contrast-enhanced MR angiography—value of a non-electrocardiographically triggered technique. Radiology. 1998;208:345–51.

265. Wolff SD, Schwitter J, Coulden R, et al. Myocardial first-pass perfusion magnetic resonance imaging: a multicenter dose-ranging study. Circulation. 2004;110:732–7.

266. Benz MG, Benz MW. Reduction of cancer risk associated with pediatric computed tomography by the development of new technologies. Pediatrics. 2004;114:205–9.

267. Brenner D, Elliston C, Hall E, et al. Estimated risks of radiation-induced fatal cancer from pediatric CT. AJR Am J Roentgenol. 2001;176:289–96.

268. Modan B, Keinan L, Blumstein T, et al. Cancer following cardiac catheterization in childhood. Int J Epidemiol. 2000;29:424–8.

269. Wall BF. Radiation protection dosimetry for diagnostic radiology patients. Radiat Prot Dosimetry. 2004;109:409–19.

270. National Cancer Institute. Radiation risks and pediatric computed tomography (CT): a guide for health care providers. Available at: http://www.cancer.gov/cancertopics/causes/radiation-risks-pediatric-CT. Accessed November 18, 2008.

271. Warnes CA, Williams RG, Bashore TM, et al. ACC/AHA 2008 guidelines for the management of adults with congenital heart disease: a report of the American College of Cardiology/American Heart Association Task Force on Practice Guidelines (Writing Committee to Develop Guidelines on the Management of Adults With Congenital Heart Disease). J Am Coll Cardiol. 2008;52: e1–121.

272. Stein PD, Woodard PK, Weg JG, et al. Diagnostic pathways in acute pulmonary embolism: recommendations of the PIOPED II Investigators. Radiology. 2007;242:15–21.

273. Stein PD, Woodard PK, Hull RD, et al. Gadolinium-enhanced magnetic resonance angiography for detection of acute pulmonary embolism: an in-depth review. Chest. 2003;124:2324–8.

274. Gupta A, Frazer CK, Ferguson JM, et al. Acute pulmonary embolism: diagnosis with MR angiography. Radiology. 1999;210:353–9.

275. Kluge A, Luboldt W, Bachmann G. Acute pulmonary embolism to the subsegmental level: diagnostic accuracy of three MRI techniques compared with 16-MDCT. AJR Am J Roentgenol. 2006;187: W7–14.

276. Meaney JF, Weg JG, Chenevert TL, et al. Diagnosis of pulmonary embolism with magnetic resonance angiography. N Engl J Med. 1997;336:1422–7.

277. Oudkerk M, van Beek EJ, Wielopolski P, et al. Comparison of contrast-enhanced magnetic resonance angiography and conventional pulmonary angiography for the diagnosis of pulmonary embolism: a prospective study. Lancet. 2002;359:1643–7.

278. Kluge A, Mueller C, Strunk J, et al. Experience in 207 combined MRI examinations for acute pulmonary embolism and deep vein thrombosis. AJR Am J Roentgenol. 2006;186:1686–96.

279. Stein PD, Fowler SE, Goodman LR, et al. Multidetector computed tomography for acute pulmonary embolism. N Engl J Med. 2006; 354:2317–27.

280. Evans AJ, Sostman HD, Witty LA, et al. Detection of deep venous thrombosis: prospective comparison of MR imaging and sonography. J Magn Reson Imaging. 1996;6:44–51.

281. Fraser DG, Moody AR, Morgan PS, et al. Diagnosis of lower-limb deep venous thrombosis: a prospective blinded study of magnetic resonance direct thrombus imaging. Ann Intern Med. 2002;136: 89–98.

282. Laissy JP, Cinqualbre A, Loshkajian A, et al. Assessment of deep venous thrombosis in the lower limbs and pelvis: MR venography versus duplex Doppler sonography. AJR Am J Roentgenol. 1996;167: 971–5.

283. Hudsmith LE, Cheng AS, Tyler DJ, et al. Assessment of left atrial volumes at 1.5 Tesla and 3 Tesla using FLASH and SSFP cine imaging. J Cardiovasc Magn Reson. 2007;9:673–9.

284. Jarvinen V, Kupari M, Hekali P, et al. Assessment of left atrial volumes and phasic function using cine magnetic resonance imaging in normal subjects. Am J Cardiol. 1994;73:1135–8.

285. Matsuoka H, Hamada M, Honda T, et al. Measurement of cardiac chamber volumes by cine magnetic resonance imaging. Angiology. 1993;44:321–7.

286. Mohiaddin RH, Hasegawa M. Measurement of atrial volumes by magnetic resonance imaging in healthy volunteers and in patients with myocardial infarction. Eur Heart J. 1995;16:106–11.

287. Rodevan O, Bjornerheim R, Ljosland M, et al. Left atrial volumes assessed by three- and two-dimensional echocardiography compared to MRI estimates. Int J Card Imaging. 1999;15:397–410.

288. Sievers B, Kirchberg S, Addo M, et al. Assessment of left atrial volumes in sinus rhythm and atrial fibrillation using the biplane area-length method and cardiovascular magnetic resonance imaging with TrueFISP. J Cardiovasc Magn Reson. 2004;6:855–63.

289. Therkelsen SK, Groenning BA, Svendsen JH, et al. Atrial and ventricular volume and function in persistent and permanent atrial fibrillation, a magnetic resonance imaging study. J Cardiovasc Magn Reson. 2005;7:465–73.

290. Ghaye B, Szapiro D, Dacher JN, et al. Percutaneous ablation for atrial fibrillation: the role of cross-sectional imaging. Radiographics. 2003;23 Spec No:S19–S33.

291. Dill T, Neumann T, Ekinci O, et al. Pulmonary vein diameter reduction after radiofrequency catheter ablation for paroxysmal atrial fibrillation evaluated by contrast-enhanced three-dimensional magnetic resonance imaging. Circulation. 2003;107:845–50.

292. Kato R, Lickfett L, Meininger G, et al. Pulmonary vein anatomy in patients undergoing catheter ablation of atrial fibrillation: lessons learned by use of magnetic resonance imaging. Circulation. 2003;107:2004–10.

293. Yang M, Akbari H, Reddy GP, et al. Identification of pulmonary vein stenosis after radiofrequency ablation for atrial fibrillation using MRI. J Comput Assist Tomogr. 2001;25:34–5.

294. Arentz T, von Rosenthal J, Blum T, et al. Feasibility and safety of pulmonary vein isolation using a new mapping and navigation system in patients with refractory atrial fibrillation. Circulation. 2003;108:2484–90.

295. Dickfeld T, Calkins H, Zviman M, et al. Anatomic stereotactic catheter ablation on three-dimensional magnetic resonance images in real time. Circulation. 2003;108:2407–13.

296. Chen SA, Hsieh MH, Tai CT, et al. Initiation of atrial fibrillation by ectopic beats originating from the pulmonary veins: electrophysiological characteristics, pharmacological responses, and effects of radiofrequency ablation. Circulation. 1999;100:1879–86.

297. Gerstenfeld EP, Guerra P, Sparks PB, et al. Clinical outcome after radiofrequency catheter ablation of focal atrial fibrillation triggers. J Cardiovasc Electrophysiol. 2001;12:900–8.

298. Haissaguerre M, Jais P, Shah DC, et al. Electrophysiological end point for catheter ablation of atrial fibrillation initiated from multiple pulmonary venous foci. Circulation. 2000;101:1409–17.

299. Shah DC, Haissaguerre M, Jais P, et al. Curative catheter ablation of paroxysmal atrial fibrillation in 200 patients: strategy for presentations ranging from sustained atrial fibrillation to no arrhythmias. Pacing Clin Electrophysiol. 2001;24:1541–58.

300. Kauczor HU, Kreitner KF. MRI of the pulmonary parenchyma. Eur Radiol. 1999;9:1755–64.

301. Kessler R, Fraisse P, Krause D, et al. Magnetic resonance imaging in the diagnosis of pulmonary infarction. Chest. 1991;99:298–300.

302. Peters DC, Wylie JV, Hauser TH, et al. Detection of pulmonary vein and left atrial scar after catheter ablation with three-dimensional navigator-gated delayed enhancement MR imaging: initial experience. Radiology. 2007;243:690–5.

303. Mohrs OK, Nowak B, Petersen SE, et al. Thrombus detection in the left atrial appendage using contrast-enhanced MRI: a pilot study. AJR Am J Roentgenol. 2006;186:198–205.

304. Ohyama H, Hosomi N, Takahashi T, et al. Comparison of magnetic resonance imaging and transesophageal echocardiography in detection of thrombus in the left atrial appendage. Stroke. 2003;34:2436–9.

305. Hirsch AT, Haskal ZJ, Hertzer NR, et al. ACC/AHA 2005 practice guidelines for the management of patients with peripheral arterial disease (lower extremity, renal, mesenteric, and abdominal aortic): a collaborative report from the American Association for Vascular Surgery/Society for Vascular Surgery, Society for Cardiovascular Angiography and Interventions, Society for Vascular Medicine and Biology, Society of Interventional Radiology, and the ACC/AHA Task Force on Practice Guidelines (Writing Committee to Develop Guidelines for the Management of Patients With Peripheral Arterial Disease). J Am Coll Cardiol. 2006;47:e1–192.

306. Selvin E, Erlinger TP. Prevalence of and risk factors for peripheral arterial disease in the United States: results from the National Health and Nutrition Examination Survey, 1999–2000. Circulation. 2004;110:738–43.

307. Baum RA, Rutter CM, Sunshine JH, et al. Multicenter trial to evaluate vascular magnetic resonance angiography of the lower extremity. American College of Radiology Rapid Technology Assessment Group. JAMA. 1995;274:875–80.

308. Owen RS, Carpenter JP, Baum RA, et al. Magnetic resonance imaging of angiographically occult runoff vessels in peripheral arterial occlusive disease. N Engl J Med. 1992;326:1577–81.

309. Foo TK, Ho VB, Hood MN, et al. High-spatial-resolution multistation MR imaging of lower-extremity peripheral vasculature with segmented volume acquisition: feasibility study. Radiology. 2001;219:835–41.

310. Ho KY, Leiner T, de Haan MW, et al. Peripheral vascular tree stenoses: evaluation with moving-bed infusion-tracking MR angiography. Radiology. 1998;206:683–92.

311. Meaney JF, Ridgway JP, Chakraverty S, et al. Stepping-table gadolinium-enhanced digital subtraction MR angiography of the aorta and lower extremity arteries: preliminary experience. Radiology. 1999;211:59–67.

312. Pereles FS, Collins JD, Carr JC, et al. Accuracy of stepping-table lower extremity MR angiography with dual-level bolus timing and separate calf acquisition: hybrid peripheral MR angiography. Radiology. 2006;240:283–90.

313. Andreisek G, Pfammatter T, Goepfert K, et al. Peripheral arteries in diabetic patients: standard bolus-chase and time-resolved MR angiography. Radiology. 2007;242:610–20.

314. Hahn WY, Hecht EM, Friedman B, et al. Distal lower extremity imaging: prospective comparison of 2-dimensional time of flight, 3-dimensional time-resolved contrast-enhanced magnetic resonance angiography, and 3-dimensional bolus chase contrast-enhanced magnetic resonance angiography. J Comput Assist Tomogr. 2007;31:29–36.

315. Prince MR, Chabra SG, Watts R, et al. Contrast material travel times in patients undergoing peripheral MR angiography. Radiology. 2002;224:55–61.

316. Ho VB, Corse WR. MR angiography of the abdominal aorta and peripheral vessels. Radiol Clin North Am. 2003;41:115–44.

317. Leiner T, Kessels AG, Nelemans PJ, et al. Peripheral arterial disease: comparison of color duplex US and contrast-enhanced MR angiography for diagnosis. Radiology. 2005;235:699–708.

318. de Vries M, Ouwendijk R, Flobbe K, et al. Peripheral arterial disease: clinical and cost comparisons between duplex US and contrast-enhanced MR angiography—a multicenter randomized trial. Radiology. 2006;240:401–10.

319. Ouwendijk R, de Vries M, Pattynama PM, et al. Imaging peripheral arterial disease: a randomized controlled trial comparing contrast-enhanced MR angiography and multi-detector row CT angiography. Radiology. 2005;236:1094–103.

320. Sacks D, Bettmann M, Casciani T, et al. Expert panel on cardiovascular imaging: claudication appropriateness criteria 2005. Available at: http://www.acr.org/ac. Accessed June 30, 2008.

321. Beneficial effect of carotid endarterectomy in symptomatic patients with high-grade carotid stenosis. North American Symptomatic Carotid Endarterectomy Trial Collaborators. N Engl J Med. 1991;325:445–53.

322. Carr JC, Ma J, Desphande V, et al. High-resolution breath-hold contrast-enhanced MR angiography of the entire carotid circulation. AJR Am J Roentgenol. 2002;178:543–9.

323. Yang CW, Carr JC, Futterer SF, et al. Contrast-enhanced MR angiography of the carotid and vertebrobasilar circulations. AJNR Am J Neuroradiol. 2005;26:2095–101.

324. Wright VL, Olan W, Dick B, et al. Assessment of CE-MRA for the rapid detection of supra-aortic vascular disease. Neurology. 2005;65:27–32.

325. Nael K, Villablanca JP, Pope WB, et al. Supraaortic arteries: contrast-enhanced MR angiography at 3.0 T—highly accelerated parallel acquisition for improved spatial resolution over an extended field of view. Radiology. 2007;242:600–9.

326. Nael K, Villablanca JP, Saleh R, et al. Contrast-enhanced MR angiography at 3T in the evaluation of intracranial aneurysms: a comparison with time-of-flight MR angiography. AJNR Am J Neuroradiol. 2006;27:2118–21.

327. Villablanca JP, Nael K, Habibi R, et al. 3 T contrast-enhanced magnetic resonance angiography for evaluation of the intracranial arteries: comparison with time-of-flight magnetic resonance angiography and multislice computed tomography angiography. Invest Radiol. 2006;41:799–805.

328. Oktar SO, Yucel C, Karaosmanoglu D, et al. Blood-flow volume quantification in internal carotid and vertebral arteries: comparison of 3 different ultrasound techniques with phase-contrast MR imaging. AJNR Am J Neuroradiol. 2006;27:363–9.

329. Tanaka H, Fujita N, Enoki T, et al. Relationship between variations in the circle of Willis and flow rates in internal carotid and basilar arteries determined by means of magnetic resonance imaging with semiautomated lumen segmentation: reference data from 125 healthy volunteers. AJNR Am J Neuroradiol. 2006;27:1770–5.

330. Fayad ZA, Sirol M, Nikolaou K, et al. Magnetic resonance imaging and computed tomography in assessment of atherosclerotic plaque. Curr Atheroscler Rep. 2004;6:232–42.

331. Yuan C, Zhao XQ, Hatsukami TS. Quantitative evaluation of carotid atherosclerotic plaques by magnetic resonance imaging. Curr Atheroscler Rep. 2002;4:351–7.

332. Fattori R, Nienaber CA. MRI of acute and chronic aortic pathology: preoperative and postoperative evaluation. J Magn Reson Imaging. 1999;10:741–50.

333. Russo V, Renzulli M, Buttazzi K, et al. Acquired diseases of the thoracic aorta: role of MRI and MRA. Eur Radiol. 2006;16:852–65.

334. Schmidta M, Theissen P, Klempt G, et al. Long-term follow-up of 82 patients with chronic disease of the thoracic aorta using spin-echo and cine gradient magnetic resonance imaging. Magn Reson Imaging. 2000;18:795–806.

335. White RD, Higgins CB. Magnetic resonance imaging of thoracic vascular disease. J Thorac Imaging. 1989;4:34–50.

336. Gebker R, Gomaa O, Schnackenburg B, et al. Comparison of different MRI techniques for the assessment of thoracic aortic pathology: 3D contrast enhanced MR angiography, turbo spin echo and balanced steady state free precession. Int J Cardiovasc Imaging. 2007;23:747–56.

337. Gaubert JY, Moulin G, Mesana T, et al. Type A dissection of the thoracic aorta: use of MR imaging for long-term follow-up. Radiology. 1995;196:363–9.

338. Kawamoto S, Bluemke DA, Traill TA, et al. Thoracoabdominal aorta in Marfan syndrome: MR imaging findings of progression of vasculopathy after surgical repair. Radiology. 1997;203:727–32.

339. Loubeyre P, Delignette A, Bonefoy L, et al. Magnetic resonance imaging evaluation of the ascending aorta after graft-inclusion surgery: comparison between an ultrafast contrast-enhanced MR sequence and conventional cine-MRI. J Magn Reson Imaging. 1996;6:478–83.

340. Fayad ZA, Fallon JT, Shinnar M, et al. Noninvasive in vivo high-resolution magnetic resonance imaging of atherosclerotic lesions in genetically engineered mice. Circulation. 1998;98:1541–7.

341. Macura KJ, Szarf G, Fishman EK, et al. Role of computed tomography and magnetic resonance imaging in assessment of acute aortic syndromes. Semin Ultrasound CT MR. 2003;24:232–54.

342. Troxler M, Mavor AI, Homer-Vanniasinkam S. Penetrating atherosclerotic ulcers of the aorta. Br J Surg. 2001;88:1169–77.

343. Salanitri GC, Huo E, Miller FH, et al. MRI of mycotic sinus of valsalva pseudoaneurysm secondary to *Aspergillus pericarditis*. AJR Am J Roentgenol. 2005;184:S25–7.

344. Givehchian M, Kramer U, Miller S, et al. Aortic root remodeling: functional MRI as an accurate tool for complete follow-up. Thorac Cardiovasc Surg. 2005;53:267–73.

345. Weigel S, Tombach B, Maintz D, et al. Thoracic aortic stent graft: comparison of contrast-enhanced MR angiography and CT angiography in the follow-up: initial results. Eur Radiol. 2003;13:1628–34.

346. Suzuki T, Mehta RH, Ince H, et al. Clinical profiles and outcomes of acute type B aortic dissection in the current era: lessons from the International Registry of Aortic Dissection (IRAD). Circulation. 2003;108 Suppl 1:II312–7.

347. Trimarchi S, Nienaber CA, Rampoldi V, et al. Role and results of surgery in acute type B aortic dissection: insights from the International Registry of Acute Aortic Dissection (IRAD). Circulation. 2006;114:I357–64.

348. Murray JG, Manisali M, Flamm SD, et al. Intramural hematoma of the thoracic aorta: MR image findings and their prognostic implications. Radiology. 1997;204:349–55.

349. Oliver TB, Murchison JT, Reid JH. Serial MRI in the management of intramural haemorrhage of the thoracic aorta. Br J Radiol. 1997;70:1288–90.

350. Sueyoshi E, Sakamoto I, Fukuda M, et al. Long-term outcome of type B aortic intramural hematoma: comparison with classic aortic dissection treated by the same therapeutic strategy. Ann Thorac Surg. 2004;78:2112–7.

351. Ozkan U, Oguzkurt L, Tercan F, et al. Renal artery origins and variations: angiographic evaluation of 855 consecutive patients. Diagn Interv Radiol. 2006;12:183–6.

352. Weizer AZ, Silverstein AD, Auge BK, et al. Determining the incidence of horseshoe kidney from radiographic data at a single institution. J Urol. 2003;170:1722–6.

353. Boatman DL, Cornell SH, Kolln CP. The arterial supply of horseshoe kidneys. Am J Roentgenol Radium Ther Nucl Med. 1971;113:447–51.

354. Kramer U, Nael K, Laub G, et al. High-resolution magnetic resonance angiography of the renal arteries using parallel imaging acquisition techniques at 3.0 T: initial experience. Invest Radiol. 2006;41:125–32.

355. Nael K, Saleh R, Lee M, et al. High-spatial-resolution contrast-enhanced MR angiography of abdominal arteries with parallel acquisition at 3.0 T: initial experience in 32 patients. AJR Am J Roentgenol. 2006;187:W77–85.

356. Li A, Wong CS, Wong MK, et al. Acute adverse reactions to magnetic resonance contrast media—gadolinium chelates. Br J Radiol. 2006;79:368–71.

357. Dellegrottaglie S, Sanz J, Rajagopalan S. Technology insight: clinical role of magnetic resonance angiography in the diagnosis and management of renal artery stenosis. Nat Clin Pract Cardiovasc Med. 2006;3:329–38.

358. Michaely HJ, Schoenberg SO, Ittrich C, et al. Renal disease: value of functional magnetic resonance imaging with flow and perfusion measurements. Invest Radiol. 2004;39:698–705.

359. Kucher C, Steere J, Elenitsas R, et al. Nephrogenic fibrosing dermopathy/nephrogenic systemic fibrosis with diaphragmatic involvement in a patient with respiratory failure. J Am Acad Dermatol. 2006;54:S31–4.

360. Kanal E, Barkovich AJ, Bell C, et al. ACR guidance document for safe MR practices: 2007. AJR Am J Roentgenol. 2007;188:1447–74.

361. Thomsen HS. Nephrogenic systemic fibrosis: a serious late adverse reaction to gadodiamide. Eur Radiol. 2006;16:2619–21.

362. Institute for Magnetic Resonance Safety, Education, and Research home page. Available at: http://www.MRIsafety.com. Accessed June 19, 2009.

363. ASTM International. Active Standard: ASTM F2503-08 standard practice for marking medical devices and other items for safety in the magnetic resonance environment. West Conshohocken, Pa: ASTM International; 2008.

364. Friedrich MG, Strohm O, Kivelitz D, et al. Behaviour of implantable coronary stents during magnetic resonance imaging. Int J Cardiovasc Intervent. 1999;2:217–22.

365. Scott NA, Pettigrew RI. Absence of movement of coronary stents after placement in a magnetic resonance imaging field. Am J Cardiol. 1994;73:900–1.

366. Shellock FG, Shellock VJ. Metallic stents: evaluation of MR imaging safety. AJR Am J Roentgenol. 1999;173:543–7.

367. Syed MA, Carlson K, Murphy M, et al. Long-term safety of cardiac magnetic resonance imaging performed in the first few days after bare-metal stent implantation. J Magn Reson Imaging. 2006;24:1056–61.

368. Nehra A, Moran CJ, Cross DT III, et al. MR safety and imaging of neuroform stents at 3T. AJNR Am J Neuroradiol. 2004;25:1476–8.

369. Sommer T, Maintz D, Schmiedel A, et al. High field MR imaging: magnetic field interactions of aneurysm clips, coronary artery stents and iliac artery stents with a 3.0 Tesla MR system. Rofo. 2004;176:731–8.

370. Gerber TC, Fasseas P, Lennon RJ, et al. Clinical safety of magnetic resonance imaging early after coronary artery stent placement. J Am Coll Cardiol. 2003;42:1295–8.

371. Porto I, Selvanayagam J, Ashar V, et al. Safety of magnetic resonance imaging one to three days after bare metal and drug-eluting stent implantation. Am J Cardiol. 2005;96:366–8.

372. Rutledge JM, Vick GW III, Mullins CE, et al. Safety of magnetic resonance imaging immediately following Palmaz stent implant: a report of 3 cases. Catheter Cardiovasc Interv. 2001;53:519–23.

373. Schroeder AP, Houlind K, Pedersen EM, et al. Magnetic resonance imaging seems safe in patients with intracoronary stents. J Cardiovasc Magn Reson. 2000;2:43–9.

374. Shellock FG, Forder JR. Drug eluting coronary stent: in vitro evaluation of magnet resonance safety at 3 Tesla. J Cardiovasc Magn Reson. 2005;7:415–9.

375. Patel MR, Albert TS, Kandzari DE, et al. Acute myocardial infarction: safety of cardiac MR imaging after percutaneous revascularization with stents. Radiology. 2006;240:674–80.

376. Shellock FG. Reference manual for magnetic resonance safety, implants, and devices. 2006 ed. Los Angeles, Calif: Biomedical Research Publishing Group; 2006.

377. Graft SZ. Zenith Flex AAA endovascular graft MR information. Available at: http://www.cookmedical.com/ai/content/mmedia/FLX_MRINFO107.pdf. Accessed October 26, 2009.

378. Edwards MB, Taylor KM, Shellock FG. Prosthetic heart valves: evaluation of magnetic field interactions, heating, and artifacts at 1.5 T. J Magn Reson Imaging. 2000;12:363–9.

379. Khambadkone S, Coats L, Taylor A, et al. Percutaneous pulmonary valve implantation in humans: results in 59 consecutive patients. Circulation. 2005;112:1189–97.

380. Shellock FG, Morisoli SM. Ex vivo evaluation of ferromagnetism, heating, and artifacts produced by heart valve prostheses exposed to a 1.5-T MR system. J Magn Reson Imaging. 1994;4:756–8.

381. Shellock FG. Prosthetic heart valves and annuloplasty rings: assessment of magnetic field interactions, heating, and artifacts at 1.5 Tesla. J Cardiovasc Magn Reson. 2001;3:317–24.

382. Shellock FG. Biomedical implants and devices: assessment of magnetic field interactions with a 3.0–Tesla MR system. J Magn Reson Imaging. 2002;16:721–32.

383. Soulen RL, Budinger TF, Higgins CB. Magnetic resonance imaging of prosthetic heart valves. Radiology. 1985;154:705–7.

384. Edwards MB, Draper ER, Hand JW, et al. Mechanical testing of human cardiac tissue: some implications for MRI safety. J Cardiovasc Magn Reson. 2005;7:835–40.

385. Pruefer D, Kalden P, Schreiber W, et al. In vitro investigation of prosthetic heart valves in magnetic resonance imaging: evaluation of potential hazards. J Heart Valve Dis. 2001;10:410–4.

386. Randall PA, Kohman LJ, Scalzetti EM, et al. Magnetic resonance imaging of prosthetic cardiac valves in vitro and in vivo. Am J Cardiol. 1988;62:973–6.

387. Bock M, Mohrs OK, Voigtlaender T, et al. MRI safety aspects and artifacts of atrial septal defect and patent foramen ovale occluders at 1.5 tesla: a phantom study. Rofo. 2006;178:272–7.

388. Shellock FG, Morisoli SM. Ex vivo evaluation of ferromagnetism and artifacts of cardiac occluders exposed to a 1.5-T MR system. J Magn Reson Imaging. 1994;4:213–5.

389. Bartels LW, Bakker CJ, Viergever MA. Improved lumen visualization in metallic vascular implants by reducing RF artifacts. Magn Reson Med. 2002;47:171–80.

390. Grassi CJ, Matsumoto AH, Teitelbaum GP. Vena caval occlusion after Simon nitinol filter placement: identification with MR imaging in patients with malignancy. J Vasc Interv Radiol. 1992;3:535–9.

391. Kim D, Edelman RR, Margolin CJ, et al. The Simon nitinol filter: evaluation by MR and ultrasound. Angiology. 1992;43:541–8.

392. Kiproff PM, Deeb ZL, Contractor FM, et al. Magnetic resonance characteristics of the LGM vena cava filter: technical note. Cardiovasc Intervent Radiol. 1991;14:254–5.

393. Liebman CE, Messersmith RN, Levin DN, et al. MR imaging of inferior vena caval filters: safety and artifacts. AJR Am J Roentgenol. 1988;150:1174–6.

394. Watanabe AT, Teitelbaum GP, Gomes AS, et al. MR imaging of the bird's nest filter. Radiology. 1990;177:578–9.

395. Hartman J, Nguyen T, Larsen D, et al. MR artifacts, heat production, and ferromagnetism of Guglielmi detachable coils. AJNR Am J Neuroradiol. 1997;18:497–501.

396. Shellock FG, Detrick MS, Brant-Zawadski MN. MR compatibility of Guglielmi detachable coils. Radiology. 1997;203:568–70.

397. Hennemeyer CT, Wicklow K, Feinberg DA, et al. In vitro evaluation of platinum Guglielmi detachable coils at 3 T with a porcine model: safety issues and artifacts. Radiology. 2001;219:732–7.

398. Marshall MW, Teitelbaum GP, Kim HS, et al. Ferromagnetism and magnetic resonance artifacts of platinum embolization microcoils. Cardiovasc Intervent Radiol. 1991;14:163–6.

399. Shellock FG, Gounis M, Wakhloo A. Detachable coil for cerebral aneurysms: in vitro evaluation of magnetic field interactions, heating, and artifacts at 3T. AJNR Am J Neuroradiol. 2005;26:363–6.

400. Teitelbaum GP, Bradley WG Jr, Klein BD. MR imaging artifacts, ferromagnetism, and magnetic torque of intravascular filters, stents, and coils. Radiology. 1988;166:657–64.

401. Hartnell GG, Spence L, Hughes LA, et al. Safety of MR imaging in patients who have retained metallic materials after cardiac surgery. AJR Am J Roentgenol. 1997;168:1157–9.

402. Faris OP, Shein MJ. Government viewpoint: U.S. Food and Drug Administration: Pacemakers, ICDs and MRI. Pacing Clin Electrophysiol. 2005;28:268–9.

403. Hayes DL, Holmes DR Jr, Gray JE. Effect of 1.5 tesla nuclear magnetic resonance imaging scanner on implanted permanent pacemakers. J Am Coll Cardiol. 1987;10:782–6.

404. Irnich W, Irnich B, Bartsch C, et al. Do we need pacemakers resistant to magnetic resonance imaging? Europace. 2005;7:353–65.

405. Levine PA. Industry viewpoint: St. Jude Medical: Pacemakers, ICDs and MRI. Pacing Clin Electrophysiol. 2005;28:266–7.

406. Prasad SK, Pennell DJ. Safety of cardiovascular magnetic resonance in patients with cardiovascular implants and devices. Heart. 2004;90:1241–4.

407. Shellock FG, Tkach JA, Ruggieri PM, et al. Cardiac pacemakers, ICDs, and loop recorder: evaluation of translational attraction using conventional ("long-bore") and "short-bore" 1.5- and 3.0-Tesla MR systems. J Cardiovasc Magn Reson. 2003;5:387–97.

408. Smith JM. Industry viewpoint: Guidant: Pacemakers, ICDs, and MRI. Pacing Clin Electrophysiol. 2005;28:264.

409. Avery JK. Loss prevention case of the month. Not my responsibility! J Tenn Med Assoc. 1988;81:523.

410. Martin ET, Coman JA, Shellock FG, et al. Magnetic resonance imaging and cardiac pacemaker safety at 1.5-Tesla. J Am Coll Cardiol. 2004;43:1315–24.

411. Gimbel JR, Kanal E, Schwartz KM, et al. Outcome of magnetic resonance imaging (MRI) in selected patients with implantable cardioverter defibrillators (ICDs). Pacing Clin Electrophysiol. 2005;28:270–3.

412. Roguin A, Zviman MM, Meininger GR, et al. Modern pacemaker and implantable cardioverter/defibrillator systems can be magnetic resonance imaging safe: in vitro and in vivo assessment of safety and function at 1.5 T. Circulation. 2004;110:475–82.

413. Del Ojo JL, Moya F, Villalba J, et al. Is magnetic resonance imaging safe in cardiac pacemaker recipients? Pacing Clin Electrophysiol. 2005;28:274–8.

414. Gimbel JR, Johnson D, Levine PA, et al. Safe performance of magnetic resonance imaging on five patients with permanent cardiac pacemakers. Pacing Clin Electrophysiol. 1996;19:913–9.

415. Goldsher D, Amikam S, Boulos M, et al. Magnetic resonance imaging for patients with permanent pacemakers: initial clinical experience. Isr Med Assoc J. 2006;8:91–4.

416. Roguin A, Donahue JK, Bomma CS, et al. Cardiac magnetic resonance imaging in a patient with implantable cardioverter-defibrillator. Pacing Clin Electrophysiol. 2005;28:336–8.

417. Sommer T, Vahlhaus C, Lauck G, et al. MR imaging and cardiac pacemakers: in-vitro evaluation and in-vivo studies in 51 patients at 0.5 T. Radiology. 2000;215:869–79.

418. Gimbel JR, Kanal E. Can patients with implantable pacemakers safely undergo magnetic resonance imaging? J Am Coll Cardiol. 2004;43:1325–7.

419. Martin ET. Can cardiac pacemakers and magnetic resonance imaging systems co-exist? Eur Heart J. 2005;26:325–7.

420. Nazarian S, Roguin A, Zviman MM, et al. Clinical utility and safety of a protocol for noncardiac and cardiac magnetic resonance imaging of patients with permanent pacemakers and implantable-cardioverter defibrillators at 1.5 tesla. Circulation. 2006;114:1277–84.

421. Sommer T, Naehle CP, Yang A, et al. Strategy for safe performance of extrathoracic magnetic resonance imaging at 1.5 tesla in the presence of cardiac pacemakers in non-pacemaker-dependent patients: a prospective study with 115 examinations. Circulation. 2006;114:1285–92.

422. Cowper SE, Su LD, Bhawan J, et al. Nephrogenic fibrosing dermopathy. Am J Dermatopathol. 2001;23:383–93.

423. Ting WW, Stone MS, Madison KC, et al. Nephrogenic fibrosing dermopathy with systemic involvement. Arch Dermatol. 2003;139:903–6.

424. Mackay-Wiggan JM, Cohen DJ, Hardy MA, et al. Nephrogenic fibrosing dermopathy (scleromyxedema-like illness of renal disease). J Am Acad Dermatol. 2003;48:55–60.

425. Sadowski EA, Bennett LK, Chan MR, et al. Nephrogenic systemic fibrosis: risk factors and incidence estimation. Radiology. 2007;243:148–57.

426. Perazella MA. Current status of gadolinium toxicity in patients with kidney disease. Clin J Am Soc Nephrol. 2009;4:461–9.

APPENDIX 1. AUTHOR RELATIONSHIPS WITH INDUSTRY AND OTHER ENTITIES—ACCF/ACR/AHA/NASCI/SCMR 2010 EXPERT CONSENSUS DOCUMENT ON CARDIOVASCULAR MAGNETIC RESONANCE

Committee Member	Consultant	Speaker	Ownership/ Partnership/ Principal	Research	Institutional, Organizational, or Other Financial Benefit	Expert Witness
Dr. W. Gregory Hundley (Chair)	None	• Pfizer	• MRI Cardiac Services	• Bracco Diagnostics*	None	None
Dr. David A. Bluemke	• Berlex • GE Healthcare	None	None	• Epix Medical*	• Research agreements between Johns Hopkins University and magnetic resonance imaging equipment manufacturers Siemens, GE Healthcare, Philips Medical Systems.	None
Dr. J. Paul Finn	• GE Healthcare • Siemens Medical Solutions*	• Berlex Laboratories, Inc.	None	None	None	None
Dr. Scott D. Flamm	• Vital Images	None	None	• EagleVision Pharmaceutical, Inc. • GE Healthcare • Philips Medical Systems • Siemens Medical Solutions • Tyco/Mallinckrodt Healthcare	None	None
Dr. Mark A. Fogel	• Siemens	• Siemens	None	• Edwards Life Sciences • National Institutes of Health • Siemens	None	None
Dr. Matthias G. Friedrich	None	None	• Circle Cardiovascular Imaging Inc., Calgary	None	• Research agreement between the Libin Cardiovascular Institute (University of Calgary) and Siemens Medical Solutions. No personal financial benefit to disclose.	None
Dr. Vincent B. Ho	None	None	None	• GE Healthcare* (research support)	None	None
Dr. Michael Jerosch-Herold	None	None	None	None	None	None
Dr. Christopher M. Kramer	• Siemens Medical Solutions*	• Merck/ Schering-Plough	None	• GlaxoSmithKline	None	None
Dr. Warren J. Manning	None	None	None	• Philips Medical Systems*	None	None
Dr. Manesh Patel	None	None	None	None	None	None
Dr. Gerald M. Pohost	None	None	None	None	None	None
Dr. Arthur E. Stillman	None	None	None	None	None	None
Dr. Richard D. White	None	None	None	• Siemens Medical Solutions*	None	None

Committee Member	Consultant	Speaker	Ownership/ Partnership/ Principal	Research	Institutional, Organizational, or Other Financial Benefit	Expert Witness
Dr. Pamela K. Woodard	None	• GE Healthcare	None	• Astellas Pharma* • GE Healthcare* • Siemens Medical (research agreement)	None	None

This table represents the relationships of committee members with industry and other entities that were reported by authors to be relevant to this document. These relationships were reviewed and updated in conjunction with all meetings and/or conference calls of the writing committee during the document development process. The table does not necessarily reflect relationships with industry at the time of publication. A person is deemed to have a significant interest in a business if the interest represents ownership of 5% or more of the voting stock or share of the business entity, or ownership of $10 000 or more of the fair market value of the business entity; or if funds received by the person from the business entity exceed 5% of the person's gross income for the previous year. A relationship is considered to be modest if it is less than significant under the preceding definition. Relationships in this table are modest unless otherwise noted.

　*Significant (greater than $10 000) relationship.

APPENDIX 2. PEER REVIEWER RELATIONSHIPS WITH INDUSTRY AND OTHER ENTITIES—ACCF/ACR/AHA/ NASCI/SCMR 2010 EXPERT CONSENSUS DOCUMENT ON CARDIOVASCULAR MAGNETIC RESONANCE

Peer Reviewer	Representation	Consultant	Speaker	Ownership/ Partnership/ Principal	Research	Institutional, Organizational, or Other Financial Benefit	Expert Witness
Dr. James C. Carr	Official Reviewer—North American Society for Cardiovascular Imaging	None	None	None	None	None	None
Dr. Michael G. Del Core	Official Reviewer—ACCF Board of Governors	None	None	None	None	None	None
Dr. Andre Duerinckx	Official Reviewer— American College of Radiology	None	None	None	• Philips Medical Systems • Schering-Plough	None	None
Dr. Mark J. Eisenberg	Official Reviewer—ACCF Task Force on Clinical Expert Consensus Documents	None	None	None	None	None	None
Dr. Victor A. Ferrari	Official Reviewer— Society for Cardiovascular Magnetic Resonance Imaging	None	None	None	None	None	None
Dr. Gautham Reddy	Official Reviewer— American College of Radiology	None	None	None	None	None	None
Dr. Orlando Simonetti	Official Reviewer—North American Society for Cardiovascular Imaging	None	None	• Siemens Healthcare	None	None	None
Dr. James E. Udelson	Official Reviewer—ACCF Board of Trustees; American Heart Association	None	None	None	None	None	None
Dr. Sanjay Kaul	Content Reviewer— ACCF Task Force on Clinical Expert Consensus Documents	None	None	None	None	None	None
Dr. Debabrata Mukherjee	Content Reviewer— ACCF Task Force on Clinical Expert Consensus Documents	None	None	None	None	None	None

Peer Reviewer	Representation	Consultant	Speaker	Ownership/ Partnership/ Principal	Research	Institutional, Organizational, or Other Financial Benefit	Expert Witness
Dr. Robert S. Rosenson	Content Reviewer— ACCF Task Force on Clinical Expert Consensus Documents	• Abbott • Anthera • AstraZeneca* • Daiichi Sankyo • LipoScience* • Roche	None	• LipoScience*	None	• Grain Board	None
Dr. Jonathan W. Weinsaft	Content Reviewer— *Individual	None	None	None	• Lantheus Medical Imaging	None	None

This table represents the relevant relationships with industry and other entities that were disclosed by reviewers at the time of peer review. It does not necessarily reflect relationships with industry at the time of publication. A person is deemed to have a significant interest in a business if the interest represents ownership of 5% or more of the voting stock or share of the business entity, or ownership of $10 000 or more of the fair market value of the business entity; or if funds received by the person from the business entity exceed 5% of the person's gross income for the previous year. A relationship is considered to be modest if it is less than significant under the preceding definition. Relationships in this table are modest unless otherwise noted. Names are listed in alphabetical order within each category of review. Participation in the peer review process does not imply endorsement of this document.

  *Significant (greater than $10 000) relationship.